Characterisation of the human immune response from AVP vaccine against anthrax

Characterisation of the Human Immune Response from AVP Vaccine against Anthrax

Tapasvi Modi, MSc

Porton Biopharma Ltd, Porton Down, Manor Farm Road, Salisbury SP4 0JG

&

Birkbeck, University of London, Malet Street, Bloomsbury, London WC1E 7HX

Thesis submitted for the degree of Doctor of Philosophy

September 2020

CONTENTS

TABLE OF CONTENTS

Declaration

I, Tapasvi Modi, declare that the work presented in this thesis is my own. Where information has been derived from other sources, or is of a collaborative nature, I confirm that this has been explicitly indicated in the text.

Acknowledgements

This project has been possible as a result of lasting support from many people. Although there are too many to name, I am pleased to acknowledge the people who have helped me through this journey. Firstly, I would like to thank my seniors at work, who have shown confidence in me and encouraged me throughout these years. I would like to thank Porton Biopharma's Managing Director Dr. Roger Hinton and Development Group's Director Dr. Julie Miller for sponsoring this project. I would like to thank my manager and supervisor Dr. Dave Gervais who has guided me throughout this project, who has been my mentor and has always encouraged me to explore my ideas.

I would like to thank my previous manager and colleague Stuart Smith for giving me invaluable career advice and encouraging me to pursue this project. I would like to thank all my work colleagues (too many to name here), who have always been supportive and flexible with me when I needed to work on this project in parallel with other work projects. Thank you, Dr. Diane Williamson at DSTL for your expertise on Anthrax, for helpful advice during the *in vitro* study and for reviewing my publication.

I would like to thank my supervisor Dr. Adrian Shepherd who has always been so patient with me and who I have had long discussions with - whether it be project related or about exploring nature. Thank you for your invaluable help and direction in writing my paper and thesis. I would like to thank my supervisor Dr. Konstantinos Thalassinos for welcoming me into his group and for help and guidance through this project. I would also like to thank Shaan Subramaniam who helped me with Mass Spectrometry work on this project and also made me feel so welcome when I spent time doing lab work at UCL.

Finally, I would like to thank my friends and family who are the pillars of my life. Ma and Papa - your love, support and blessings have shaped me to become who I am. I hope I am making

you two proud! To my little brother Parth - although we are siblings, you have become a best friend. You have stuck with me throughout my ups and downs; your love, support and advice help me immensely. To Bhargavi Aunty, Jani Sir and Aunty Gillian – I am glad to have you as second parents in my life. Thanks to my friends Pushpa, Laura, Peter, Filia and Sophie who have helped me maintain a life perspective outside of work and PhD. And to life time buddies – Khyati, Janvi, Siddhi and Riddhi!

LIST OF FIGURES

LIST OF TABLES

Research Abstract

The UK Anthrax vaccine (AVP) is an alum precipitate of a sterile culture filtrate of the *Bacillus anthracis* Sterne strain designed to maximise the production of protective antigen (PA). Although AVP has been in use for decades, several of its fundamental properties are poorly understood, including its exact composition, the extent to which proteins other than PA may contribute to protection, and how the degree of protection may differ between individuals.

This study involved three innovative investigations. Firstly, the composition of AVP was analysed using liquid chromatography tandem mass-spectrometry (LC-MS/MS). This required the development of a novel desorption method for releasing *B. anthracis* proteins from the vaccine's aluminium-containing adjuvant. Secondly, computational MHC-binding predictions were made for the eight most abundant proteins of AVP using the NetMHCIIpan tool, focusing on the most common HLA alleles in several ethnic groups and multiple *B. anthracis* strains. Thirdly, antibody levels and toxin neutralising antibody (TNA) levels were measured for both PA and lethal factor (LF) in sera from AVP human vaccinees.

Using LC-MS/MS it was demonstrated that AVP is composed of at least 138 *B. anthracis* proteins, including PA (65%), LF (8%) and edema factor (EF) (3%). NetMHCIIpan predicted that peptides from all eight abundant proteins are likely to be presented to T cells, a pre-requisite for protection; however, the number of such peptides varied considerably for different HLA alleles.

These analyses highlighted two important properties of the AVP vaccine that have not been previously established. Firstly, the effectiveness of AVP within humans does not depend on PA alone; there is compelling evidence to suggest that LF has a protective role, with computational predictions suggesting that additional proteins may be important for individuals

with specific HLA allele combinations. Secondly, in spite of differences in the sequences of key antigenic proteins from different *B. anthracis* strains, computational analysis suggested that these do not affect the protection that AVP affords to strains other than the vaccine's source strain.

ABBREVIATIONS

ADCC - Antibody-dependent cell-mediated cytotoxicity

Alum – Aluminium potassium sulphate

APC – Antigen presenting cells

ATP – Adenosine Triphosphate

AVA - Anthrax Vaccine Absorbed

AVP - Anthrax Vaccine Precipitate

BCA - Bicinchoninic acid

cAMP – Cyclic Adenosine Monophosphate

CGM2 - Capillary Morphogenesis gene-2

CID – Collision Induced Dissociation

CF – Culture Filtrate

CPC - Cetylpyridinium chloride

CRM – Charge Residue Model

DDA – Data Dependent Acquisition

DIA – Data Independent Acquisition

ECD – Electron Capture Dissociation

EDTA - Ethylenediaminetetraacetic acid

EF - Edema Factor

ELISA – Enzyme-linked immunosorbent assay

ERK - Extracellular-signal regulated kinase

ESI – Electrospray Ionisation

ET - Edema Toxin

ETD – Electron Transfer Dissociation

FDR – False Discovery Rate

GFPB – [Glu1] – Fibrinopeptide B

GM-CSF - Granulocyte macrophage colony-stimulating factor

GPCR – G-protein coupled receptor

HLA – Human leukocyte antigen

IgG – Immunoglobulin G

IgM – Immunoglobulin M

IFN – Interferon gamma

JNK - Jun N terminus kinase

LC - Liquid Chromatography

LC-MS/MS – Tandem Mass Spectrometry

LF - Lethal Factor

LT - Lethal Toxin

MAPK - Mitogen-activated protein kinases

MCL – Macrophage cell lysis

MEKs - Mitogen-activated protein kinase kinases

MHC – Major histocompatibility complex

MS – Mass Spectrometry

MTT - (3-(4, 5-Dimethylthiazol-2-yl)-2, 5-Diphenyltetrazolium Bromide)

m/z – Mass to charge ratio

NaOH – Sodium hydroxide

nESI – Nano Electrospray Ionisation

NIBSC – National Institute of Biological Standards and Controls

NK cells – Natural killer cells

PA - Protective Antigen

PBS – Phosphate buffer saline

PBMC – Peripheral blood mononuclear cells

PES – Polyethersulfone

PHE- Public Health England

PKA – Protein Kinase A

PMNs – Polymorphonuclear cells

Q-ToF – Quadrupole - Time of Flight

RPLC – Reversed phase liquid chromatography

SDS – Sodium dodecyl sulphate

TEM8 - Tumour Endothelium Marker 8

TCR – T cell receptor

Th cell – Helper T cell (or T helper cell)

T_{FH} - T follicular helper cells

TLR- Toll-like receptor

TNA – Toxin Neutralising Assay

TNF- Tumour necrosis factor

ToF – Time of Flight

TWIMS – Travelling Wave Ion Mobility Separation

vWA - von Willebrand factor A

2D-DIGE – 2-dimensional gel electrophoresis

1.0 INTRODUCTION

1.1 Project Aims and Objectives

Bacillus anthracis is a highly virulent bacterium that is responsible for causing Anthrax. Anthrax spores survive in the environment for a long time, are easily transmitted, and are associated with high rates of morbidity and mortality. For these reasons, Anthrax has gained increasing attention as a potential bioterrorism agent. As a consequence, government agencies are interested in stockpiling Anthrax vaccines that exhibit long-term stability and efficacy as a means to safeguard public health through mass immunisation, should the need arise.

There are two widely-used vaccines against Anthrax: the US Anthrax Vaccine Adsorbed (AVA) vaccine, and the UK Anthrax Vaccine Precipitate (AVP) vaccine. AVP, which has been in production since the 1950s and is now manufactured by Porton Biopharma Ltd (PBL), is the focus of this research. AVP is, in essence, an alum precipitate of a sterile culture filtrate of the *B. anthracis* Sterne ($34F_2$) strain. Previous proteomic studies [1, 2] have shown that AVP contains at least 21 proteins including protective antigen (PA), lethal factor (LF) and edema factor (EF). However, the exact composition of AVP remains unknown, although – perhaps significantly – it is thought to contain more LF than AVA, based on antibody titres measured in sera from animal or human studies [3-5].

One of the main objectives of this project was to identify and quantify proteins in AVP. This was done using highly sensitive tandem mass spectrometry (LC-MS/MS) methods. An introduction to the technique is detailed in Section 1.5. The MS work carried out on AVP is described in Chapter 3. Potassium aluminium sulphate (alum) is used as an adjuvant in AVP. In order to characterise the proteins in AVP using LC-MS/MS methods, the proteins in AVP needed to be desorbed from alum. The development of a novel desorption method is described in Chapter 2.

Numerous studies have confirmed that PA is the principle immunogen of both AVP and AVA, with anti-PA antibody and TNA (toxin neutralising antibody) levels generally accepted as correlates of protection when measuring vaccine efficacy [3, 6, 7]. These terms are explained in more detail in Section 1.3.3. However, it is currently unknown whether AVP proteins other than PA have a significant protective role. Several studies have highlighted the additional protective role of LF, either because it enhances the PA-specific antibody response [6, 8, 9], or via the independent protective role of anti-LF antibodies [3, 10, 11]. Additionally, EF is shown to protect from *B. anthracis* spore challenge in animal studies [12, 13], and that anti-EF antibodies can neutralise Edema Toxin (ET) [14]. Other *B. anthracis* proteins such as cell wall proteins are also shown to trigger a protective immune response against Anthrax in mice [15].

In Anthrax research, there has been a heavy reliance on animal studies, owing to the life-threatening nature of *B. anthracis* and the low rates of human infection. Large-scale studies of human AVA vaccinees are possible because of mandatory US military vaccination programmes, whereas comparable studies for AVP are infeasible, given the comparatively smaller number of AVP vaccinees. One AVA study involving 1000 vaccinated individuals concluded that African Americans have lower toxin neutralising antibodies than European Americans [16], raising the possibility that genetic differences play a role in the immune response to AVA and calling into question the relevance of non-human studies.

Given their known associations with ethnicity and with differential responses to vaccination, HLA haplotypes are prime candidates as potential genetic factors underpinning the stratification of human responses to Anthrax vaccines. Computational studies were carried out to predict MHC-binding (a pre-requisite for T cell response) for the most abundant proteins of AVP (these were identified by LC-MS/MS studies – Chapter 3). The differences in peptide-MHC binding were investigated across common HLA alleles in several ethnic groups and multiple *B. anthracis* strains. Section 1.6 gives a brief introduction to the underlying

computational methods. Computational work carried out in this project is detailed in Chapter 4.

Finally, a small proof of concept study was designed to characterise the immune response from PA and LF in human AVP vaccinees (Chapter 5). This study evaluated T cell response by measuring IFNy and IL10 cytokine response, anti-PA IgG, anti-LF IgG and TNA levels in vaccinees. These terms will be explained in more detail in Chapter 5.

1.2 Background

1.2.1 Bacillus anthracis

B. anthracis is a highly virulent, non-motile, encapsulated, gram-positive, rod shaped, spore forming, aerobic, facultative unaerobic bacterium (Figure 1) [17, 18]. Exposure to *B. anthracis* or its spores causes the infectious disease Anthrax.

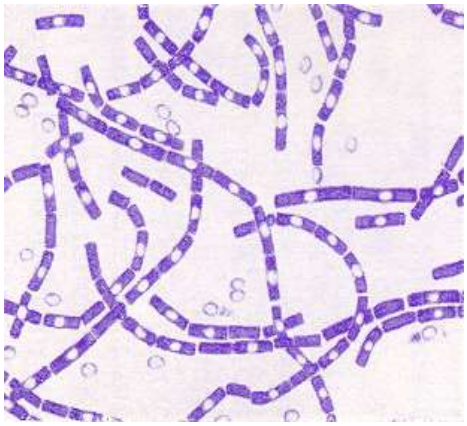

Figure 1 - Gram stained *B. anthracis* (1500x). Typically, the cells are 1-1.2µm in width x 3-5µm in length with distinctive square ends. The endospore is ellipsoidal in shape and is located in the middle of the cell [19].

1.2.2 Anthrax Spore

Robert Koch first observed that the bacterium associated with Anthrax formed endospores in 1877 and demonstrated the disease by injecting into animals [20]. His work on *Bacillus anthracis* lead to the development of Koch's four postulates, which became widely accepted principles in microbiology: first - the microbe is present in each case of the disease, second - the microbe can be taken from infected host and grown independently, third - when the microbe is introduced into healthy host, it causes disease, fourth - the microbe can then be isolated from the new infected host and identified to the source microbe [21].

An Anthrax spore is a special cell type produced by the bacteria in response to starvation. It lacks metabolic activity and is resistant to various environmental stresses such as heat, chemicals, desiccation, starvation and other stresses [22-24]. Hence, the spore can survive in the environment for decades in its dormant state; however, when the spore senses the presence of nutrients in a suitable host, it can rapidly return to a vegetative state. This also helps it survive the host defence systems after entering the host and before secreting toxins that cause disease when it has reached suitable location in the host after germination [25].

The spore is formed of a series of concentric shells, and with each shell performing a specific function. First on the inside, there is a peptidoglycan layer which surrounds the spore core (containing the chromosome). Then there is a protein shell that can resist a variety of stresses, and on the outside, there is another protein and glycoprotein layer that is important for surface interactions with the environment and with the host [25].

1.2.3 *B. anthracis* Virulence Factors

B. anthracis has two virulence factors, namely the poly-D-glutamic acid capsule and the Anthrax toxins. It contains a single chromosome and two extrachromosomal plasmids. The

poly-D-glutamic acid capsule is encoded by the pXO2 plasmid (182 kb) and suppresses phagocytosis by immune effectors. Anthrax toxins is an A/B type tripartite toxin, encoded by the pX01 plasmid (96 kb) [26-28]. These toxins are the main virulence factors of *B. anthracis* [18, 26-29]. The toxins are formed from the synergistic effects of three proteins – protective antigen (PA), lethal factor (LF) and edema factor (EF). These proteins are not toxic individually, but PA binds with LF to form lethal toxin (LT) and with EF to form edema toxin (ET). Typically, bacteria release toxins into the host as a survival strategy, to promote bacterial spread and growth and suppress host immune response. The function of PA, LF and EF, and their effects on the host immune system are detailed later in Section 1.3.

1.2.4 Exposure to Anthrax and Mortality

Exposure to Anthrax spores can result in high levels of morbidity and mortality. Anthrax typically affects wild or domestic herbivorous animals in its natural state. Human exposure to Anthrax is usually due to contact with infected animals or their products. There are three possible routes of exposure to Anthrax spores - cutaneous, gastrointestinal and pulmonary. People working in the tanning industry, woollen mills and veterinarians are at a high risk of an Anthrax infection. Recently, Anthrax infection was reported in class IV drug users due to contaminated heroin in Scotland [30].

Cutaneous Anthrax infection is the most common type of Anthrax and accounts for more than 95% of total cases. It is caused by the vegetative bacteria or its spore coming into contact with cuts or abrasions on the skin. The mortality rate for cutaneous Anthrax is approximately 20% without antibiotics. Clinical symptoms of cutaneous Anthrax develop within 1-2 days of exposure with the formation of a pruritic papule or vesicle that enlarges and erodes into a necrotic ulcer and subsequently into a black eschar. Other related symptoms such as fever, myalgia, swollen glands, headache and vomiting also persist. If the infection is not treated, it can progress into compartment syndrome in the affected area [17, 18].

Gastrointestinal Anthrax is caused by the ingestion of contaminated meat. The mortality rate for gastrointestinal Anthrax is approximately 25-75% with antibiotics, depending on the stage of infection and the start of treatment. The incubation period can range between 1-7 days. Clinical symptoms of gastrointestinal Anthrax include pharyngeal lesions with sore throat, difficulty in swallowing, marked neck swelling and regional lymphadenopathy, or intestinal infection showing symptoms of fever, severe abdominal pain, massive ascites, hematemesis, and bloody diarrhoea [17, 18].

Inhalation Anthrax is the most severe and rare form of Anthrax, caused by breathing in Anthrax spores. The mortality rate for inhalation Anthrax is 45-90% with antibiotics, depending on the stage of infection and the start of treatment. The incubation period ranges between 1-43 days post exposure. Clinical symptoms of inhalation Anthrax start with fever, chills, cough, chest pain, headache, myalgia and malaise for the first few days. When the lymph nodes are overwhelmed with Anthrax toxin, the toxin ends up entering systemic circulation, resulting into acute respiratory distress with pulmonary edema and pleural effusion, and eventually severe breathlessness, hypoxia and septic shock [17, 18].

1.2.5 Anthrax Incidences

Anthrax incidences are rare and it is estimated that there are approximately 1000-2000 deaths per year worldwide [31]. However, Anthrax has gained significant attention as a bioterrorism agent. The first reported use of Anthrax as a biological agent was during World War I, when Germany wanted to spread it to the Allied Forces by contaminating livestock feed [32]. Post-World War I and II, many countries instigated research into Anthrax vaccines [33]. Eventually in 1972, a treaty was signed between 103 countries to never use such biological warfare agents. Despite that, the bioterrorism threat of Anthrax continued during the Cold War and the Gulf War in 1991. In recent times, there is a threat from individuals and terrorist groups to use Anthrax as a bioterrorism agent. There have been two reported incidents of such attacks

namely the 1995 attack by the Aum Shinrikyo cult in Japan [34] and the 2001 Anthrax mail event in the USA [18, 35]. Hence, for the purpose of public health preparedness, government agencies are interested in Anthrax vaccines that can be used for mass immunisation. It is important that the vaccine has long term safety and efficacy so that it can be stockpiled.

1.2.6 Treatment for Anthrax post exposure

The success of antibiotic treatment for Anthrax can be variable depending on the type of Anthrax infection. Nevertheless, the treatment is only effective if started early in the infection. Antibiotic treatment can kill the bacteria, but if Anthrax toxins have been released in the host, the treatment would be unsuccessful. Most cases of cutaneous Anthrax can be successfully treated with antibiotics involving a 60-day course of ciprofloxacin or doxycycline, with ciprofloxacin being the first line of treatment (EMA 2002). Other alternative antibiotic treatments include ofloxacin, levofloxacin and penicillin. Two or more types of antibiotics are necessary for the treatment of inhalation Anthrax [18].

The antibiotic treatment regimen for Anthrax is lengthy and it can result in irregular medication, often resulting into antibiotic resistance. Although, antibiotic resistance to *B. anthracis* occurring naturally has been reported rarely, *in vitro* studies have shown that *B. anthracis* can develop resistance to ciprofloxacin, doxycycline and β-lactam antibiotics [36-39]. Cavallo *et al.,* [40] studied antibiotic susceptibility in 96 *B. anthracis* isolates from France *in vitro* and reported that *B. anthracis* is susceptible to 25 different antibiotics. However, all of the isolates studied were resistant to cotrimoxazole, whilst 11 isolates were resistant to penicillin G and amoxicillin. Doxycycline and fluoroquinolones showed good activity; ofloxacin, pefloxacin, gatifloxacin, and levofloxacin are potentially suitable for the treatment of ciprofloxacin resistant strains.

1.2.7 Current Anthrax Vaccines

There are two types of Anthrax vaccines currently available for human use:

1. Live attenuated vaccine – The vaccine contains spores from attenuated strains of *B. anthracis*. It was first licenced in Russia in 1953 for administration by scarification, and by subcutaneous injection in 1959. Booster injections are given on an annual basis [4, 18, 35].
2. Cell-free vaccines
    a. AVP - The UK Anthrax vaccine Anthrax Vaccine Precipitate (AVP) is a sterile CF of avirulent *B. anthracis* Sterne strain precipitated adsorbed to alum. The vaccine was first licenced in the UK in 1978. The AVP immunisation schedule includes four 0.5mL intramuscular injections at 0, 3, 6 and 32 weeks. Booster injections were previously given on an annual basis [18], but since 2018 the booster frequency has been changed to 10 years.
    b. AVA - Anthrax Vaccine Adsorbed (AVA) is a culture supernatant of non-virulent *B. anthracis* V770-NP1-R adsorbed to aluminium hydroxide. The vaccine was first licenced in the USA in 1972. The AVA immunisation schedule includes five 0.5mL intramuscular injections at 0 and 4 weeks, and 6, 12 and 18 months. Booster injections are given on an annual basis, after the initial 18-month period [41].

1.3 Anthrax toxin

As described earlier in Section 1.2.3, Anthrax toxins are formed from synergistic effects of three proteins namely PA, LF and EF. PA binds with LF to lethal toxin (LT) and with EF to form edema toxin (ET). PA is the 83 kDa receptor binding subunit, which facilitates the entry of LF (90 kDa) and EF (89 kDa) into the host cell.

1.3.1 Receptor binding, Entry and Cellular Trafficking

PA (83 kDa) is proteolytically activated by cleaving a 20 kDa fragment of PA at the N-terminus by furin-type proteases [28, 42-44]. The activated PA (63 kDa) monomer (PA_{63}) is thus enabled to form a heptamer or an octamer, which can bind to LF or EF. Each PA_{63} oligomer can bind to three or four EF and/or LF molecules due to steric limitations [28, 44]. Mammalian endosomal lumen has low pH, which induces a conformational change in the PA oligomer. As a result, PA inserts into the lipid bilayer via cell surface receptors forming a prepore [42, 45-47]. PA targets two cell surface receptors in mammalian cells namely, tumour endothelium marker 8 (TEM8) and capillary morphogenesis gene-2 (CMG2). TEM8 is also commonly known as Anthrax toxin receptor 1 and CMG2 is known as Anthrax toxin receptor 2. These proteins are homologous and contain an extracellular von Willebrand factor A (vWA) domain which binds to PA and its associated ligands [28, 46, 48]. LF and EF molecules are thus translocated into the cytosol by endocytosis [28, 42, 49-52].

1.3.2 Mechanism of Action

LF is the catalytic component of LT, which contains a thermolysin-like active site and a zinc binding consensus motif HExxH [53]. It acts as a zinc-dependent metalloproteinase [54], which cleaves mitogen-activated protein kinase kinases (MEKs) 1-4, 6 and 7 at the N-terminus. This results in the inactivation of three important mitogen-activated protein kinase (MAPK) cellular signalling pathways namely extracellular-signal regulated kinase (ERK) via MEK 1/2 [55], Jun N terminus kinase (JNK) via MEK 4/7 and p38 via MEK 3-6 [28, 56-61].

EF is the catalytic component of ET and acts as a calcium/calmodulin-dependent adenylate cyclase [62]. It converts intracellular ATP to cAMP 1000-fold faster compared to host adenylyl cyclases. Increased levels of cAMP disrupt many cell signalling pathways [63].

1.3.3 Immune Response to Anthrax toxins

Since LT and ET are the major virulence factors responsible for causing Anthrax, this section summarises the effect of Anthrax toxins on the host innate and adaptive immune systems. These proteins suppress the host immune system by impairing the functions of several phagocytes including neutrophils, macrophages, monocytes and dendritic cells, T and B cells [28, 64].

T follicular helper cells (T_{FH}) are a type of $CD4^+$ T cells that help the production of highly specific antibodies in germinal centres of secondary lymphoid tissue, that are associated with long-term humoral immunity [65, 66]. Secondary lymphoid tissues are those sites where lymphocytes and nonlymphoid cells facilitate the generation of immune responses to antigens; these include the spleen, lymph nodes, and mucosa-associated lymphoid tissues [67]. New evidence suggests that Anthrax spores germinate and release toxins at the site of infection, i.e. during inhalation infection in nasal-associated lymphoid tissues and during gastrointestinal infection in Peyer's patches, before spreading to draining lymph nodes [68]. Given the importance of T_{FH} cells for the generation of antigen-specific memory B cell antibody response and their relevance with respect to respiratory and gastro-intestinal lymphoid tissues, it is important to understand the factors underpinning the activation and induction of T_{FH} cells during an anthrax infection or vaccination.

1.3.3.1 Effect on Phagocytes

Neutrophils

Neutrophils (a type of white blood cell) are one of the first phagocytes recruited to fight infection. They migrate to the site of infection by chemotaxis, orchestrated by the expression of pro-inflammatory cytokines (*e.g.* IL-1β) and facilitated by actin filaments [69]. LT and ET

suppress neutrophil function by suppressing their actin-based motility [70, 71]. Further, ET suppresses the expression of β2 integrin, which affects their surface adhesion ability [71]. LT is thought to inhibit phagocytosis by suppressing the production of superoxides, which kill bacteria [72].

Monocytes

Monocytes (a type of white blood cell) are recruited to phagocytose pathogens and modulate cytokine-based inflammatory responses [73, 74]. Monocytes are derived from monoblasts in the bone marrow and differentiate into macrophages and dendritic cells [75-77]. LT is not thought to cause monocyte cell apoptosis directly but interferes with monocyte function. LT not only disrupts MAPK pathways, but also affects genes involving IL18, Toll-like receptor (TLR) [78], IFN alpha signalling and G protein family signalling pathway functions [74]. As a result, regulation of transcription processes, cytokine signalling pathways, actin regulation and signal transduction functions may be impaired [74]. The differentiation of monocytes into dendritic cells is also suppressed by inhibiting the production of chemokines [58, 74, 79-81]. ET has been shown to increase cAMP levels in human monocytes and adversely affecting cytokine expression (increased IL-1 and IL-6, decreased TNF-α) [82, 83]. Further, the production of heparanase may be suppressed, which plays a vital role in producing an inflammatory response [74].

Research has shown that prior exposure to anthrax toxins modulate TEM8 receptor expression in monocytes [84]. TEM8 receptor expression in monocytes was shown to be low in naturally-infected individuals, whilst it was higher in AVP-vaccinated individuals and control individuals. This was also corroborated by the relative percentages of monocytes found to bind to PA within blood samples from these individuals. The hypothesis is that high expression of TEM8 receptors makes the individual more susceptible to anthrax infection. Despite the fact that AVP vaccinees would have been exposed to anthrax toxins, TEM8 receptor expression

was high in monocytes from vaccinees. This could be attributable to differences in the concentration/ratio of PA, LF and EF proteins in comparison to naturally-infected individuals.

Macrophages

Macrophages are critical components of the innate immune system that phagocytose pathogens. LT supresses macrophage activation and chemotaxis by disrupting MAPK pathways and inhibiting the expression of pro-inflammatory cytokines (*e.g.* TNF-α and IL-1β [85]) [81, 86]. LT also disrupts mitochondrial function, inhibits the expression of prosurvival or anti-apoptopic genes, and induces cell death by initiating proteasome and inflammasome dependent pathway [64, 87, 88].

ET supresses the phagocytic ability of human macrophages by increasing cAMP levels in the cells, which disrupts protein kinase A (PKA) dependent signalling pathways and actin remodelling processes [89, 90]. An *in vitro* study [91] suggested that ET also prevents phagocytosis by inhibiting the expression of TNF-α cytokine in murine macrophages. Although ET is thought to supress chemotaxis [86], evidence suggests that it may enhance the migration of infected macrophages (anti-inflammatory GPCR-activated macrophages) through lymph nodes, thereby promoting bacterial spread [92].

Dendritic cells

Dendritic cells (DCs) are part of both innate and adaptive immune systems. They are the antigen presenting cells responsible for delivering antigen-specific signals for mounting a T cell response. When a dendritic cell encounters a pathogen, it expresses inflammatory chemokines and recruits inflammatory effectors at the site of infection [93]. Typically, immature dendritic cells capture the bacterial antigens and accumulate them in the peripheral tissues. In lymph nodes, DCs become mature after going through terminal differentiation and present

the bacterial antigens necessary for a helper T response (Th1 (interferon (IFN-γ) producing), Th2 (interleukin (IL)-4-, IL-5- and IL-13-producing) or Th17 (IL-17- and IL-22-producing)) [81, 94, 95].

Both LT and ET prevent the initiation of adaptive immunity by preventing DC activation and maturation. An *in vivo* study using a mouse model [96] demonstrated that LT prevents an antigen-specific T cell response by inhibiting the expression of pro-inflammatory cytokines and disrupting the MAPK pathways. Other studies [97, 98] have corroborated this finding in dendritic cells derived from mice bone marrow and lungs respectively and suggested that ET inhibits the production of IL-12p70, LT inhibits the production of IL-10, whilst both toxins collectively prevent the secretion of TNF-α. Further, it has been suggested that helper T cell differentiation in dendritic cells is suppressed by inhibiting the expression of TNF-α, IL-10 and IL-12 cytokines [99, 100]. LT also inhibits the production of chemokines from dendritic cells and epithelial cells in lungs [81, 99, 101], which prevents the recruitment of polymorphonuclear neutrophils at the site of infection [70]. LT is thought to kill immature dendritic cells and not mature dendritic cells [102]. On the other hand, ET promotes dendritic cell migration towards lymph nodes, thus allowing the spread of bacteria to other parts of the body [86, 103].

1.3.3.2 Effect on T cells and B cells

LT and ET are thought to disrupt the T cell and B cell functions [64]. PA in the toxins bind to the TEM8 (ANTXR1) and CMG2 (ANTXR2) receptors expressed by T cells [48, 104]. Both PA receptors have been found in mouse and human macrophages [105]. After the toxins have been transported into the cytosol, they disrupt MAPK and PKA signalling pathways, which control the expression of certain gene activation and proliferation of T cells [55, 106]. T cell activation is regulated by the proliferation of antigen-specific T cells [107].

In vitro studies [108, 109] have shown that LT inhibits T cell activation and proliferation by modulating the expression of certain cytokines (IL-2, TNF-α, IFN-γ, IL-5) and activation markers (CD69, CD25) in human T cells. Comer *et al.,* [91] demonstrated that LT and ET had inhibitory effects on T cell antigen receptor-mediated activation, secretion of cytokines (IL-3, IL-4, IL-5, IL-6, IL-10, IL-17, GM-CSF, TNF-α, IFN-γ) and proliferation of $CD4^+$ T cells in a mouse model.

Due to ET induced high cAMP levels, protein kinase A (PKA) pathway is activated, which inhibits Ras protein activation and disrupts the extracellular signal-regulated kinase (ERK) pathway via MEK1/2. Further, PKA induces inactivation of p38 and JNK mediated pathways [107, 110]. In addition, it is proposed that even after the toxins have been released into the cytosol, ET remains bound to the endosomes and continues to release high levels of cAMP. This results in high amounts of PKA locally, which indirectly affects T cell receptor (TCR) signalling [107, 111, 112]. Further, ET is thought to disrupt TCR signalling independently due to elevated cAMP levels [107]. Rossi Paccani *et al.,* [113] demonstrated that ET disrupted TCR signalling *in vitro* using human T cells; it is thought to inhibit tyrosine kinase Lck activation, which adversely affects CD3ζ phosphorylation. Figure 2 shows the effects of Anthrax toxins on T cell activation and proliferation.

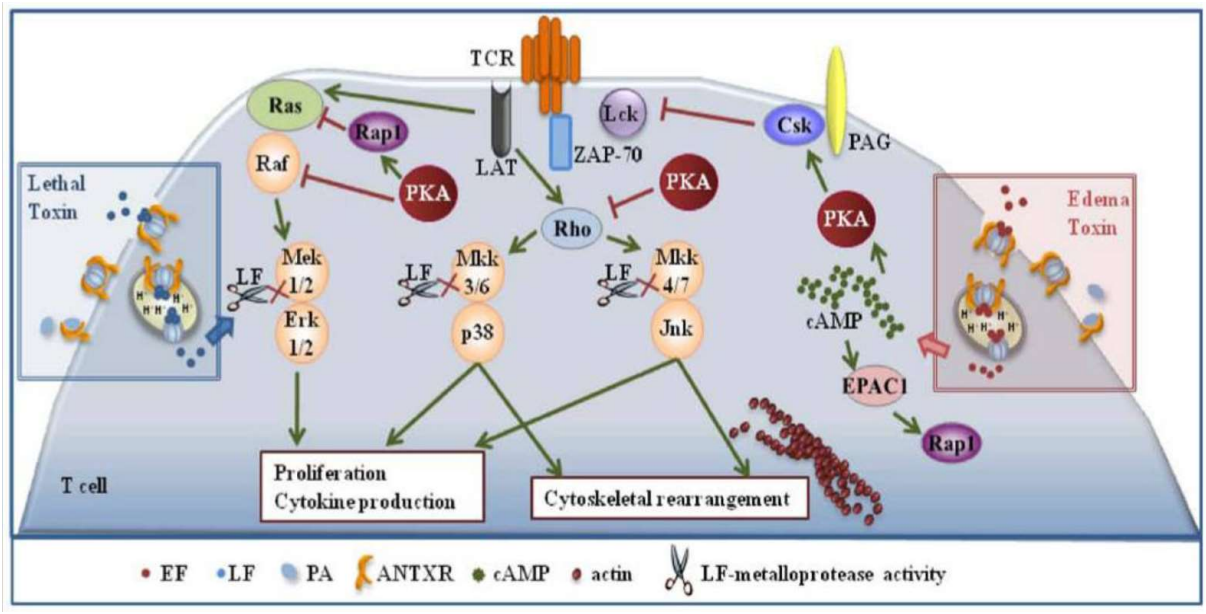

Figure 2 - Effects of LT and ET on T cell activation and proliferation. LT disrupts MAPK signalling pathways and ET disrupts PKA-dependent pathways by elevating cAMP levels [107].

In addition, both LT and ET have been shown to restrict T cell chemotaxis [86]. This involves migration of naïve T cells to lymph nodes, preventing initiation of an adaptive immune response; and migration of T cell effectors from lymph nodes to peripheral tissues at the site of infection [86, 114]. Chemotaxis is regulated by chemokine receptors (seven spanning transmembrane receptors) which are coupled with Gi proteins. When there is an inflammatory chemokine response, chemokine receptors have an inhibitory effect on cAMP production. This instigates a tyrosine kinase-dependent pathway, which in turn activates MAPK signalling pathways. LT and ET suppress both APC and T cell chemotaxis by inhibiting the chemokine-based activation of MAPK-dependent signalling pathway, thereby preventing the initiation of the adaptive immune response [86]. Figure 3 describes the effect of LT and ET on T cell chemotaxis.

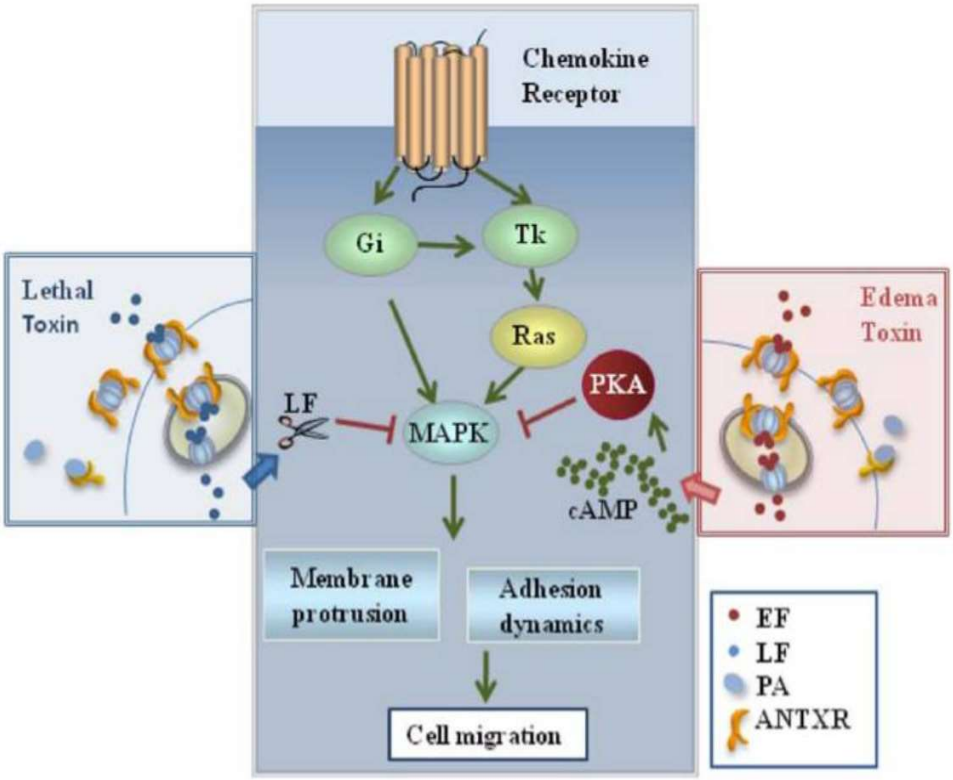

Figure 3 - Effect of Anthrax toxins on T cell chemotaxis. LT and ET inhibit the chemokine based activation of MAPK-dependent signalling pathways modulated by chemokine receptors [107].

$CD4^+$ T cells are very important in mediating the adaptive immune response. During TCR activation when the $CD4^+$ T cells are presented with major histocompatibility complex (MHC) bound antigen by antigen presenting cells (APC), they differentiate into various types of helper T cells (*e.g.* Th1, Th2 and Th17). The differentiation of helper T cells depends on the antigen presented, the types of cytokine, or the lipid mediators produced [107, 115-117]. Th1 cells are usually responsible for cell-mediated immunity and aid macrophages by producing pro-inflammatory cytokines. Th17 cells are also thought to help phagocytes with their functions by producing pro-inflammatory cytokines. Th2 cells have an important role in promoting the maturation of activated B cells into antibody producing plasma cells [107, 118-120]. ET has been shown to promote the differentiation of naïve $CD4^+$ human T cells into Th2 and Th17

cells by increasing cAMP levels and activating PKA-dependent pathways [107]. Figure 4 describes the effect of ET on T cell polarisation of $CD4^+$ T cells into Th2 and Th17 cell types.

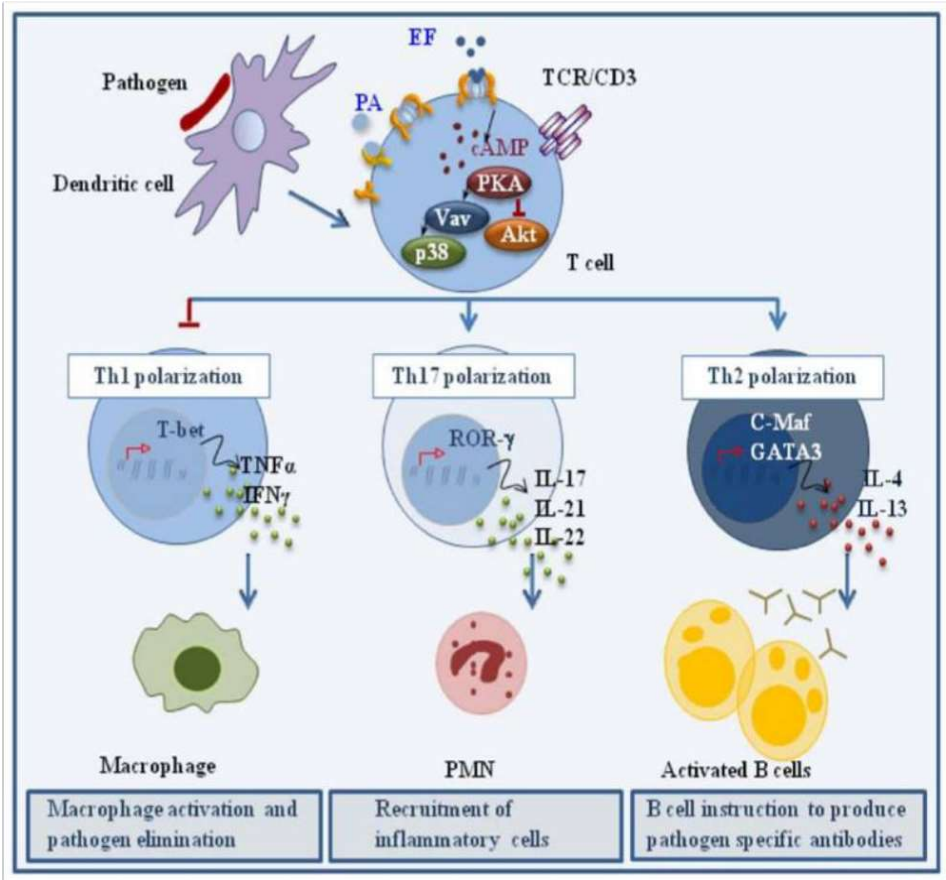

Figure 4 - The effect of ET on helper T cell polarisation into Th2 and Th17 cell types. ET regulates TCR signalling and stimulates the expression of certain transcription factors, which in turn promote the expression of certain cytokines. The specific cytokines promote differentiation of naïve helper T cells into Th2 and Th17 cell types [107].

LT is also thought to impact $CD4^+$ T cell differentiation due to its interference with MAPK-dependent signalling pathways, however the mechanism has not been studied yet [121].

LT and ET are believed to affect B cell activation, proliferation and antibody production [122]. Typically, helper T cells (specifically Th2) are required for the production of B cells, which

produce antibodies specific to the required antigen (affinity maturation) and isotype switching (*e.g.* from isotype IgM to IgG) in maturing B cells [123, 124]. New evidence suggests that a subset of natural effector B cells can be generated independent of T cell help and are capable of isotype switching [125]. Th2 helper cells produce IL-4 transcription factor and CD40 ligand necessary for the terminal differentiation of B cells [126]. The differentiation of Th2 cells from its naïve precursor is dependent on the production of IL-4, IL-5, IL-10 and IL-13 cytokines [127]. Further, the production of IL-4 and IL-5 cytokines is dependent on PKA pathways. Although, increased cAMP levels (due to ET) promote Th2 cell differentiation, increased cAMP levels inhibit naïve Th cell development by regulating cytokine production. The IL-4 and IL-10 cytokines are upregulated which promotes Th2 production, whilst inhibition of IL-12 cytokine inhibits Th1 production. Thus, ET disrupts Th1/Th2 balance by promoting differentiation of naïve $CD4^+$ Th cells into Th2 cells [64, 128-131]. Further, ET has been described to inhibit B cell chemotaxis and modulates B cell cytokine production [63].

1.4 Immune Response to AVP/AVA Vaccination

Both AVP and AVA were developed as prophylactic vaccines against Anthrax. Both vaccines are cell-free culture filtrate or supernatant of *B. anthracis*, grown in culture conditions designed to maximise the production of PA. The idea is that the generation of anti-PA antibodies post vaccination can protect the individual from subsequent Anthrax infection. Anti-PA antibodies are thought to prevent the toxin functions at many stages including binding of PA to its receptors, activation of PA, LT and ET formation, and translocation into the cell [132], thus neutralising the toxins from Anthrax infection. Hence, when measuring efficacy of AVA/AVP vaccination, anti-PA antibody titres and toxin neutralising activity (the capacity of the anti-PA antibodies to neutralise LT *in vitro*) are measured. These are generally accepted as correlates of protection [6, 133-138].

The production of anti-PA IgG antibodies post AVP vaccination describes a predominant T cell-dependent immune response; a robust $CD4^+$ T cell response generates a mature antibody response (B cell) associated with T cell class switching (IgM to IgG) and the development of memory B cells of higher affinity and that are longer-lived. A T cell response is generated when foreign antigens are taken up by specific antigen-presenting cells (APC) and proteolytically digested into small peptides. Major Histocompatibility Complex (MHC) molecules bind to a number of these peptides and present them on the APC surface. In humans, MHC molecules are described as Human Leukocyte antigen (HLA). The formation of antigen-MHC complex enable the presentation of antigen-MHC complex on the APC cell surface [139]. $CD4^+$ helper T cells or $CD8^+$ cytotoxic T cells recognise the peptide-HLA II or peptide-HLA I interaction respectively and promote the expression of co-stimulatory effectors. Only a subset of peptide-HLA complexes are immunodominant.

1.4.1 Characterisation of the Immune Response

1.4.1.1 Antibody Subtypes

There are five isotypes of immunoglobulin (antibody) molecules found in human blood sera: IgA, IgD, IgE, IgM and IgG. They are differentiated based on the type of heavy chain they contain [140].

The IgM isotype constitutes around 5% of all antibodies in blood sera. It is the first class of antibody produced on exposure to an antigen in the early stages of the primary antibody response. It is the largest in size, typically exists as pentavalent identical sub-units, attached by disulphide bonds. It has high binding strength and plays an important role in activating the complement system and agglutination [140]. Since this is the first major antibody class produced on exposure to an antigen, it might be important to measure IgM titres during the onset of anthrax infection or vaccination.

IgD antibodies are secreted in small quantities on the surface of mature B cells, mainly functions as a B cell antigen receptor, and are co-expressed with IgM antibodies in naïve B cells.

IgG is the most common isotype of antibodies (70-75%), and is produced in large quantities during the secondary immune response. It exists as a monomeric subunit, activates complement system, binds to Fc receptors on macrophages and neutrophils, and is responsible for initiating the antibody-dependent cell-mediated cytotoxicity (ADCC) response. Depending on the molecular weight of the antibody, the position of the disulphide bonds and the size of the hinge region, IgG can be further divided into four sub-classes - IgG1, IgG2, IgG3, and IgG4. Generally, IgG1 and IgG3 production is triggered by proteins, whereas IgG2 and IgG4 is triggered by foreign polysaccharides [140, 141].

IgA isotype constitutes around 10-15% of all antibodies in blood sera; it is also the most prevalent class of antibody in secretions (respiratory and intestinal secretions, saliva, tears, breast milk). IgA exists as a monomeric subunit in blood, whilst it is dimeric in secretions. It has two subtypes (IgA1 and IgA2), based on differences in the hinge region. IgA provides the primary antibody response against inhaled and ingested pathogens at mucosal surfaces [140]. Hence, this antibody class could be important in characterising anthrax infections, given that gastro-intestinal and inhalation anthrax act across mucosal membranes.

IgE is the least prevalent antibody isotype in blood sera (typically a 10,000 times lower concentration that IgG). This isoform is increased significantly in allergic reactions. In response to pathogens, IgE binds to mast cells in tissues and blood via specific receptors in response to pathogens, acting as passively-acquired receptors for antigens. This results in recruitment of eosinophil at the site of infection and destruction of pathogens via ADCC-type mechanisms [140].

1.4.1.2 Characterisation of the Immune Response to AVA and AVP

Baillie and co-workers [142, 143] characterised the types of anti-PA IgG detected in AVP vaccinees who had received the full AVP vaccination schedule. These studies confirmed that IgG_1 was principally generated; however, IgG_2, IgG_3 and IgG_4 were also detected in the serum samples from AVP vaccines. The presence of IgG_2 and IgG_3 indicates Th1-generated response, whilst IgG_1 and IgG_4 represent a Th2-generated response [144].

Allen *et al.,* [145] evaluated T cell response from AVP in Gulf war veterans who had been vaccinated 10-15 years prior to the study. Based on cytokine profiles, they reported that the vaccinees has long-lasting mixed Th1 (IFN-γ and IL-2) and Th2 (IL-13) response. Two other studies [6, 146] have corroborated this finding and reported mixed Th1 and Th2 cytokine response induced by AVA vaccination. Kwok *et al.,* [147] evaluated $CD4^+$ T cell immune response in 36 AVA vaccinees and reported bias towards PA-specific Th2 response (higher amounts of IL-5 and IL-13 in comparison to IFN-γ). Further, PA-specific pre-Th2 memory T cells were also detected in the vaccinees, meaning that the development of PA $CD4^+$ T cells was skewed towards a Th2 response, due to the pre-exposure of PA in AVA vaccinees.

1.4.2 Vaccine Efficacy

AVP and AVA are known to be efficacious based on historical animal and human data [7, 18, 148-151]; however, the immune response is not fully understood. The only efficacy data in humans is the observation that since AVP vaccination started in 1958, there was a decrease in the number of Anthrax infection cases in the employees at the Government Wool Disinfection Station in Liverpool [18, 149]. A field study in the US [7] found 92.5% AVA vaccination efficacy in workers exposed to inhalation Anthrax at four US mills. Protection had failed in workers who had either incomplete, placebo or no vaccine inoculation; except in one case where protection failed in a vaccine-inoculated individual.

Several hurdles are encountered when assessing the data from various studies. Variables such as different animal models, different *B. anthracis* strains, route of infection, vaccine dosing schedules, etc. further complicate the issue and have prevented robust conclusions from being drawn. Further, the genetic diversity of the human host has also been reported to contribute to differences in immune response.

1.4.2.1 Animal Models

The pathophysiology of Anthrax infections varies in different animals. Vaccine efficacy in different animal models is also different [18, 33]. AVP is shown to be least efficacious in mice, rats and guinea pigs, whilst it provides good protection in rabbits and monkeys. The non-human primate model *e.g.* Rhesus macaque (being the closest to human) is considered to be the most suitable model for bridging animal data to humans and measuring probability of survival for vaccine efficacy [152]. However, it is unclear the extent to which genetic differences between humans and animals, such as those associated with MHC molecules and the encoding of T cell receptors, undermine the ability of animal models to provide reliable insights into the efficacy of the vaccine.

1.4.2.2 *B. anthracis* strains

Several studies have been carried out to assess whether AVP/AVA would be protective against different *B. anthracis* strains. Inhalation Anthrax challenge studies in guinea pigs [153-155] demonstrated that AVP and AVA provided different levels of protection to different strains. It conferred full protection against the Vollum strain, limited protection against the Ames strain and showed no protection against the New Hampshire and penicillin-resistant strain, despite having high anti-PA antibody titres. AVA vaccination was shown to be protective against 18 out of 27 *B. anthracis* strains in guinea pigs [156]. Another study found that the level of

protection by AVA from 33 different *B. anthracis* strains varied considerably (6-100%) in guinea pigs [157]. However, AVA was shown to be protective in macaques and rabbits against several virulent B. *anthracis* strains in the same study. As mentioned previously, AVP and AVA are manufactured from avirulent Sterne strain and non-virulent V770-NP1-R strain, respectively. It remains to be assessed whether there are differences in sequences of key antigenic proteins in AVP and, if so, does this impact the protection afforded against different *B. anthracis* strains in humans?

1.4.2.3 Route of Anthrax infection

The route of Anthrax infection can also result in a differential immune response. The following studies in survivors of Anthrax infection demonstrate that the immune response varies considerably in different human hosts, depending on the type of Anthrax infection. Quinn *et al.,* [158], reported that anti-PA IgG titres, TNA and memory B cell response, time course for production, and maintenance of antibodies varied significantly depending on the type of infection (inhalation or cutaneous Anthrax) in 22 patients. Anti-PA IgG was detected in inhalation Anthrax patients after 11 days and after 21-34 days in cutaneous Anthrax patients from the start of symptoms. Anti-PA IgG was detectable for 8-16 months in 6 survivors of inhalation Anthrax and 7 of 11 survivors of cutaneous Anthrax. PA-specific IgG memory B cells could be detected in all 6 survivors of inhalation Anthrax and in only 2 out of 7 survivors of cutaneous Anthrax. This suggests that the degree of protection afforded by AVP/AVA vaccination would also differ depending on the type of Anthrax infection encountered.

1.4.2.4 Human Genetic Diversity

Genetic diversity in humans can cause significant differences in immune response from AVP/AVA vaccination and vaccine efficacy. Baillie and co-workers [143] reported that anti-PA antibody titres in human AVP vaccinees varied significantly and suggested that this may be

due to the genetic diversity of the human host. Further, a study found that despite having high anti-PA antibody titres in 200 AVA vaccinees, 43% of the samples lacked toxin neutralisation activity *in vitro* [16]. PA may not induce protective antibody immunity in some people due to immunodominant responses to non-protective PA epitopes [159].

Another study evaluated the immune response generated in 1000 AVA vaccinees and described that serum samples from African American individuals had lower toxin neutralising activity than European Americans samples [160]. Similarly, Marano *et al.* [161] also reported differences in immunogenicity in 1564 AVA vaccinees as a result of human racial diversity. There are a number of factors that could contribute to such variation, including different epitopes being presented by MHC molecules, differences in HLA haplotypes, cytokine or cytokine receptor gene polymorphisms or differences in cell surface molecules [160, 162, 163]. Given their known associations with ethnicity and with differential responses to vaccination, HLA haplotypes are prime candidates as potential genetic factors underpinning the stratification of human responses to Anthrax vaccines. Indeed, a significant association between HLA-DRB1-DQA1-DQB1 haplotypes and anti-PA Ab titres has already been demonstrated for European-Americans vaccinated with AVA in a GWAS study. Specifically, three distinct haplotypes were associated with lower titres, with the HLA-DRB1*15:01-DQA1*01:02-DQB1*06:02 haplotype having the highest statistical significance, and with the affect accentuated for homozygous carriers compared to heterozygous carriers [164].

1.4.3 Composition of AVA / AVP

The composition of AVA has not been published yet. However, studies indicate that AVA contains similar levels of PA and lower levels of LF, EF and certain surface proteins compared to AVP [4, 153, 160, 165-168].

The exact composition of AVP is unknown. Studies carried out by a group at the National Institute of Biological Standards and Controls (NIBSC) [1, 2] determined that AVP contains a complex mixture of at least 21 proteins from the *B. anthracis* proteome, including PA, LF and EF. The average PA and LF content in AVP supernatant is reported to be 3.71 and 0.99 µg/ml respectively, as determined by ELISA [18]. One of the main objectives of this project is to determine the composition of AVP using tandem mass spectrometry (LC-MS/MS) studies. An introduction to the technique is detailed in Section 1.5, the MS work carried out on AVP is described in Chapter 3. Potassium aluminium sulphate (alum) is used as an adjuvant in AVP. In order to characterise the proteins in AVP using LC-MS/MS methods, the proteins in AVP needed to be desorbed from alum. The development of a novel desorption method for proteins in AVP is described in Chapter 2.

1.4.4 Are other AVP proteins Immunogenic?

Although, PA is the main immunogen in both AVA and AVP, it is possible that other *B. anthracis* proteins could also play an important protective role against Anthrax. For instance, AVP is thought to contain more LF than AVA, based on antibody titres measured in sera from animal or human studies [3-5]. Many studies have highlighted the additional protective role of LF, either because it enhances the PA-specific antibody response [6, 8, 9], or via the independent protective role of anti-LF antibodies [3, 10, 11]. Ingram *et al.* [169] had reported that a strong, long-lasting $CD4^+$ T cell response to LF was measured in both AVP vaccinees and cutaneous Anthrax patients.

Another study reported that higher anti-LF antibody titres than anti-PA antibody were measured in two out of 4 AVP vaccinees [123]. Further, based on humoral immune response data from cutaneous Anthrax patients, Brenneman and co-workers [170] suggest that the anti-LF IgG antibody response is fast and lasts longer in comparison to the anti-PA IgG response.

These studies suggest that AVP contains significant amount of LF that could be playing an important role in protecting vaccinees against Anthrax.

Additionally, AVP is thought to contain minute amounts of EF, based on anti-EF antibody titres measured in AVP vaccinee sera [14, 153], whereas AVA does not contain any EF [154]. EF is also shown to protect from *B. anthracis* spore challenge in animal studies [12, 13], and that anti-EF antibodies can neutralise ET [14]. Other *B. anthracis* proteins such as cell wall proteins are also shown to trigger a protective immune response against Anthrax in mice [15]. Baillie and co-workers [142, 143] further suggested that other components of AVP such as bacterial cell wall proteins may also trigger an immune response. An *in vivo* study in mice [15] corroborated this and demonstrated that EA1 (S layer protein) in combination with PA might contribute to protection during the early stages of infection.

In this research, computational studies were carried out to predict MHC-binding (given that presentation by MHC molecules is a pre-requisite for a T cell response) for the most abundant proteins of AVP (as identified by LC-MS/MS studies – Chapter 3). The differences in peptide-MHC binding were investigated for common HLA alleles in several ethnic groups and multiple *B. anthracis* strains. Section 1.6 gives a brief introduction to computational methods. Computational work carried out in this project is detailed in Chapter 4.

1.5 Mass Spectrometry-based Proteomic Studies

This section describes the “Bottom-up” proteomics workflow that was used to characterise AVP in this project. See Figure 5 for a Shotgun Bottom-Up Proteomics workflow. Tandem Mass Spectrometry (LC-MS/MS) analysis performed on proteolytically-digested proteins for the characterisation of proteins is known as shotgun “Bottom-up” proteomics [171]. The available approaches for sample preparation, mass analysers and data acquisition methods and data processing are described here. In a typical shotgun bottom-up proteomics

experiment, the proteins are solubilised and digested with an enzyme to generate peptides. The peptides are then separated and fractionated usually by reverse phase (RP) chromatography and subjected to MS/MS analysis.

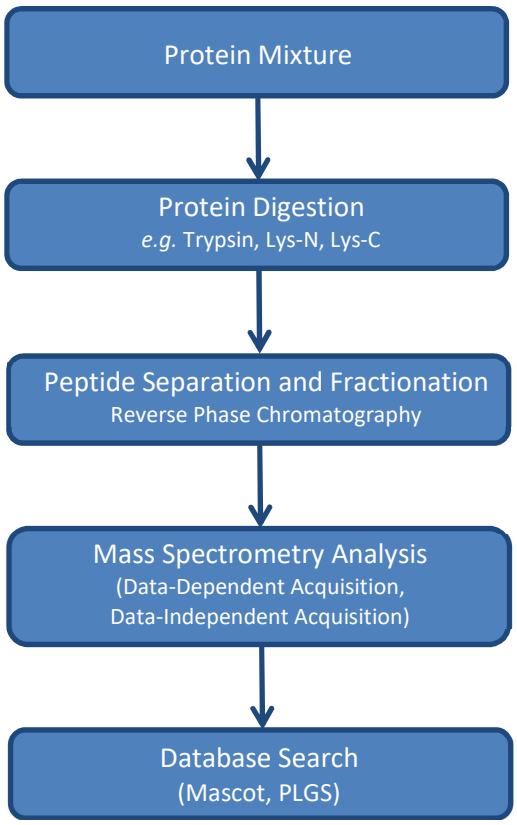

Figure 5 - Shotgun Bottom-Up Proteomics Workflow

1.5.1 Solubilisation and Proteolytic Digestion

For optimum proteolytic digestion efficiency, it is important that the protein is solubilised and unfolded for access to protease cleavage sites. Commonly-used solubilisation agents include organic solvents, surfactants and salts (*e.g.* acetonitrile [171-174], urea and SDS [171], custom-made surfactants such as ProteaseMax, Invitrosol, Rapigest, PPS Silent surfactant [171, 174], volatile surfactants such as Perfluorooctanoic acid and 1-butyl-3-methyl imidazolium tetrafluoroborate [171, 175]).

Common proteases used in bottom-up proteomics are detailed in Table 1. Each of the proteolytic enzymes has different cleavage specificity for cleaving at the amide or carboxyl bonds of protein residues by hydrolysis. Trypsin is the most widely-used proteolytic enzyme, often described as a “gold standard” [171].

Protease	Cleavage Specificity
Trypsin	Carboxyl side of Arg and Lys
Endoproteinase Lys-C	Carboxyl side of Lys
Chymotrypsin	Carboxyl side of Trp, Tyr and Phe; less specificity for Leu, Met and His
Elastase	Carboxyl side of Val or Ala
Endoproteinase Lys-N	Amine side of Lys
Endoproteinase Glu-C	Carboxyl side of Glu and Asp
Endoproteinase Arg-C	Carboxyl side of Arg
Endoproteinase Asp-N	Amine side of Asp and Cys

Table 1 - Common Proteases used for Bottom-Up Proteomics (Adapted from [171])

1.5.2 Mass Spectrometry

Mass spectrometry has now become a technique of choice for proteomic studies due to its high sensitivity, accuracy and throughput. In simple terms, a mass spectrometer is composed of an ion source, a mass analyser and a detector. The ion source ionises the sample, the mass analyser measures the mass-to-charge ratio (m/z) of ionised analytes in vacuum and the detector records the intensity of each m/z value ion. In this section, the components of the mass spectrometer that are relevant to this project are described. There are other ionisation

techniques or mass analysers available, however discussing those is beyond the scope of this project.

1.5.2.1 Electrospray Ionisation

ESI is known as a soft ionisation technique, as it is suitable for polar, thermally- unstable and least volatile samples [176]. This method can ionise a liquid sample, hence it is typically combined with reversed phase-liquid chromatography (RPLC) [171, 177, 178]. The sample is drawn up into a glass capillary (maintained at a high voltage), which aerosolises the sample. ESI is a soft ionisation process and does not generate fragmented ions. Further, ESI generates multiply-charged ions, which means that during peptide or protein analysis, the mass range can be optimal for data acquisition by commercial mass analysers [176, 179]. NanoESI is analogous to ESI, albeit at a lower flow rate (20-50 nL/min) [180, 181]. This means that lower sample concentration (nmol/mL) and volume are required, resulting in less interference from salt contaminants [180-182]. The nanoESI generates tiny droplets, allowing aerosolisation of samples without applying high heat or sheath gas [181].

1.5.2.2 Mass Analysers

The mass analyser generates accurate ion mass spectra data by separating ions based on their mass-to-charge ratio (m/z). Commonly used Mass Analysers for Proteomics work include linear ion trap, orbitrap, fourier transform ion cyclotron resonance, quadrupole and time of flight [183] [171, 178]. These mass analysers derive and measure peptide masses using different mechanisms, hence selecting a mass analyser is a trade-off between sensitivity, accuracy and speed depending upon the application [171, 178]. This section focuses exclusively on quadrupole and time-of-flight mass analysers only, as these are used in this work.

1. Quadrupole

Quadrupole mass analysers are popular for proteomics work, as they are operationally simple, relatively inexpensive and can perform both quantitative and qualitative mass analysis. A quadrupole mass analyser comprises of four parallel electrodes (cylindrical metal rods with a hyperboloidal interior surface) positioned at the same distance from the central axis, inside a vacuum chamber [176, 179]. See Figure 6 for a diagram of quadrupole mass analyser. These operate at relatively low vacuum levels compared to other mass analysers, enabling easy interface with an LC system [176].

A quadrupole mass analyser has a high scan speed (6000 amu/sec), which enables a mass measurement range of up to 2000 m/z. This allows mass measurement in a practical range generating qualitative data. Furthermore, it can switch between high-speed scans, generating high-sensitivity quantitative data on multiple ions, known as selected ion monitoring [176].

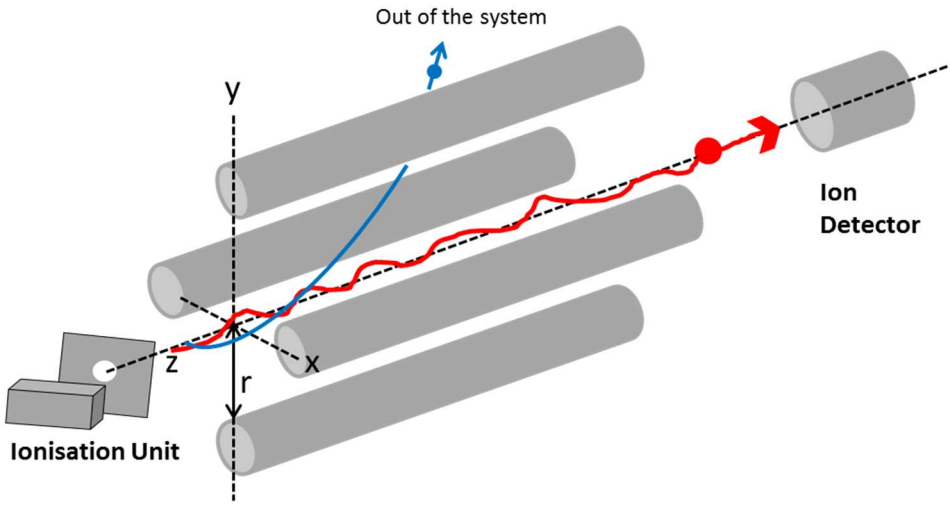

Figure 6 - Diagram of a Quadrupole mass analyser (Adapted from [176]). Ions enter the quadrupole through a small orifice (in z direction) under low applied voltage. An alternating direct and high frequency current voltage is applied to each electrode, oscillating ions in the x and y direction. Certain ions of a specific m/z attain stable oscillation under specific voltage conditions, enabling them to exit the quadrupole and reach the detector. Oscillations of other ions become unstable and collide with the electrodes and not be detected [176].

2. Time of Flight

A ToF analyser consists of an accelerator contained within a strong vacuum (See Figure 7 for a diagram of ToF). ToF can measure ions of any mass range. However, as a result linear ToF suffers from low resolution, as ions with similar m/z can have similar flight times. Reflectrons are used to improve resolution, by correcting initial kinetic energy dispersion and ToF difference by increasing the ion path length of the ion. Essentially, the higher velocity ions would travel into the reflectron more deeply and thus take longer to reverse under a decreasing electric field (See Figure 8).

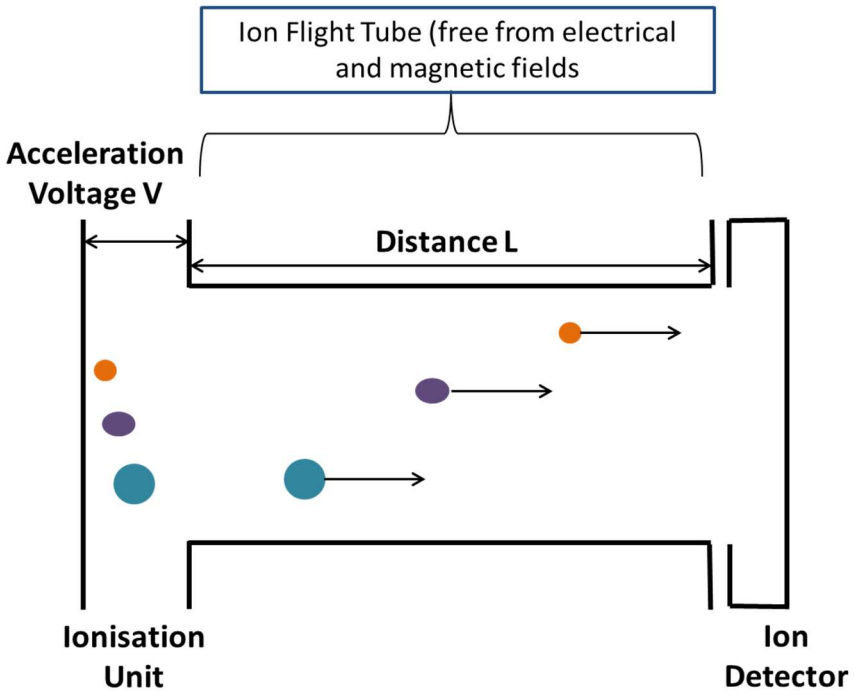

Figure 7 – Diagram of a ToF mass analyser (Adapted from [176]). It extracts ions from the ion source in pulses or intermittently, and measures the time required by the ions to travel from the ion source to the detector (m/z ratio).

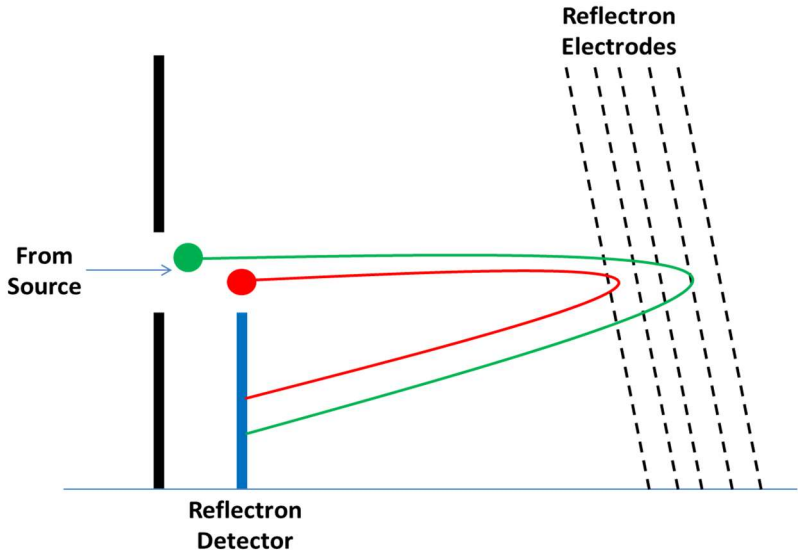

Figure 8 - Schematic of a Reflectron in a ToF (Adapted from [184]). Two ions of the same m/z ratio but different initial kinetic energies are depicted in red and green colour. Consequently, the green ion has a longer path length than the red ion.

1.5.3 Tandem Mass Spectrometry (MS/MS)

Different mass analysers are combined to allow mass analysis of LC separated peptides (MS1) and their fragments (MS2) [185]. This is known as tandem mass spectrometry (MS/MS).

1.5.4 Peptide Fragmentation

The two most popular peptide fragmentation methods are collision induced dissociation (CID) [82] [171] and electron capture dissociation (ECD) [186] or electron transfer dissociation (ETD) [187]. This section focuses on CID only, as this was the peptide fragmentation method used in this work.

Collision Induced Dissociation

CID involves the acceleration of molecular ions in gas phase to high kinetic energy in vacuum using electric potential to collide with neutral molecules (*e.g.* helium, nitrogen or argon). During the collision, some of the ion's kinetic energy is internalised, resulting in peptide bond cleavage and fragmentation of molecular ions into fragments. The fragmentation pathways mostly rely on proton transfer [171]. Fragmentation pathways can now be predicted (Figure 9 details the fragmentation ion nomenclature).

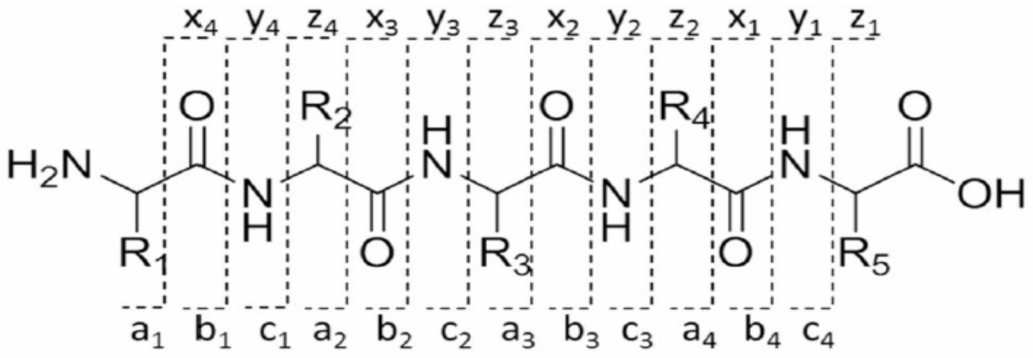

Figure 9 – Fragmentation Ion Nomenclature for Peptides [171]

In a beam-type CID on a quadrupole mass analyser, both precursor ion and fragmented ions are activated and dissociated, resulting in further dissociation of relatively unstable b ions into y-type ion fragments [171].

1.5.5 Data Acquisition

1.5.5.1 Data-Dependent Acquisition (DDA)

Data-dependent acquisition is the traditional method of data acquisition. It involves identification and fragmentation of the high-intensity precursor ions with specific m/z values. This process is repeated until all of the high-intensity ions have been sampled. The frequency of ion scans and fragmentation can be adjusted, based on signal-to-noise threshold. Figure 10 shows a schematic of DDA.

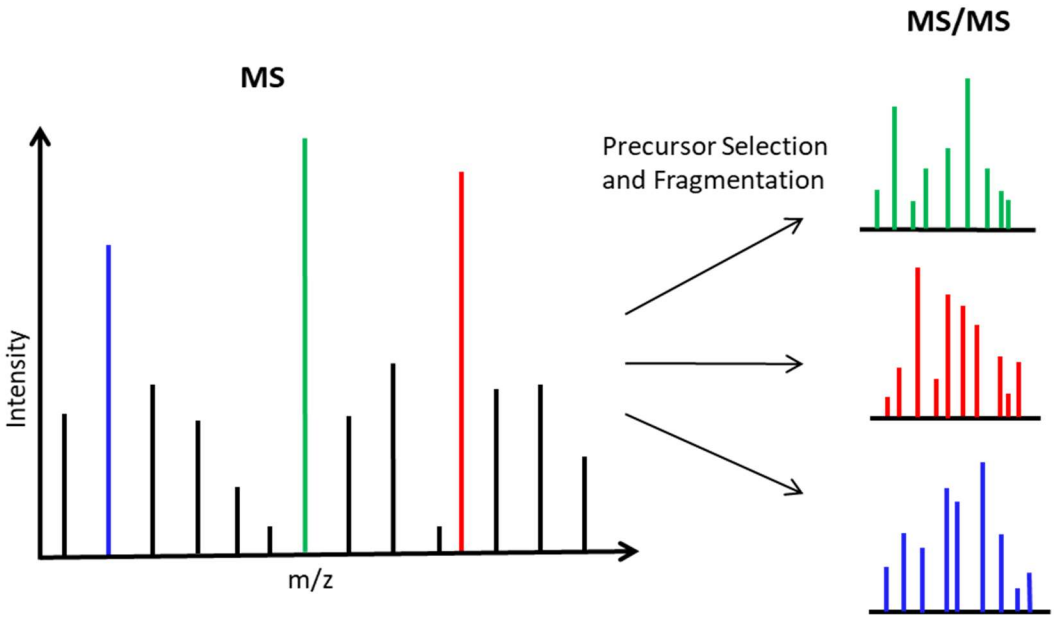

Figure 10 – Schematic of Data Dependent Acquisition (Adapted from [188]) MS scan selects the 3 most abundant precursor ions (blue, green and red), subsequent fragmentation generates MS/MS scans of each ion.

Obviously, DDA creates a bias, where only most abundant proteins in the sample are identified. Reproducibility of low-abundance peptide quantification is challenging with DDA [189]. Further, repeatability in peptide identification decreases due to variability of LC and MS time alignment between replicate runs, along with inherent variability from ionisation method (*e.g.* ESI) [190].

1.5.5.2 Data Independent Acquisition (DIA)

In DIA analysis, all peptides within a certain m/z window and retention-time range are fragmented at the same time. This process is repeated until all of the m/z windows and retention-time ranges are covered. This allows unbiased peptide identification and accurate quantification of all abundances [191].

Different DIA approaches with different instrument types, duty cycles and precursor selection ranges have been described in the literature previously. Silva *et al.,* [192] have described the MS^E approach, which involves the fragmentation of all precursor ions and simultaneous acquisition of MS and MS/MS data at high and low collision energy. The precursor ion and fragment ions are then matched up by either retention time and/or mass difference. Figure 11 shows a schematic of the DIA-based MS^E approach. The MS^E approach was shown to be more reproducible than the traditional DDA acquisition on MS/MS [193].

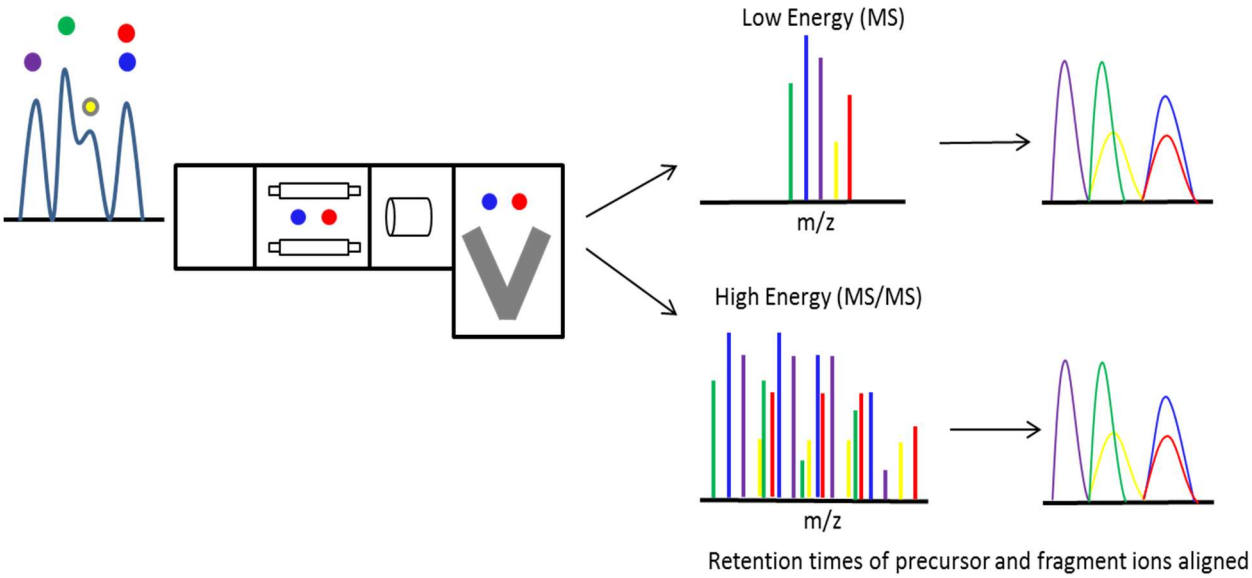

Figure 11 – Schematic of Data Independent Acquisition based MS^E approach (Adapted from [194, 195]). The peptides are separated on reversed phase column, then ionised before entering triple quadrupole mass analyser. Precursor ions are fragmented, and MS and MS/MS data is acquired at high and low collision energy, simultaneously. The precursor ion and fragment ions are then matched up by either retention time and/or mass defect.

Similarly, Panchaud *et al.,* [196] have described the PAcIFIC approach, which involves fragmentation of precursors within a small m/z window of 2.5 m/z, where precursor selection is independent of ion count. PAcIFIC was shown to perform more efficiently than traditional DDA acquisition and identified hundreds of proteins across 8 orders of magnitude. The main difficulty with DIA analysis is that the resulting MS/MS spectra can be very complex [189], which increases the time required for data analysis, or else the DIA comprises a larger precursor selection window [191]. Recently, Aebersold and co-workers have described a DIA-based SWATH approach, which is a targeted data extraction method [197], combined with software that facilitates automation (OpenSWATH) [191]. The SWATH method involves the selection and fragmentation of sequential 25 m/z ion windows across a 400-1200 m/z range and the generation of high resolution and accurate mass data. Peptide identification is done

by matching fragment ion data with a spectral library containing prior information based on representative sample analysis. Further, OpenSWATH facilitates automated retention time alignment, chromatogram extraction, peak group scoring and statistical estimation of false discovery rate [191].

1.5.6 Peptide Identification

Peptide identification is performed by matching the measured mass of peptides from MS/MS data with a protein library [185]. A theoretical protein sequence library based on relevant genomic data is supplemented with enzyme cleavage sites and the prediction of fragmentation ions. Search engine tools have been developed to search and analyse mass spectrometry data. The most popular tools include Sequest [198], Mascot [199], Andromeda [200], ProteinLynx Global Server [201] [201], OMSSA [202], X!tandem [203] and CRUX [204]. Several statistical algorithms have been developed to determine the false discovery rate (FDR) for a particular dataset, and thus limit the number of false identifications [205-207]. The most popular approach for determining FDR is to create a target decoy database [185, 208, 209], which combines both a target sequence database and a decoy database. A decoy database is created by either reversing or scrambling the protein sequences from the target database. It is assumed that the sequences in these databases will not overlap and if they do the FDR rate will be very high.

1.5.7 Label-Free Quantitation

There are several approaches to label-free quantification of proteins by LC-MS/MS. One of the most popular methods for relative quantification of proteins is spectral counting, which involves counting the number of times a peptide mass spectrum is measured [185]. Several studies have described other approaches for the relative quantification of proteins [192, 210-213].

More recently, label-free absolute quantification methods have been described. One of the most popular approaches is the incorporation of a standard of known concentration, creating a calibration curve and extrapolating the protein concentration [193, 214, 215]. Additionally, peptide peak intensity predictions can be made and these can help deduce absolute protein concentration [216]. Schwanhausser *et al.,* [217] have described "iBAQ" for absolute quantification of proteins, which is an extension of the spectral counting method. This method involves dividing the number of theoretically observable peptides from the sum of peak intensities of all peptides from a specific protein for inferring proxy absolute protein concentration.

Silva *et al.,* [193] describe a method for the absolute quantification of proteins by LCMS^{E}, known as the Hi3 method. This method calculates the average MS signal for the three most intense peptides of each protein and the internal standard. A universal signal response factor is calculated from the average MS signal of the internal standard (counts/mol of protein). The absolute protein concentration is derived by dividing the universal signal response factor from the average MS signal for the three most intense peptides for that protein.

1.6 Computational Studies

As described previously in Section 1.4.2, the assessment of Anthrax vaccine efficacy is complex. Firstly, owing to the nature of the organism, studies in humans is not possible. Owing to genetic differences between humans and animals, animal models cannot give us reliable insights into the human immune response from vaccination and its efficacy. Secondly, the genetic diversity of humans has been reported to cause significant variation in immune response from AVP / AVA. Even though high anti-PA antibody titres are measured in AVA vaccinees, TNA levels are low in some individuals and this raises questions about the efficacy of the vaccine. Previously, studies have focused on certain alleles for experimental feasibility [146, 169, 218, 219]. It is important that many alleles that represent the diverse human

population are studied so that the potential differences in human ethnicities/populations can be investigated. This would not be feasible experimentally.

Thirdly, there has never been a systematic study to investigate the efficacy of AVP in humans against different *B. anthracis* strains. For these reasons, in this project we have taken a computational approach. Computational tools that have been developed using large sets of experimental binding data have afforded the opportunity to gain insights into AVP protein-specific $CD4^+$ and $CD8^+$ T cell responses by human hosts. These tools enabled us to investigate peptide-MHC binding affinities (peptide-MHC binding is a pre-requisite for a T cell response to develop) for multiple antigens in AVP across common HLA alleles. Further, the immunogenicity of PA, LF and EF proteins from AVP in humans was also investigated across several *B. anthracis* strains.

The likelihood that a given T cell epitope will emerge as an important contributor to the host immune response is partly dependent on the specificity and affinity of the complex between (on the one hand) the relevant peptide bound to an MHC molecule and (on the other hand) a T cell receptor (TCR) T cell [220]. T cells are known to be antigen specific, which allows them to distinguish between self and non-self-peptides [220, 221]. However, it is worth noting that T cells are also cross-reactive, having the ability to recognise multiple peptide-MHC complexes; the diversity of presented antigenic peptides is much larger than T cell TCR repertoire diversity [220, 222, 223]. Although there are multiple steps on antigen presentation-recognition pathways (including enzymatic cleavage of a given peptide from its parent antigen, and transportation), peptide-MHC binding is arguably the most crucial step in T cell response [220, 224]. However, the likelihood and quality of the overall T cell response is dependent on many additional factors such as: the abundance of MHC-bound peptides; TCR recognition, specificity and abundance; T cell phenotypes and the presence of secondary co-stimulatory signals [139, 225-229]; and the genetic diversity associated with an individual's HLA haplotype

and the germline genes that encode their T cell receptors (TCRs) and B cell receptors (BCRs) [139].

1.6.1 *In silico* HLA II epitope prediction

HLA II molecules are highly polymorphic, with thousands of known alleles belonging to each of the HLA genes HLA-A, HLA-B, HLA-C, HLA-DRB, HLA-DQB1 and HLA-DPB1 [230]. HLA II cleft is formed by two protein chains (α and β chain), encoded in one of the three loci – HLA-DR, -DQ or -DP located in the peptide-carrying region [220, 231]. Both clefts have binding pockets conforming primary and secondary anchor positions on the binding peptide. Thus, HLA II binding cleft is open-ended, allowing longer length peptides to bind [224].

It has been observed that HLA-DR binding peptides are commonly 12 amino acids long [139, 232], although longer peptides are commonplace (up to around 30 residues) with MHC class II, owing to the open groove [233, 234]. In nearly all cases, the peptide binding core (comprising the residues within the MHC groove) consists of 9 amino acid residues [220], with residues outside the core contributing to binding strength and affinity [220, 232, 235]. Of the several thousand known HLA-DR alleles, 8 representative alleles encompass the genetic backgrounds of most human populations globally [139, 236]. HLA-DP and HLA-DQ alleles are less well characterised [139, 237]. It is suggested that some peptides can bind to several alleles, either by sharing common anchors across different alleles or by sharing common allele-specific anchors and overlapping binding cores [220].

Considerable efforts have been dedicated to developing MHC class II epitope prediction computational methods using machine learning methods, software algorithms and data transformation [139]. Two pan-specific methods are available that make interpolated predictions for those HLA types for which insufficient binding data is available to train a

conventional predictor, namely TEPITOPEpan [238] and NetMHCIIpan [220]. Prediction of class II binding is more challenging than class I, and hence typically less accurate; owing to the open ends of the MHC class II groove, it is necessary to predict the register of peptide binding as well as the strength. Nevertheless, based on assessments by Andreatta and co-workers [220, 239], the predictions made by recent incarnations of NetMHCIIpan are reasonably accurate (*e.g.* AUC values for DRB1*01:01, DRB1*07:01, DRB1*15:01 HLA-DQA1*01:02-DQB1*06:02 are 0.830, 0.857, 0.831 and 0.887 respectively [239]); whereas individual predictions may be erroneous, the overall picture provided by a large-scale computational project is likely to be substantially correct. The predictive performance of the method is measured using the area under the receiver operating characteristics curve (AUC), AUC = 1 meaning perfect prediction.

1.6.2 *In silico* HLA I epitope prediction

The highly polymorphic nature of MHC I molecules contributes to different position, number and physiochemical properties of the binding pockets within the MHC groove. Hence different sets of peptides bind to different MHC molecules. HLA I cleft is formed by a single protein chain (α-chain) and is closed at both ends, which typically restricts the peptide length to 8-11 amino acids, although longer peptides are possible [224, 240]. Recent studies have confirmed that the most abundant length of peptide binding to most MHC class I molecules consist of 9 residues [241], although certain allelic variants are known to have a strong preference for other peptide length (*e.g.* HLA-B*18:01 has a preference for a peptide length of 8 amino acids [242], whereas HLA-B*44:03 has a preference for 10 or 11 amino acids [243]) [240].

MHC I molecules have distinct preference for specific amino acid types within each binding pocket; these are known as the anchor residues of the peptide. In MHC class I, the canonical binding pocket positions are 2 and 9 (numbered with respect to the 9 residue locations within

the binding core) [244]. The preference at these positions vary between alleles, for example: HLA-A*02:01 is associated with a preference for Leucine and either Valine or Isoleucine at positions 2 and 9 respectively [245]; HLA-B*08:01 is associated with a preference for positively charged amino acids at position 5; and HLA-A*01:01 is associated with a preference for Aspartic Acid at position 3 [246]. Structural limitations or interactions within the peptide may also contribute to presentation and ultimately recognition of the peptide-HLA complex [247].

Many computational tools have been developed to predict the epitopes binding to MHC I molecules, based on different approaches including similarity matrices [248], linear regression [249], and artificial neural networks [250-252]. NetMHCpan is available for molecules that have inadequate binding data [253]. Several studies [240, 254, 255] have shown NetMHCpan to be the most reliable tool for predicting MHC I epitopes.

2.0 DESORPTION METHOD

2.1 Introduction

Aluminium-containing adjuvants are used to enhance the immune response and increase vaccine stability [256-260]. Potassium aluminium sulphate (alum) is used as an adjuvant in Anthrax Vaccine Precipitated (AVP). The chemical name of alum is potassium aluminium sulphate; however aluminium hydroxide and aluminium phosphate are often incorrectly termed alum [261]. During the final steps of the AVP manufacturing process, the proteins in the sterile CF are precipitated under gravity by adding sterile 10% w/v aluminium potassium sulphate solution. The pH is adjusted to 5.9-6.2 by adding hydrochloric acid. The supernatant is removed such that the bulk vaccine precipitate is 15x concentrated. The bulk vaccine concentrate is diluted with sterile saline to achieve 5x concentrated product [18]. See Figure 12 for a flow chart of AVP manufacture from CF.

In order to characterise the proteins in AVP, they need to be released or desorbed from alum precipitate. This chapter describes an investigation into finding a suitable desorption method for AVP proteins. The adsorption and desorption of proteins from aluminium adjuvants depend on several interactions between proteins and alum, including electrostatic forces, hydrophobic interactions, hydrogen bonding, van der Waals forces, ligand exchange, pH, temperature, ionic strength, etc. [260-266]. Historically, sodium hydroxide is used to desorb proteins from alum (sodium hydroxide dissolves aluminium, thereby releasing the proteins); however, this approach was considered potentially inappropriate on the grounds that the proteins may be degraded. Hence, other mild conditions using salts and surfactants were investigated for desorbing protein from the adjuvant in AVP. Commonly used salts for desorption include sodium citrate, ammonium sulphate, sodium phosphate, etc. Surfactants such as Triton X-100, lauryl maltoside and cetylpyridinium chloride (CPC), may also be used for desorption [259, 260, 263, 267]. Some of these reagents were investigated for efficiency and robustness.

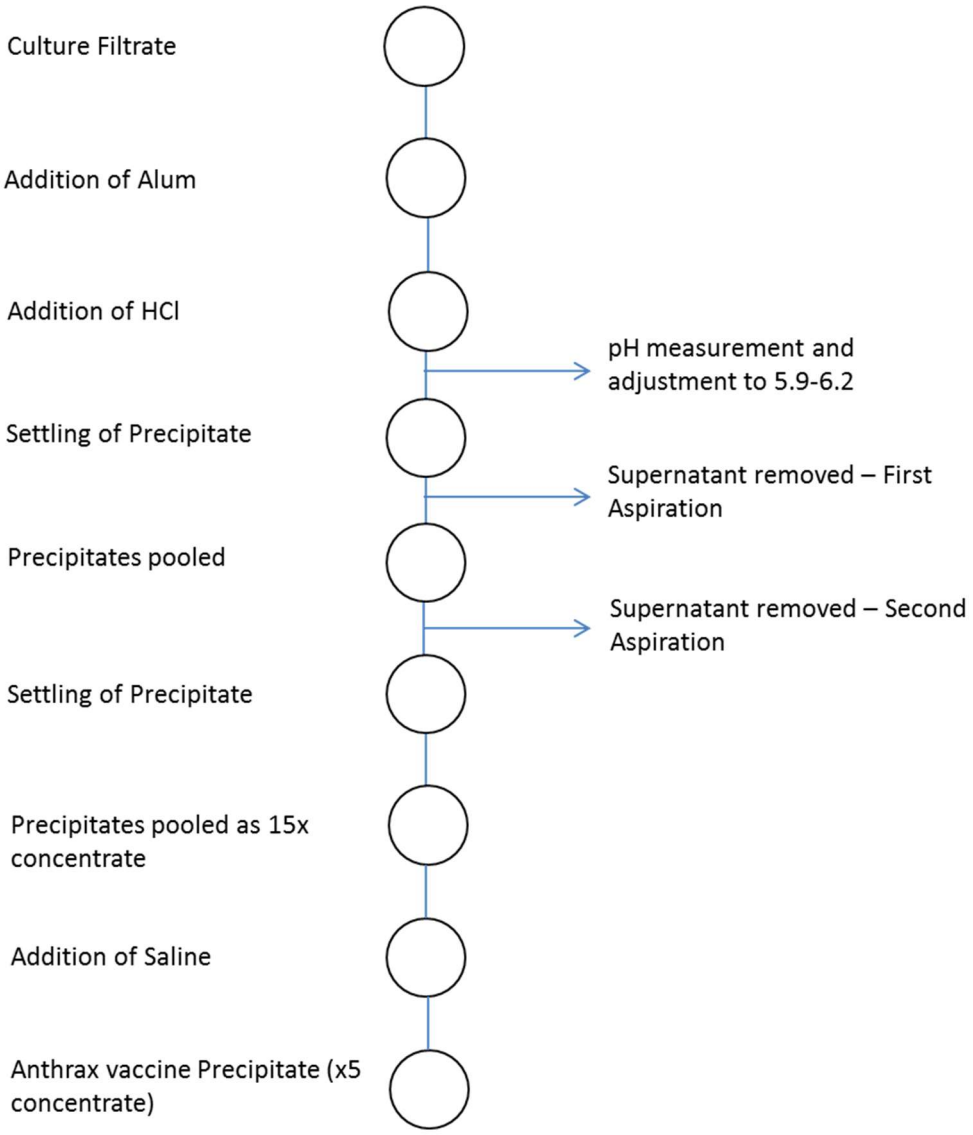

Figure 12 - Process flow chart describing the process of AVP manufacture from CF

2.2 Materials and Methods

AVP was obtained from Porton Biopharma Ltd. Sodium hydroxide (NaOH), sodium citrate, succinic acid, sodium phosphate dibasic, guanidine hydrochloride, urea, ammonium sulphate, cetylpyridinium chloride (CPC) and ethylenediaminetetraacetic acid (EDTA) were purchased from Sigma Aldrich. RapiGest™ SF surfactant was purchased from Waters (Cat No: 186001860) and ProteaseMAX™ surfactant was purchased from Promega (Cat No: V2072).

Regenerated cellulose centrifugal concentrators were purchased from Millipore (Amicon Ultra-0.5 Centrifugal Filter Unit, Cat No. UFC500308). Polyethersulfone (PES) membrane centrifugal concentrators were purchased from VWR (Vivaspin 500 3000 MW, Cat No. 512-2838). Protein estimation Micro BCA kit was purchased from ThermoFisher (Cat No: 23235). MES running buffer, 4-12% bis-tris gels, and Coomassie stain were purchased from Invitrogen.

The following nine desorption methods were assessed; each procedure was performed on 1 vial of AVP (~620 µL).

1. 5µL of sodium hydroxide was added. The solution was vortexed for 30 seconds until it turned clear. In order to neutralise the solution, 10µL of 3M sodium citrate was added immediately.
2. 500µL of 250mM succinic acid, pH 3.5 was added and incubated for 30 min at room temperature with shaking at 40 rpm [259].
3. 500µL of 0.66M sodium phosphate dibasic, 3mM EDTA, pH 7.0 was added and incubated for 3 hours at room temperature, with shaking at 40 rpm [267].
4. 1mg of RapiGest™ SF surfactant was dissolved in AVP and incubated at 37°C for 24 hours.
5. 1mg of ProteaseMAX™ surfactant was dissolved in AVP and incubated at 37°C for 24 hours.
6. 500µL of 4M guanidine hydrochloride, pH 7.0 was added and incubated for 24 hours at room temperature, with shaking at 40 rpm.
7. B500µL of 8M urea, pH 7.0 was added and incubated for 24 hours at room temperature, with shaking at 40 rpm.
8. 500µL of 1M ammonium sulphate, 27mM CPC, pH 7.0 was added and incubated for 24 hours at room temperature, with shaking at 40 rpm [260].

9. 500µL of 0.66M sodium phosphate dibasic, 3mM EDTA, pH 7.0 and 1mg of RapiGest™ SF surfactant was added and incubated for 3 hours at room temperature, with shaking at 40 rpm [267].

After the desorption process was completed, each solution was centrifuged at 14,000xg for 2 min. The supernatants were transferred into regenerated cellulose centrifugal filter units and concentrated to ~100 µL by centrifuging at 14,000xg. The solutions were buffer exchanged into phosphate buffer saline (PBS - 100 mM Sodium Phosphate and 150 mM NaCl, pH 7.2) 5 times, by adding 400µL of PBS each time. The final volume of each sample was ~100µL. The protein concentration of each sample was determined by Micro BCA kit using the manufacturer's recommended procedure. Desorbed proteins were analysed by 1D gel electrophoresis. The samples for 1D gel electrophoresis were treated as follows: 10 µL of 4x LDS was added to 30µL of sample and incubated at 70°C for 10 min. 20µL of each sample was loaded on 4-12% bis-tris gel and run for 45 minutes at 200V using MES running buffer. The gel was stained using Coomassie blue stain.

Further, regenerated cellulose and PES membrane centrifugal concentrators were compared for protein recovery. The PES filter membrane was cleaned with water prior to use according to the manufacturer's recommendation.

Finally, the protein concentration and protein profile of CF, supernatant and AVP were determined. This work was carried out on two batches of AVP.

Amino acid analysis was also performed on AVP after desorption to find the protein concentration of desorbed proteins, and the proteins bound to alum after desorption. After desorption the solution was centrifuged at 14,000xg for 5 min. The supernatant (collected in a separate Eppendorf tube) and the pellet were sent to Alta BioSciences for amino acid analysis.

2.3 Results and Discussion

2.3.1 Screening of Desorption Methods

As described above, several different salts and surfactants were investigated for desorption of AVP proteins from alum. Figure 13 shows the size-based separation of desorbed AVP proteins on 1D gel electrophoresis, using nine different desorption methods. The desorption methods with NaOH (Lane 3), EDTA (Lane 5), ammonium sulphate and CPC (Lane 11), and a combination of RapiGest™ SF surfactant and EDTA (Lane 12) gave good recovery of desorbed proteins (Figure 13). The measured protein concentration of recovered proteins from desorption methods with NaOH, EDTA, ammonium sulphate plus CPC and RapiGest™ SF surfactant plus EDTA was 27.1, 18.6, 11.6 and 18.1 µg/mL using a Micro BCA assay, respectively. The desorption methods with succinic acid (Lane 4), RapiGest™ SF surfactant (Lane 6), ProteaseMAX™ surfactant (Lane 7), guanidine hydrochloride (Lane 8) and urea (Lane 10) did not desorb AVP proteins from alum (Figure 13). This correlated with the Micro BCA assay results.

Although the maximum desorption of proteins from alum in AVP was using the NaOH method, the higher molecular weight bands on the corresponding 1D gel (Lane 3, Figure 13) were faint in comparison to other methods, confirming that the harsh condition associated with NaOH degrades proteins. Hence, this method was not taken forward. The EDTA desorption reagent (Lane 5, Figure 13) gave good recovery of proteins. The desorption mechanism of EDTA is probably due to chelation of aluminium ions, thus enabling release of proteins from alum. The ammonium sulphate and CPC method (Lane 11, Figure 13) produced a pellet in the sample after the desorption process, hence this method was also not taken forward. The combination of RapiGest™ SF surfactant and EDTA (Lane 12, Figure 13) did not enhance the recovery of proteins in comparison to EDTA alone.

Thus, 0.66M Sodium Phosphate Dibasic, 3mM EDTA, pH 7.0 was found to be the most suitable reagent for protein desorption. This mixture was further optimised, which is discussed in the section below.

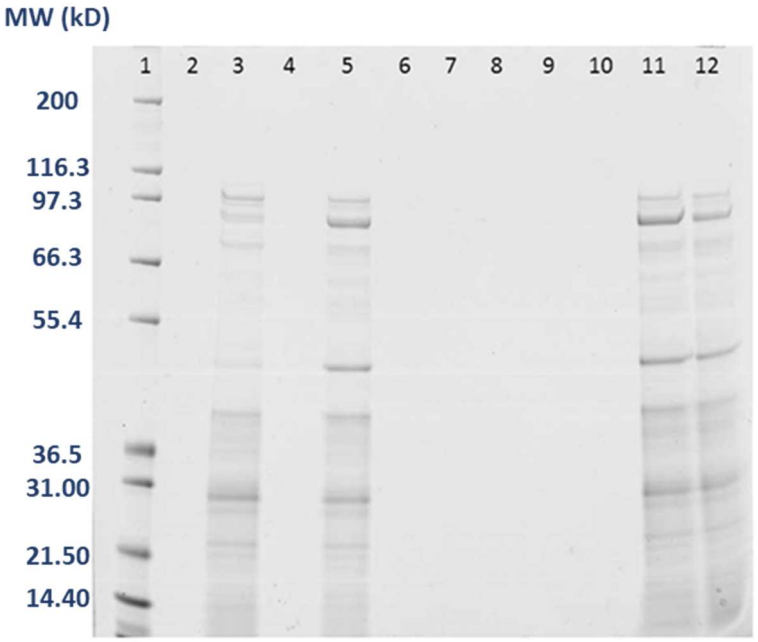

Figure 13 - Comparison of Desorption methods - size based separation of desorbed AVP proteins on 1D gel electrophoresis. Lane 1 – Molecular Weight Std; Lane 2 – Blank; Lane 3 – Sodium Hydroxide and Sodium Citrate method, Sodium Citrate method; Lane 4 – Succinic Acid method; Lane 5 – Sodium phosphate dibasic, EDTA method; Lane 6 – RapiGest™ SF surfactant method; Lane 7 – ProteaseMAX™ surfactant method; Lane 8 – Guanidine hydrochloride method; Lane 9 – Blank, Lane 10 – Urea method, Lane 11 – Ammonium sulphate, CPC method; Lane 12 – RapiGest™ SF surfactant, EDTA method.

2.3.2 Optimum EDTA Concentration and pH range

Further work was carried out to investigate the optimum conditions of EDTA concentration (1-5mM) and pH range (5-9). Table 2 details the concentration of desorbed AVP proteins with various amounts of EDTA reagent. Figure 14A and 14B shows the size-based separation of desorbed AVP proteins on 1D gel electrophoresis from pH and EDTA concentration screening. All investigated EDTA concentrations were found to be effective; hence the least amount of EDTA (1mM) was found to be optimum to enable easy removal of EDTA from the final sample. The recovery of proteins was acceptable at pH 7, 8 and 9; whilst the recovery was low at pH 5 and 6. Hence, the pH of 7.0 was chosen as a convenient pH that also allowed efficient onward processing of the samples.

EDTA and pH reagent conditions		**Average desorbed Protein Conc. (µg/ml)**
EDTA Conc. (mM)	**pH**	
3	5.0	11.6
3	6.0	14.5
3	7.0	18.7
3	8.0	17.2
3	9.0	17.2
1	7.0	18.7
2	7.0	18.9
3	7.0	17.4
4	7.0	19.2
5	7.0	17.4

Table 2 – Investigation into optimum conditions for EDTA desorption reagent – Based on desorbed AVP protein concentration determined using Micro BCA assay.

Figure - 14A

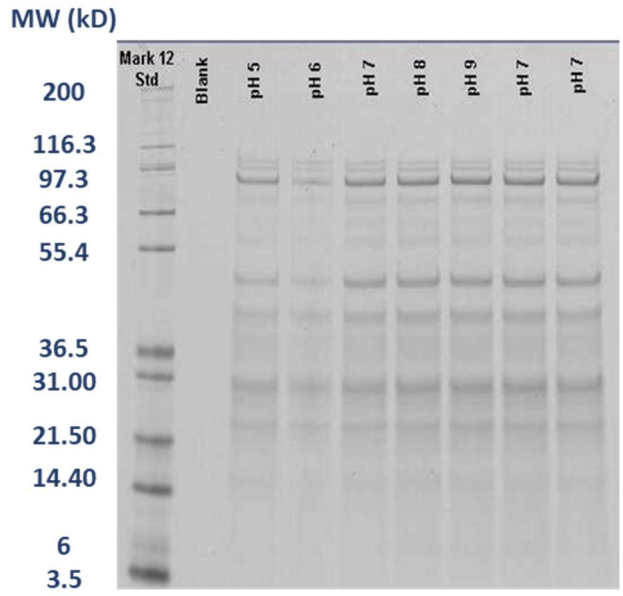

Figure - 14B

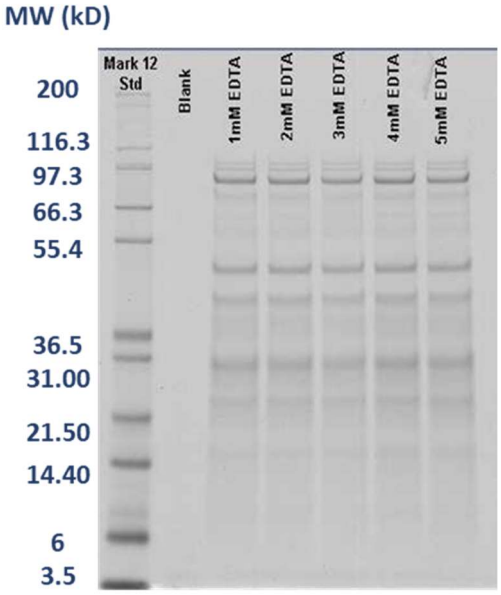

Figure 14 - Investigation into optimum conditions for EDTA desorption reagent - Size based separation of desorbed AVP proteins on 1D gel electrophoresis; 14A - Comparison of protein recovery from 0.66M Sodium Phosphate Dibasic, 3mM EDTA pHs 5-9 desorption; 14B - Comparison of protein recovery from 0.66M Sodium Phosphate Dibasic, 1-5mM EDTA, pH 7.0 desorption.

2.3.3 Comparison of Centrifugal Membrane Filters

The recovery of proteins was found to be similar using both cellulose and PES membrane filters. The process time for the desorption method using a PES membrane filter was much longer than the regenerated cellulose membrane (data not shown here). Hence, the regenerated cellulose membrane centrifugal filter was found to be optimum for the concentration and buffer exchange process during desorption.

2.3.4 Efficiency and Robustness of Desorption Method

Finally, the protein concentration and protein profile of CF, supernatant and AVP were determined. Thus, the amount of protein being adsorbed onto alum precipitate, the amount of protein being removed in supernatant, and the amount of protein being desorbed from alum precipitate using the 0.66M Sodium Phosphate Dibasic, 3mM EDTA, pH 7.0 reagent were ascertained. Table 3 shows the total protein recovered in CF, supernatant and desorbed AVP proteins from two AVP batches after desorption with 0.66M Sodium Phosphate Dibasic, 3mM EDTA, pH 7.0 reagent, determined using Micro BCA assay. Note that the final protein concentration (µg/ml) has been reported based on the total volume of each batch of CF, supernatant and AVP. Figure 15 shows the size-based separation of proteins in CF, supernatant and desorbed AVP proteins from the two AVP batches.

Samples	**Measured Protein Conc. (µg/ml)**
CF Batch 1	6.3
CF Batch 2	11.3
Supernatant Batch 1	1.6
Supernatant Batch 2	1.8
AVP Batch 1	14.3
AVP Batch 2	19.8

Table 3 – Average Protein concentration of CF, Supernatant and AVP after desorption with 0.66M Sodium Phosphate Dibasic, 3mM EDTA, pH 7.0 reagent – determined using Micro BCA assay.

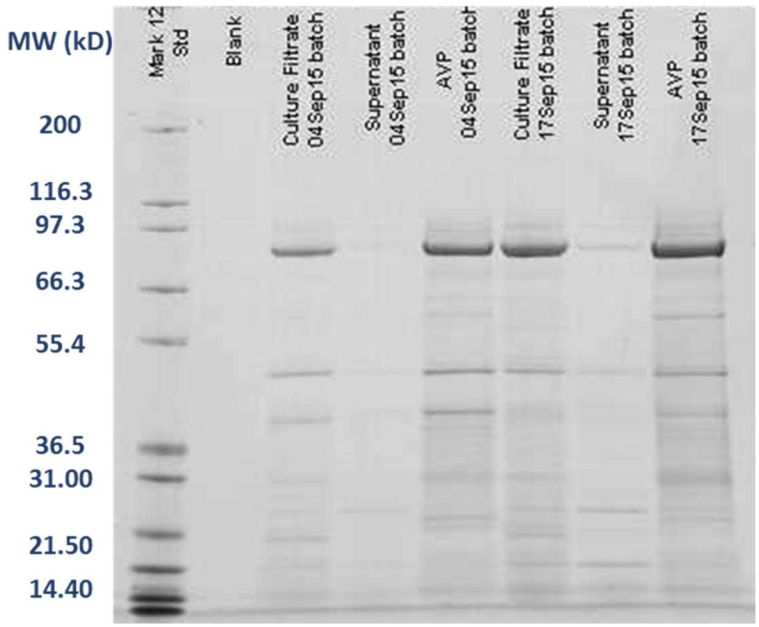

Figure 15 - Size based separation of proteins in CF, Supernatant and Desorbed AVP proteins from two batches of AVP (Batch 1 (04Sep15) and 2 (17Sep15)) on 1D gel electrophoresis.

Both protein estimation and SDS-PAGE profile show that the supernatant has some proteins present, suggesting that there is loss of CF proteins during the alum precipitation step during AVP manufacturing (Table 3, Lanes 4 and 7 in Figure 15). The final concentration of AVP is different to the CF concentration (despite the loss of protein in the supernatant). This suggested that the EDTA-based desorption method desorbs 40-60% of the proteins from alum in AVP (assuming that all the proteins from CF have been adsorbed onto alum precipitate).

Amino acid analysis was performed on desorbed AVP proteins (desorbed using 0.66M Sodium Phosphate Dibasic, 3mM EDTA, pH 7.0 reagent) and pellet. However, owing to interference from alum and excess amino acids (which are added in the media during the manufacture of AVP), the amino acid analysis was not successful.

The recovery of proteins from AVP using the down-selected EDTA-based desorption method was low. The low recovery of proteins from AVP is corroborated by similar findings by other groups investigating desorption of proteins from the closely-related adjuvant Alhydrogel® (Brenntag Biosector, Denmark) (aluminium hydroxide). Alhydrogel adjuvants are more widely used; hence several studies have reported the stability profile of alhydrogel based vaccines. Vassely *et al.,* [259] have reported that due to chemical and physical changes in proteins adsorbed to alhydrogel, the desorption of proteins from alhydrogel is difficult. Another study has shown that the strength of the protein bound to alhydrogel increases with time, and harsh desorption buffer conditions are required to recover proteins [260]. This study also highlights the difficulty of analysing alum-adsorbed vaccines.

2.4 Conclusion

Amongst all the desorption reagents and experimental conditions assessed, 0.66M Sodium Phosphate Dibasic, 1mM EDTA, pH 7.0 was found to be the best choice for desorbing protein from alum in AVP. This method was taken forward for desorbing proteins in subsequent proteomic studies.

3.0 PROTEOMICS STUDIES

3.1 Aims and Objectives

The exact composition of AVP is not known. The main objective of this study is to identify and quantify proteins in AVP. Highly sensitive Mass Spectrometry (MS) based proteomics methods will be used to identify and quantify proteins in AVP.

3.2 Introduction

The Synapt G2-Si instrument from Waters Ltd was used for proteomics studies in this project. Peptides are separated by reverse phase chromatography and the Synapt G2-Si analyses mass by high resolution mass spectrometry. Electrospray Ionisation and tandem MS/MS (utilising triple quadrupole and time of flight (ToF) mass analysers) are used in this instrument. The features of each of these components have been described previously (Section 1.5.2 and 1.5.3). Figure 16 describes the instrument schematic of Synapt G2-Si.

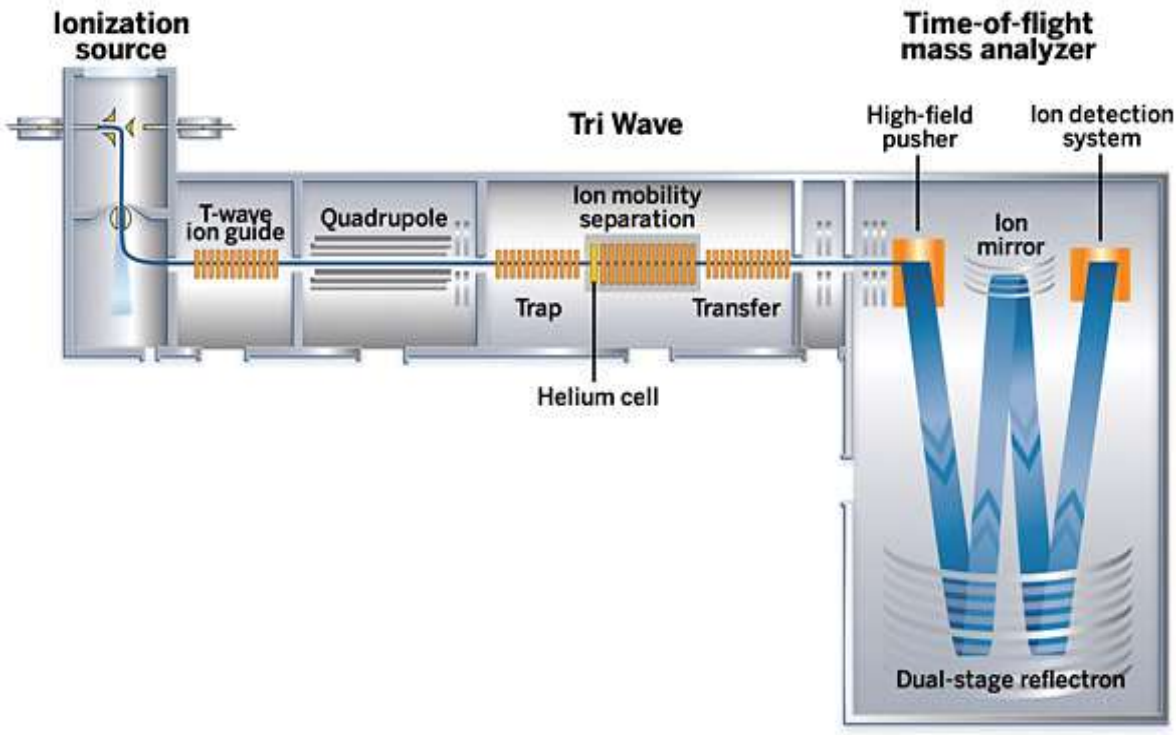

Figure 16 – Instrument Schematic of Waters Synapt G2-Si [268]

Peptide fragmentation is achieved using collision induced dissociation [82] (Section 1.5.4.1). Data is acquired using MS^E based Data Independent Acquisition (Section 1.5.5.2), data is analysed on Waters PLGS platform for identifying and quantifying proteins based on label free Hi3 quantitation method (Section 1.5.7).

As described in Chapter 2, there is variability associated with desorption process (*i.e.*, desorbing proteins from alum in AVP), hence proteomic studies were performed on CF also. CF is essentially the same material as AVP, but the CF samples are taken from the process immediately prior to the addition of alum (See Section 2.1 for detailed explanation).

3.3 Materials & Methods

3.3.1 Sample Preparation

Two batches of CF and AVP were used for this work. Two biological replicates of each batch were prepared for LC-MS/MS analysis. The sample preparation was carried out in a class I cabinet, under sterile conditions. LoBind microcentrifuge tubes were used throughout the sample preparation (Fisher Scientific UK, Cat Nos. 10708704 and 15178344).

3.3.1.1 AVP Protein Desorption

A 1 ml aliquot of AVP was incubated with 1 ml of desorption buffer (0.66 M Sodium Phosphate, 1 mM EDTA, pH 7.0) for 3 hours at room temperature, with shaking at 40 rpm.

3.3.1.2 Protein Concentration and Measurement of Protein Concentration

The CF and desorbed AVP samples were concentrated 20x using Amicon regenerated cellulose 10K centrifugal filter concentrators (UFC801096). Each solution was then buffer exchanged 3x into PBS (100 mM Sodium phosphate dibasic and 150 mM NaCl, pH 7.0). The protein concentration of all samples was measured using Micro BCA assay.

3.3.1.3 Solubilisation, Reduction and Alkylation

The CF and AVP concentrated samples were prepared using either urea or acetonitrile solubilisation protocol as detailed below:

Urea Method – The sample was incubated with 12M urea in Buffer A (50 mM Ammonium Bicarbonate), in 1.5 ml low bind Eppendorf tube at 40°C for 10 minutes shaking, to achieve a

final sample concentration of 8M urea (Urea – Sigma Aldrich, U5378; Ammonium Bicarbonate – Sigma Aldrich, 09830). The sample was centrifuged for 1 min to bring down the condensation droplets. The samples were incubated with 400mM DTT (Sigma Aldrich, GE17-1318-02) at 56°C for 30 minutes, shaking, to get final DTT concentration of 10mM. The samples were allowed to cool down for 5 minutes and incubated with 800mM iodoacetamide (IAA) (Sigma Aldrich, GERPN6302) in dark at room temperature for 30 minutes, to get IAA concentration of 20mM. The sample was then made up with 50mM Ammonium Bicarbonate solution, so that the final urea concentration was reduced from 8M to 1M.

Acetonitrile Method – The concentrated sample was mixed with Buffer A (80% Acetonitrile, 20% 50mM Trizma-HCl, 10mM CaCl2, pH 7.6) at 1:5 sample:Buffer A ratio, in 1.5 ml low bind Eppendorf tube at room temperature (Acetonitrile - Fisher Scientific 75-05-8; Trizma-HCL – Sigma Aldrich, 93363; Calcium Chloride – Sigma Aldrich, 499609). The sample was incubated with 400mM DTT (Sigma Aldrich, GE17-1318-02) at room temperature for 20 minutes, shaking, to get final DTT concentration of 10mM. The sample was incubated with 800mM Idoacetamide (IAA) (Sigma Aldrich, GERPN6302) in dark at room temperature for 15 minutes, to arrive at an IAA concentration of 10mM.

Preliminary experiments showed that the urea-based solubilisation method was more reproducible in comparison to acetonitrile-based method; hence the sample preparation for the final experiments were carried out using urea-based method.

3.3.1.4 Digestion Step

The samples were digested by incubating with sequencing-grade modified trypsin (Promega, V5117) at 1:50 trypsin: protein concentration at 37°C for 16 hours, with shaking at 40 rpm. The samples were dried down at 35°C setting on a SpeedVac system (ThermoFisher, UK).

3.3.1.5 Solid Phase Extraction Step

The samples were desalted using Empore SPE Disks C18, diam. 47 mm (Sigma, 66883-U). The following buffers were made: Buffer A - 0.5 % Acetic acid in water (Acetic acid – Sigma Aldrich, 45726; LC-MS grade Water - ThermoFisher Scientific, 51140), Buffer B - 0.5% Acetic acid in 80% Acetonitrile (Acetonitrile - ThermoFisher Scientific, USA - 51101). Briefly, the freeze-dried samples were resuspended in Buffer A. The membrane was cleaned by passing 100% methanol (Fluka 34966), and then equilibrated with Buffer A, B and A sequentially. The samples were passed through the membrane, washed with Buffer A and eluted with Buffer B. The samples were dried down at 35°C setting on the SpeedVac system.

3.3.1.6 Spiking of the Internal Standard

The samples were resuspended in Buffer A (water and 0.1% formic acid - LC-MS grade Water - ThermoFisher Scientific, USA – 51140; Formic acid - ThermoFisher Scientific, USA - 85178). An internal standard of trypsin digested BSA (Waters, UK) (125 fmole) was spiked into the samples.

3.3.2 Reversed Phase Liquid-Chromatography Mass Spectrometry Analysis

Figure 11 shows the schematic of liquid chromatography–tandem mass spectrometry (LC-MS/MS) workflow - MS^E based Data Independent Acquisition. Separation of peptides was performed using a 15 kpsi Waters NanoAcquity Ultra-Performance Liquid Chromatography system (UPLC) (Waters Corporation, USA). The following buffers were made: Buffer A - water and 0.1% formic acid (described above) and Buffer B - Acetonitrile and 0.1% formic acid (Acetonitrile - ThermoFisher Scientific, USA - 51101). A 4µL sample was injected onto a nano-UPLC, the samples were desalted using a reverse-phase SYMMETRY C_{18} trap column (180µm internal diameter, 20mm length, 5µm particle size, Waters Corporation) at a flow rate

of 8µL/min for 2 minutes. Peptides were separated by a linear gradient (0.3µL/min, 35°C; 97-60% Buffer A over 60 minutes) using a custom made Acquity UPLC M-Class Peptide BEH C_{18} column (130Å pore size, 75µm internal diameter, 400mm length, 1.7µm particle size, Waters Ltd). [Glu1]-fibrinopeptide B (GFPB, Waters, UK) was used as lockmass at 100fmol/µL. Lockmass solution was delivered from an auxiliary pump operating at 0.5µL/min to a reference sprayer sampled every 60 seconds.

The nanoLC was coupled online through a nanoflow sprayer to a Q-ToF hybrid mass spectrometer (HDMS Synapt G2-Si; Waters, UK). The instrument was operated in positive ion resolution mode and tuned to a mass resolution of 19,000-24,000 (full width at half maximum). The ToF analyser was calibrated with fragment ions of [Glu1]-fibrinopeptide B (GFPB, Waters, UK) for the m/z range 175.11 to 1285.54.

Data were lockmass-corrected with the monoisotopic mass of the doubly-charged precursor of GFPB (785.8426 *m/z*), post-acquisition. Accurate mass measurements were made using a data-independent mode of acquisition (LC-MS^E) [192]. Briefly, energy in the collision cell was alternated between low energy (4 eV) and high energy (energy ramp from 16-38 eV) modes every 0.6 seconds to acquire precursor and fragment ion spectra for retention time alignment and peptide sequencing during database processing. Measurements were made over a *m/z* range of 50-2000 Da with a scan time of 0.6s and an interscan delay of 0.05s. One cycle of MS and MS^E data were acquired every 1.3s. A radio frequency was applied to the quadrupole mass analyser to facilitate efficient transmission of ions in 300-2000 m/z range. This ensured that ions below 300 m/z observed in the MS^E spectrum were known to be derived from collision cell fragmentation. Each sample was analysed in technical triplicate.

3.3.3 Database Processing

Databases were searched using PLGS v3.0.2 (Waters, UK). The raw data was lockmass-corrected, smoothed, background subtracted and deisotoped. This provided a single centroid accurate mass for the monoisotopic species of each peptide and respective fragment ions. The peptide and fragment ion retention times were aligned [269]. Data were searched against Uniprot complete protein database for *B. anthracis* Sterne $34F_2$ strain. Carbamidomethylation of Cysteine and oxidation of Methionine were specified as fixed and variable modifications, respectively. A maximum of two missed cleavages were allowed for semi-tryptic peptide identification. For peptide identification, three corresponding fragment ions were set as a minimum criterion whereas for protein identification a minimum of two corresponding peptide ions and seven fragment ions were required. Protein level FDR rate was maintained at 1% estimated based upon the number of proteins identified from a decoy database. Database search results were outputted in .csv format for further analysis.

3.3.4 Protein Quantification

The proteins were quantified using the Hi3 method [193]. The average MS signal for three most intense peptides for each protein and the internal standard was calculated. A universal signal response factor was calculated from the average MS signal of the internal standard (counts/mol of protein). The absolute protein concentration was derived by dividing the universal signal response factor from the average MS signal for three most intense peptides of a specific protein.

3.4 Results and Discussion

3.4.1 Identification of proteins in AVP and CF

Using LC-MS/MS analysis, a total of 261 and 163 proteins were matched to the *B. anthracis* proteome from AVP and CF, respectively (Figure 17). Appendix 4 and 5 lists all the proteins identified in CF and AVP, respectively. 138 proteins were found to be common to both AVP and CF.

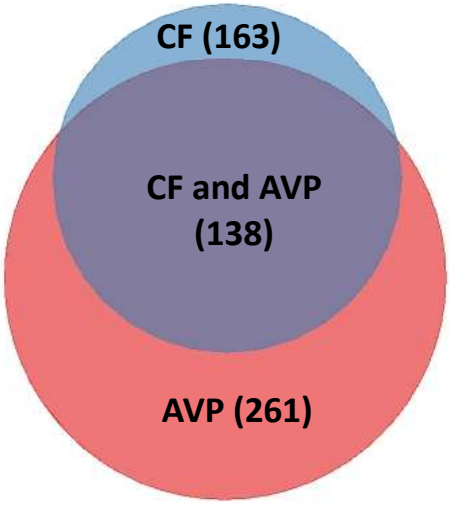

Figure 17 – Comparison of the number of proteins identified in AVP and CF by LC-MS/MS analysis, 261 proteins were found in AVP, 163 proteins were found in CF, 138 proteins were found common in CF and AVP (Two biological replicates and three analytical replicates were performed). A maximum of 11% and 19% CV was measured for two batches of CF and AVP, respectively (Figure adapted in Interactive Venn [270]).

Two biological replicates were prepared from two batches of CF and AVP, with each sample analysed by LC-MS/MS in triplicate. A maximum precision of 11% and 19% CV was recorded for the identification of proteins in the two batches of CF and AVP respectively, including the

biological replicates. More proteins were identified in AVP in comparison to CF, because AVP is five times more concentrated than CF, due to the alum precipitation step during AVP manufacture, as described before (Chapter 2 - Figure 12). Hence, low abundance proteins were identified in AVP that were not identified in CF. AVP samples had more variability in replicates, potentially due to the variability in the desorption process (Section 2.3.4).

3.4.2 Relative quantitation of PA, LF and EF in AVP and CF

PA was found to be the most abundant toxin protein in CF and AVP, followed by LF and EF (Figure 18). For CF and AVP, PA accounted for 65% and 64% of total protein respectively, LF accounted for 6% and 8% respectively, and EF accounted for 3% of total protein in both.

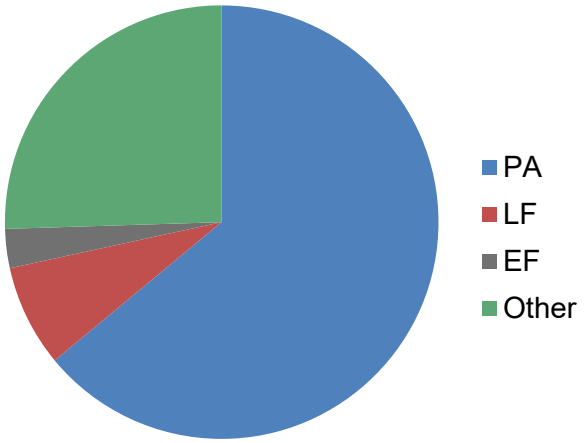

Figure 18 – Composition of AVP - PA was the principle component of the vaccine (65%), LF was found to be 8% and EF was found to be 3%, 258 proteins were found in lower abundances, comprising the other 25% (Figure adapted in Interactive Venn [270]).

Repeatability for relative quantitation of PA, LF and EF proteins in CF and AVP was good, a maximum CV of 18% was measured, including biological replicates and triplicate LC-MS/MS

analysis (Figure 19). Several Hi3 quantitation studies have reported similar CVs in complex samples [193, 195, 271].

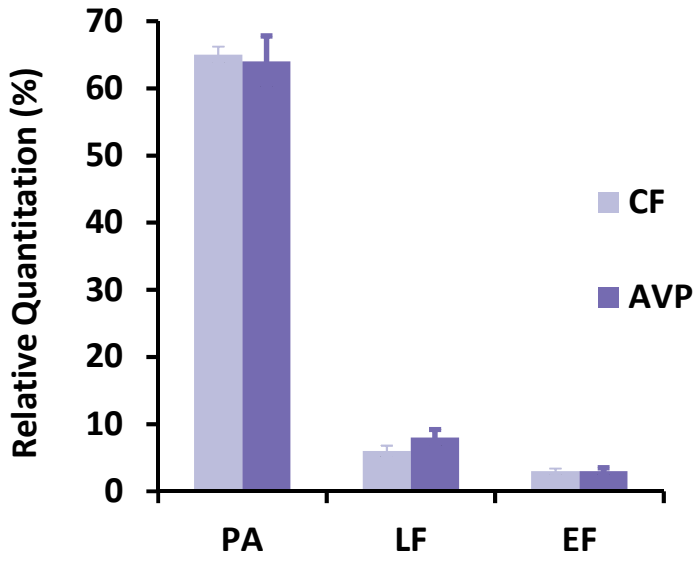

Figure 19 – Relative Quantitation of PA, LF and EF in two batches of CF and AVP. Error bars represent ± 1 SD about the mean. Two biological replicates and three analytical replicates were performed.

3.4.3 Absolute quantitation of PA, LF and EF in AVP and CF

As described before, PA was found to be the most abundant protein in CF and AVP, followed by LF, Enolase, PX01-90, EF, 60kD Chaperonin, alcohol dehydrogenase and phosphoglycerate kinase. PA was measured to be 615 and 2831 ng/mL in CF and AVP; LF was measured to be 52 and 345 ng/mL in CF and AVP; EF was measured to be 30 and 119 ng/mL in CF and AVP, respectively (Figure 20).

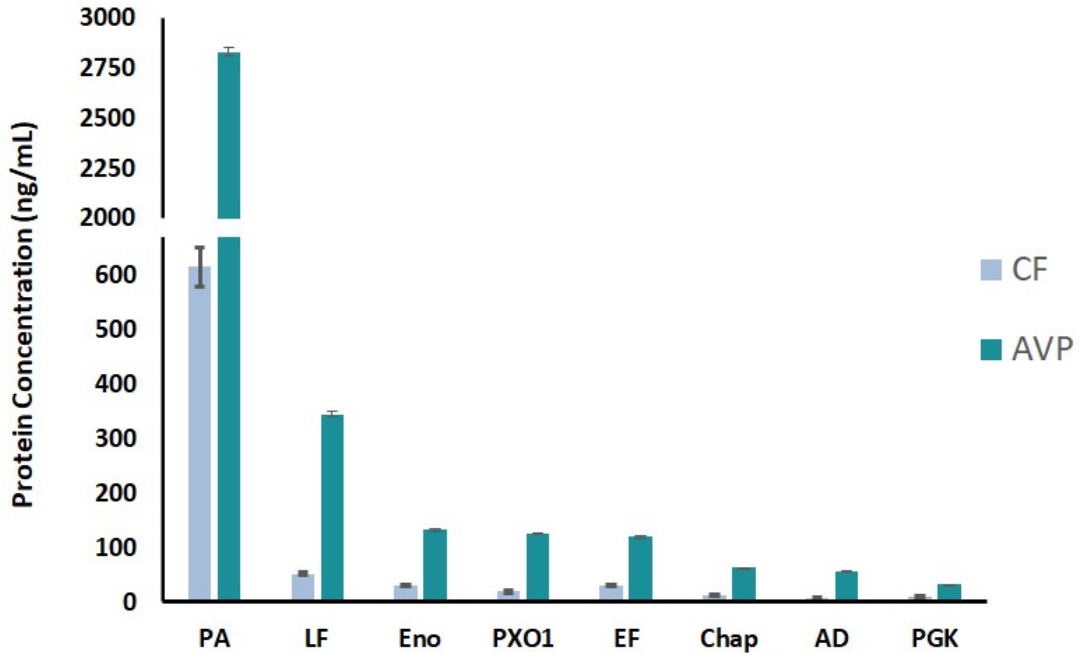

Figure 20 – Top 8 most abundant proteins in CF and AVP (PA – Protective Antigen, LF – Lethal Factor, Eno – Enolase, PX01-90, EF – Edema Factor, Chap – Chaperonin 60, AD – Alcohol Dehydrogenae, PGK – Phosphoglycerate Kinase). Error bars represent ± 1 SD about the mean. Two biological replicates and three analytical replicates were performed.

Previously, the average concentration of PA and LF was reported to be 3710 and 990 ng/ml, respectively, in culture supernatant from AVP production, determined by ELISA [18]. Although Hi3 label-free quantitation is deemed reliable for absolute quantitation of proteins [193, 195], absolute quantitation was not possible for CF and AVP. The quantitation data for PA and LF using ELISA is significantly different from LC-MS/MS data in the present study. Sample preparation steps involving desorption, sample concentration using centrifugal filters and solid phase extraction steps using C_{18} disks potentially resulted in loss of proteins. Calculations show that only 20% of the sample was recovered from LC-MS/MS experiment, based on the total protein estimation by Micro BCA assay. Sample manipulations in standard polypropylene Eppendorfs also resulted in loss of protein, hence lo-bind tubes were used.

Nevertheless, a maximum of 25% CV was measured for the quantification of abundant proteins in two batches of CF (including biological replicates). The repeatability of AVP biological replicates was poor and a CV of 15% was measured for PA (the most abundant protein in AVP), and approximately 40% for less abundant proteins. AVP samples had more variability in biological replicates, possibly due to the variability in the desorption process. The repeatability of the triplicate analysis of each AVP sample was <20%. For accurate absolute quantitation of proteins in CF and AVP, sample preparation designed to minimise the loss of protein (*i.e.* without desorption, concentration step and solid phase extraction) would be required. However, this proved unfeasible, as further investigation revealed that CF contains interfering substances that needed to be removed to achieve a reproducible LC-MS/MS analysis.

3.5 Conclusion

A total of 138 proteins were identified in AVP and CF using proteomic LC-MS/MS analysis. PA (65%), LF (8%) and EF (3%) were found to be the most abundant proteins in AVP, using DIA based Hi3 label free quantitation. A maximum of 18% CV was measured for the relative quantitation of eight abundant proteins analysed in AVP, including biological and technical replicates. The study highlights the difficulty in measuring absolute quantity of proteins in alum adjuvant-based vaccines.

4.0 COMPUTATIONAL STUDIES

4.1 Aims and Objectives

Computational studies will be carried out to predict $CD4^+$ and $CD8^+$ peptide-MHC binding for the eight most abundant proteins of AVP (Section 3.4.3 – Figure 20). The differences in peptide-MHC binding affinity were investigated across a selection of HLA alleles that provides wide coverage of the global human population and multiple *B. anthracis* strains.

4.2 Introduction

MHC II epitopes were predicted using NetMHCIIpan 3.2 [239] for the eight most abundant proteins in AVP (Section 3.4.3, Figure 20) and across multiple HLA alleles in order to assess the impact of allelic differences in human populations. As described previously (Section 1.6.1), the length of the peptide binding to HLA II molecules can vary between 9-30 amino acids. However, a length of 15 amino acids is widely used in both experimental and computational studies [272].

Given the reasonable assumptions that a) epitope binding affinity is correlated with the strength of the immune response, and b) a larger proportion of peptides predicted to bind with moderate to high affinity (≤500 nM) are likely to be true epitopes than those predicted to bind with low affinity (>500 nM and ≤5000 nM), only predicted epitopes with high and intermediate binding affinity were taken forward for analysis. Two IC_{50} binding thresholds advocated by the Immune Epitope Database (IEDB) [273], ≤50 nM and ≤500 nM, were adopted for predicted epitopes with high binding affinities (strong binders) and intermediate binding affinities (medium binders), respectively.

NetMHCIIpan is not completely accurate and may be prone to either over- and under-prediction in specific cases. It has been observed, for example, that standard computational tools predict a subset of experimentally-verified immunodominant peptides to bind too weakly to form epitopes [274]. However, in the context of this study computational methods are of sufficient accuracy to give us broad insights covering multiple antigens and many HLA alleles – a combination that poses an unsolved challenge to experimental approaches.

MHC I epitopes were predicted using NetMHCpan 3.0 [250, 253] for the eight most abundant proteins in AVP and across multiple HLA alleles in order to assess the impact of allelic differences in human populations. As described previously (Section 1.6.2), the length of the peptide binding to HLA I molecule can vary from 8-11 amino acids. However, the length of 9 amino acids has been observed to be the most abundant with most HLA alleles in recent, high-throughput immunopeptidome studies thought to be optimal and was used in this study [241, 275]. Rather than an absolute binding threshold, NetMHCpan adopts a relative ranking approach, with predicted affinity compared to those of a large set of random natural peptides; peptides with a %rank <0.5 are deemed strong binders. Only strong binders were taken forward for further analysis.

4.3 Methods

4.3.1 MHC II epitope prediction

MHC class II predictions were carried out to identify the epitopes found in the eight most abundant proteins of AVP (Section 3.4.3 - Figure 20), using NetMHCIIpan 3.2 [239]. A set of 25 HLA class II alleles were selected that provide a global population coverage of over 99% [231]. Python scripts were written to enable automation (See Appendix 1). Binding affinities of peptides with IC_{50} ≤50 nM cut off and ≤500 nM cut off were used to select strong and medium binding epitopes, respectively [273].

4.3.2 *B. anthracis* strain data

The PA, LF and EF protein sequences from 33 known *B. anthracis* strains were analysed for in order to identify mutations using the MegAlign software [276]. The list of all *B. anthracis* strains evaluated in the study are detailed in Appendix 3; genomic sequences for these strains were obtained from the NCBI database [277]. Substitutions were then analysed with respect to MHC class II antigen presentation to assess whether they changed the immunogenic properties of these proteins.

4.3.3 MHC I epitope prediction

MHC class I predictions were carried out to identify 9-mer epitopes in the eight most abundant proteins of AVP (Section 3.3 – Figure 20) using NetMHCpan 3.0 [250, 253]. The choice of HLA-I alleles (Table 4) was based on a meta-analysis of HLA allele frequency data published by Solberg and co-workers [278, 279]. From each of the HLA-A, -B and -C genes, 10 high frequency alleles were selected. Epitopes were additionally predicted for comparatively low-frequency HLA-B alleles (*e.g.* HLA-B*27:05 and HLA-B*39:05) that are considered representatives of so-called HLA supertypes [278, 279]. Python scripts were written to enable automation (See Appendix 1). Binding affinities of peptides with %Rank threshold of 0.5 was used to select strong binding epitopes.

No.	HLA Allelic Variant	Allele Frequency
1	HLA-A*01:01	0.04843
2	HLA-A*02:01	0.15284
3	HLA-A*03:01	0.04272
4	HLA-A*24:02	0.18816
5	HLA-A*11:01	0.11661
6	HLA-A*31:01	0.04093
7	HLA-A*33:03	0.04081
8	HLA-A*02:06	0.03469
9	HLA-A*26:01	0.03354
10	HLA-A*30:01	0.02505
11	HLA-B*35:01	0.05466
12	HLA-B*51:01	0.05222
13	HLA-B*40:01	0.05120
14	HLA-B*44:03	0.04473
15	HLA-B*07:02	0.04105
16	HLA-B*15:01	0.03431
17	HLA-B*08:01	0.02960
18	HLA-B*58:01	0.0289
19	HLA-B*27:05	0.01236
20	HLA-B*39:05	0.00455
21	HLA-C*07:02	0.13101
22	HLA-C*04:01	0.11177
23	HLA-C*03:04	0.09132
24	HLA-C*01:02	0.08481
25	HLA-C*07:01	0.06887
26	HLA-C*06:02	0.06160
27	HLA-C*03:03	0.05580
28	HLA-C*08:01	0.04522
29	HLA-C*15:02	0.03362
30	HLA-C*12:02	0.03191

Table 4 - MHC I alleles used in this study and their frequencies (Adapted from Solberg *et al.,* [279])

4.4 Results and Discussion

4.4.1 MHC II epitope prediction

The number of strong and medium-plus-strong binders for eight AVP proteins and 25 HLA alleles are shown in Tables 5 and 6, respectively.

Before interpreting these results, it is important to note that one needs to be cautious, as binding affinity between peptide and MHC molecule is just one of the many factors contributing to the T cell response. Whereas peptide-MHC binding affinity can be predicted with reasonable accuracy, in the present context there is no information about other important factors such as T cell precursor frequency [280-282] and the breadth of the T cell response [283]. The emerging picture from many independent research studies is a highly complex one; hence within a given individual, specific epitopes may be protective whereas others may have a negative impact, for example by blocking or slowing down the T cell response [284, 285], or by inducing autoimmunity [280, 285, 286]. In principle and presumably in practice, the same epitope may lead to different outcomes in different individuals.

Bearing these points in mind, there are nevertheless cautious but potentially important conclusions that can be drawn from the MHC II-peptide binding prediction. In interpreting these results, the confidence that a given antigen is likely to be protective with respect to a given HLA allele depends on the number of predicted epitopes, and in particular the number of epitopes predicted to be at least medium binders. If the number of medium-plus-strong epitopes is low, there is a greater possibility that an individual will lack TCRs capable of binding to any of the peptide-MHC complexes associated with that combination of antigen and HLA allele.

HLA II Alleles	No. of strong binding epitopes							
	PA	LF	EF	PX01	Chap.	AD	Eno	PGK
HLA-DPA1*01:03-DPB1*02:01	3	6	12	9	0	0	0	0
HLA-DPA1*01:03-DPB1*04:01	0	5	4	9	0	0	0	0
HLA-DPA1*02:01-DPB1*05:01	0	0	0	0	0	0	0	0
HLA-DPA1*03:01-DPB1*04:02	0	5	0	0	0	0	0	0
HLA-DQA1*01:01-DQB1*05:01	0	0	0	0	0	0	0	0
HLA-DQA1*01:02-DQB1*06:02	0	0	0	0	3	0	5	0
HLA-DPA1*02:01-DPB1*01:01	0	5	0	0	0	0	0	0
HLA-DQA1*03:01-DQB1*03:02	0	0	0	0	0	0	0	0
HLA-DQA1*04:01-DQB1*04:02	0	0	0	0	0	0	0	0
HLA-DQA1*05:01-DQB1*02:01	0	0	0	0	0	0	0	0
HLA-DQA1*05:01-DQB1*0301	5	0	0	0	12	11	7	19
HLA-DRB1*01:01	44	100	101	27	42	20	43	49
HLA-DRB1*03:01	7	21	0	0	4	2	0	0
HLA-DRB1*04:01	1	3	10	0	0	0	3	0
HLA-DRB1*04:04	5	0	5	4	0	1	0	5
HLA-DRB1*04:05	0	0	12	0	0	0	0	0
HLA-DRB1*07:01	15	33	28	7	0	2	4	12
HLA-DRB1*08:02	0	0	0	0	0	0	0	0
HLA-DRB1*09:01	0	18	14	4	3	1	4	11
HLA-DRB1*11:01	6	5	20	2	0	0	6	4
HLA-DRB1*13:02	32	36	30	9	10	10	8	11
HLA-DRB1*15:01	5	30	7	7	0	0	0	0
HLA-DRB3*01:01	4	20	0	0	0	2	0	0
HLA-DRB4*01:01	6	2	0	0	0	0	0	0
HLA-DRB5*01:01	7	25	28	11	0	0	14	14
Total No. of Epitopes	140	314	271	89	74	49	94	125

Table 5 - Predicted number of strong binding MHC II epitopes, derived using NetMHCIIpan (IC_{50} cut-off of ≤50 nM).

HLA II Alleles	No. of medium-plus-strong binding epitopes							
	PA	LF	EF	PX01	Chap.	AD	Eno	PGK
HLA-DPA1*01:03-DPB1*02:01	55	118	146	67	13	2	34	60
HLA-DPA1*01:03-DPB1*04:01	41	88	68	52	5	0	23	25
HLA-DPA1*02:01-DPB1*05:01	14	32	50	26	0	0	4	3
HLA-DPA1*03:01-DPB1*04:02	33	61	48	44	3	0	17	14
HLA-DQA1*01:01-DQB1*05:01	22	28	40	27	0	0	11	13
HLA-DQA1*01:02-DQB1*06:02	58	40	34	34	137	63	63	62
HLA-DPA1*02:01-DPB1*01:01	50	121	130	66	12	0	35	57
HLA-DQA1*03:01-DQB1*03:02	5	2	0	0	15	0	0	4
HLA-DQA1*04:01-DQB1*04:02	5	4	3	0	29	0	7	4
HLA-DQA1*05:01-DQB1*02:01	29	56	54	20	75	23	65	35
HLA-DQA1*05:01-DQB1*0301	89	48	58	39	197	114	121	111
HLA-DRB1*01:01	346	398	358	263	299	165	188	225
HLA-DRB1*03:01	107	124	53	23	45	49	30	41
HLA-DRB1*04:01	139	211	172	86	64	33	67	71
HLA-DRB1*04:04	171	223	189	121	124	57	89	105
HLA-DRB1*04:05	112	207	172	89	39	24	51	69
HLA-DRB1*07:01	195	235	205	105	113	90	100	106
HLA-DRB1*08:02	75	111	112	34	75	28	56	43
HLA-DRB1*09:01	169	214	195	74	134	97	121	115
HLA-DRB1*11:01	128	202	221	114	89	33	79	89
HLA-DRB1*13:02	244	277	224	147	122	84	92	102
HLA-DRB1*15:01	150	214	190	112	52	41	73	96
HLA-DRB3*01:01	82	130	86	31	31	32	27	34
HLA-DRB4*01:01	156	236	195	158	123	45	72	100
HLA-DRB5*01:01	176	216	258	134	115	55	86	108
Total No. of Epitopes	**2651**	**3596**	**3261**	**1866**	**1911**	**1035**	**1511**	**1692**

Table 6 - Predicted number of medium-plus-strong binding MHC II epitopes, derived using NetMHCIIpan (IC_{50} cut-off of ≤500 nM).

The NetMHCIIpan tool predicted that peptides from all eight proteins are likely to be presented to T cells, however the number of such peptides varied considerably between different HLA alleles (Tables 1 and 2). The “core” vaccine components PA, LF and EF were associated with at least 5 medium-plus-strong class II epitopes with the notable exceptions of common HLA-DQ alleles HLA-DQA1*0301-DQB1*0302 and HLA-DQA1*0401-DQB1*0402. In both these cases, a much higher number of medium-plus-strong epitopes was associated with the 60 kDa Chaperonin protein (15 and 29 epitopes respectively).

Given that individuals have multiple class II HLA alleles, the data in Table 6 suggests that most individuals vaccinated with AVP have the potential to undergo a protective T cell response, although the proteins involved may vary between individuals. From this analysis, it appears that the efficacy of PA alone is by no means guaranteed and that the presence of additional proteins enhances the prospects that AVP affords broad protection.

4.4.2 Efficacy of AVP against different *B. anthracis* strains

Multiple sequence alignments of PA, LF and EF protein sequences from 33 known *B. anthracis* strains were generated. These alignments revealed 3, 4 and 6 single amino acid differences for PA, LF and EF respectively between the vaccine (Sterne) strain and the other strains. NetMHCIIpan was used to make predictions for all 15-mers spanning each of these substitutions. The results are summarised in Table 7.

None of the predictions in Table 7 were for strong binding epitopes (≤50 nM binding affinity), and the numbers of predicted changes is very small compared to the total number of predicted epitopes for each of these proteins (Table 6). Nevertheless, there remains a small possibility that an individual’s immunodominant vaccine response, induced by the Sterne strain, may be comparatively less effective against a different strain if one or more critical epitopes are absent or different in that strain.

Amino acid change	B. *anthracis* strains	Number of missing epitopes[1]	Number of additional epitopes[2]	Number of changed epitopes[3]
PA I433V	HYU01	9	0	5
PA P565S	CDC 684, SK-102, Vollum 1B, Vollum	10	12	9
PA A600V	BA1015, Canadian Bison, CDC 684, isolate IT Carb1-6241, isolate IT Carb3-6254, PAK-1, RA3, SK-102, Turkey32, V770-NP-1R, Vollum 1B, Vollum, Pollino, P.NO_2, Larissa, HYU01, H9401, A1144	18	5	11
LFK155X	P.NO_2	4	9	13
LF S299A	1C3, 4NS, A16, A16R, A0248, A1144, A2012, Ames 0462, Ames BA1004, BA1015, Canadian Bison, CDC 684, H9401, Larissa, Ohio, P.NO_2, Pak-1, Pollino, Shikan, SK-102, Stendal, Turkey 32, V770-NP-1R, VCM1168, Vollum 1B, Vollum	0	4	16
LF S299T	BA1035, HYU01, RA3, SVA11	3	0	12
LF Q346E	H9401	0	5	1
LF E709G	BA1035, HYU01, P.NO_2, RA3, SVA11	0	0	0
EF D84G	A16R	0	40	1
EF D180G	BA1035, HYU01, RA3, SVA11	22	16	19
EF I318T	BA1035, HYU01, RA3, SVA11	10	0	0
EF G352V	A16R	0	0	0
EF E443D	Canadian Bison	0	0	0

[1]The number of HLA-II alleles for which a Sterne strain epitope in Table 6 is predicted to be a non-binder in a non-Sterne strain

[2]The number of HLA-II alleles for which an epitope is predicted with a non-Sterne strains that is not predicted to be an epitope with the Sterne strain

[3]The number of HLA-II alleles for which a Sterne strain epitope is predicted to present a different epitope in non-Sterne strains (i.e. the epitope has a different TCR-facing amino-acid residue).

Table 7 - Predicted medium-plus-strong binding MHC II epitope differences between the Sterne strain and other *B. anthracis* strains, derived using NetMHCIIpan (IC_{50} cut-off of ≤500 nM).

4.4.3 MHC I epitope prediction

Table 8 details the predicted number of strong binding MHC I epitopes for each of the analysed eight proteins in AVP. The NetMHCpan tool predicted that the peptides from all eight proteins are likely to be presented to T cells, with the largest number of strong binding MHC I epitopes observed in PA, LF and EF across different alleles. However, when the number of epitopes were normalised relative to amino acid length, these proteins did not have statistically higher number of epitopes in comparison to other proteins. This analysis suggests that many proteins in AVP have the potential to induce a $CD8^+$ T cell response

HLA I Alleles	No. of strong binding epitopes							
	PA	LF	EF	PX01	Chap.	AD	Eno	PGK
HLA-A*2402	12	11	13	7	0	0	1	3
HLA-A*0201	7	9	13	3	6	2	6	12
HLA-A*1101	14	12	16	17	11	6	7	7
HLA-A*0101	13	17	34	2	0	2	11	2
HLA-A*0301	14	18	16	13	9	4	9	5
HLA-A*3101	9	4	7	4	2	3	6	3
HLA-A*3303	8	5	13	7	1	4	4	2
HLA-A*0206	4	9	9	2	7	3	4	10
HLA-A*2601	13	20	16	9	3	3	13	6
HLA-A*3001	10	6	16	8	12	4	6	11
HLA-B*3501	10	10	17	5	6	1	3	9
HLA-B*5101	13	5	6	2	0	4	5	6
HLA-B*4001	10	16	11	10	12	3	8	14
HLA-B*4403	15	21	21	13	8	5	11	4
HLA-B*0702	9	3	8	4	10	6	1	11
HLA-B*1501	9	9	13	3	5	2	6	2
HLA-B*0801	7	7	4	7	5	0	2	3
HLA-B*5801	11	5	13	2	1	1	0	2
HLA-B*2705	9	7	5	2	3	1	3	5
HLA-B*3905	6	10	8	11	1	0	8	4
HLA-C*0702	8	10	18	7	0	1	4	2
HLA-C*0401	10	9	12	5	3	2	7	6
HLA-C*0304	14	8	10	6	12	1	4	9
HLA-C*0102	10	12	16	2	5	1	4	8
HLA-C*0701	10	11	7	12	0	1	4	3
HLA-C*0602	11	11	9	9	1	1	5	2
HLA-C*0303	14	8	10	6	12	1	4	9
HLA-C*0801	13	12	12	7	5	2	4	10
HLA-C*1502	11	13	10	3	4	3	3	9
HLA-C*1202	11	14	14	5	5	3	3	11
Total No. of Epitopes	**315**	**312**	**377**	**193**	**149**	**70**	**156**	**190**
Normalised with sequence length	**41**	**41**	**49**	**25**	**20**	**9**	**20**	**25**
No. of Alleles	**13**	**15**	**12**	**10**	**6**	**8**	**9**	**8**

Table 8 - Predicted number of strong binding MHC I epitopes, derived using NetMHCIpan (Rank cut-off of 0.5).

4.5 Conclusion

NetMHCIIpan predicted that peptides from all eight abundant proteins are likely to be presented to T cells, a pre-requisite for protection; however, the number of such peptides varied considerably for different HLA alleles. This suggests that the effectiveness of AVP within humans does not depend on PA alone; other *B. anthracis* proteins in AVP may be important for individuals with specific HLA allele combinations. Further, in spite of differences in the sequences of key antigenic proteins from different *B. anthracis* strains, computational analysis suggested that these do not affect the protection that AVP affords to strains other than the vaccine's source strain. Nevertheless, there remains a small possibility that an individual's immunodominant vaccine response, induced by the Sterne strain, may be comparatively ineffective against a different strain if one or more critical epitopes are absent or different in that strain. Further, NetMHCpan predicted that not only PA, LF and EF, but other *B. anthracis* proteins in AVP have a strong likelihood of epitope presentation across various HLA alleles and may contribute to triggering $CD8^+$ T cell response**.** This corroborates with current knowledge and understanding on anthrax toxins and the way in which LT and ET supresses the host immune system by impairing the functions of several phagocytes, T cells and B cells [28, 81], as described previously in Section 1.3.3.

5.0 *IN VITRO* STUDIES

5.1 Aims and Objectives

A small proof-of-concept study was designed to characterise the immune response from PA and LF in human AVP vaccinees. The aim of this study was to investigate the cellular and humoral (antibody) response in AVP vaccinees, including impact of genetic diversity and corroborate findings with computational studies. This study evaluated the T cell response by measuring IFNy and IL10 cytokine levels when stimulated with rPA (recombinant PA) and rLF (recombinant LF), together with anti-PA IgG, anti-LF IgG and TNA levels.

5.2 Introduction

PA is thought to be the primary immunogen in both AVP and AVA. As described previously (Section 3.3.2, Figure 18), AVP contains at least 138 proteins, including PA (65%) and LF (8%). LF is the next most abundant protein in AVP after PA. Computational studies (Section 4.4.1, Table 5 and 6) suggest that peptides from LF are likely to be presented to T cells by MHC molecules encoded by HLA alleles that provide broad coverage of the global human populations. In fact, the overall number of strong and strong-medium binding epitopes for LF is predicted to be higher in comparison to PA. This suggests that LF is an important immunogen in AVP. Previous studies have also proposed that LF enhances PA-specific antibody response [6, 8, 9], and that anti-LF antibodies are protective [3, 10, 11]. Ingram *et al.,* [169] have reported that LF shows a strong long-lasting $CD4^+$ T cell response in both AVP vaccinees and cutaneous Anthrax patients.

Hence, this study was designed to characterise the cellular and humoral response from PA and LF in AVP vaccinees. The cellular immune (T cell) response was measured by stimulating peripheral blood mononuclear cells (PBMCs) with rPA and rLF and measuring the release of

IFNy and IL10 cytokines. The humoral immunity (antibody response) was determined by measuring anti-PA antibodies, anti-LF antibodies and TNA levels. Further, the aim of the study was to correlate the T cell response with antibody response, as well as corroborate at least a subset of the computational findings discussed in Chapter 4.

IFNγ cytokine was selected in this study as it is thought to induce a Th1 immune response by regulating chemotaxis, promoting phagocytosis and upregulating antigen presentation. IFNγ is secreted by NK cells and T lymphocytes and is required for optimal antibody-mediated protection against infection [287]. It is thought to play an important role in mediating the cellular immune response against Anthrax [288-290]. IL-10 cytokine levels were also measured in this study, as it is an important immunoregulator that inhibits the excessive Th1 and $CD8^+$ T cell responses that are associated with potentially dangerous proinflammatory responses during infection [291]. It is mainly secreted by helper T cells type 2 (Th2), regulatory T cells, monocytes, some dendritic cells, activated macrophages and granulocytes [291, 292].

5.3 Materials and methods

5.3.1 Blood collection

Eight AVP-vaccinated volunteers and two non-vaccinated control volunteers based at PBL, Porton Down, participated in this study, in the context of a study protocol (Ref: R&D 325) approved by the PHE Independent Ethics Committee, UK. The subjects were all adults aged over 18 years and all provided written, informed consent. A total of 29 ml of blood was collected from each volunteer. Although volunteers were not recruited based on their vaccination dates, details of their AVP vaccination history were recorded.

From each volunteer, 10 ml x 2 blood was collected in sodium heparin plasma tubes (Midmeds Cat No. MD368480), 4 ml in K_2EDTA tubes (Midmeds Cat No. MD367839) and 5 ml in clot activator

coated tubes (Midmeds Cat No. MD367954). Blood collection was performed by a PBL Occupational Health phlebotomist nurse. Each donor blood sample was labelled 1-10 anonymously and stored at room temperature. Samples 5 and 10 were blood collected from control individuals (i.e. individuals who had never been vaccinated with AVP).

On the same day as blood collection, PBMCs were isolated from 20 ml of volunteer blood collected in sodium heparin plasma tubes. The work was performed in Culture Collections labs at PHE, Porton Down. Each sample was treated as follows: Blood was transferred from each donor into 50 ml falcon tube and was made up to 40 ml with RPMI-1640 medium (Sigma R8758). To prepare the Accuspin tubes 50 ml (Sigma A2055), the tubes were filled with 15 ml of Ficoll Plaque Plus (Sigma GE17-1440-02) and spun at 1000g for 2 min. Blood was then transferred to the Accuspin tubes and spun at 1000g for 20 min for PBMC separation. The white layer (PBMCs) was recovered and transferred to a fresh 50 ml falcon tube. The solution was then made up to 40 ml using RPMI-1640 medium. The sample was centrifuged at 300g for 10 min. The supernatant was discarded, and the pellet was recovered with 15 ml of RPMI-1640 medium. Cell counting was done using NucleoCounter (Chemometec, UK). The sample was again spun at 300g for 5 min. The supernatant was discarded, and the pellet was diluted in 5 ml of chilled Foetal bovine serum + 10% DMSO. 5 x 1 ml sample was transferred to cryovials and transferred to a Mr. Frosty container, before transfer into -80°C.

5.3.2 HLA tissue typing

HLA tissue typing analysis was contracted to Proimmune Ltd, UK. Blood (4 ml) was collected in K_2EDTA tubes (Midmeds, UK) and stored at -80°C. The MHC II alleles for each donor for the 6x loci (2 x DRB1, 2 x DQB1 and 2 x DPB1) were reported.

5.3.3 Anti-PA and anti-LF IgG ELISA assay

Blood (5 ml) that was collected in clot activator coated tubes (Midmeds, UK) was centrifuged at 2,000 x g for 10 minutes. The supernatant was recovered and stored at -80°C for anti-PA and anti-LF IgG ELISA and TNA assay.

These tests were performed by the Medical Interventions Group (MIG) at Public Health England (PHE), Porton Down. Briefly, 96-well plates (NUNC flat bottomed wells, ThermoFisher, UK) were coated overnight with either purified rPA (*E. coli*-derived, PHE Porton) or rLF (*B. anthracis*-derived, PHE Porton), before the addition of serial-diluted human serum samples and reference (IAG/AIQC/04, PHE Porton). The reference serum was prepared by plasma conversion of plasma collected from AVP-vaccinated individuals (not originating from this study). Anti-human IgG Fcγ-specific antibody conjugated to Alkaline Phosphatase (Jackson Immunoresearch) was used to produce a colorimetric response proportional to the amount of PA or LF specific antibody when substrate (AP Yellow, BioFX & surmodics) was added. Plates were read using a Versamax plate reader with SoftMax Pro 5.2 analysis software (Molecular Devices). Each sample was assigned a titre against a 5PL human sera reference curve. The reference serum was assigned values of 960U/ml (PA) and 500 U/ml (LF) based on the mean ED_{50} value of multiple runs on previous occasions (not included in this study).

5.3.4 Toxin neutralising assay

Sera were serially diluted and incubated with Lethal Toxin (PHE Porton) at a controlled concentration. This was transferred to 96-well plates seeded with a mouse macrophage cell line (J774A.1, ECACC 9105151) known to be sensitive to Anthrax toxin-mediated cytotoxicity. Cell survival was assessed through uptake of methylthiazolyldiphenyl-tetrazolium bromide (MTT, Sigma, UK) by surviving cells; this provided a colorimetric readout of survival. Plates were read using a Versamax plate reader with SoftMax Pro 5.2 analysis software (Molecular Devices, US). Sample ED_{50} values (the dilution of serum required for a 50% reduction in cytotoxicity) were compared to a reference serum (IAG/AIQC/07, PHE Porton), which allows an NF_{50} value to be calculated for each sample. The reference serum was prepared by plasma conversion of plasma collected from AVP-vaccinated individuals (not originating from this study). The ED_{50} of the reference and samples and NF_{50} of the samples are reported.

5.3.5 rPA and rLF peptide library

rPA (5.5 mg/mL) and rLF (2 mg/mL) were acquired from Porton Biopharma Ltd. Peptides were acquired from Pepscan, Netherlands. PA and LF peptides (15mers) of ≥90% purity were synthesized (Table 9). These peptides were selected as they were previously described as immunodominant epitopes. The peptides were delivered in lyophilised form. The complete list of synthesized peptides (including amino acid composition) is detailed in Appendix 6.

Antigen	Peptides	Reference
PA	397-411, 408-422, 501-515, 512-526, 709-723, 720-734	[218]
	177-191, 188-202, 253-267, 264-278, 275-289, 633-647, 644-658, 655-669	[16]
LF	570-584, 581-595, 650-664, 661-675, 672-686, 683-697, 710-724, 721-735	[169]
	453-467, 464-478*, 475-489*, 543-557, 554-568	[219]

*Peptides LF 464-478 and LF 475-489 could not be synthesised to required purity levels.

Table 9 – rPA and rLF Peptide library

5.3.6 Measurement of cytokine response

IFNy and IL10 cytokine response in PBMCs to various AVP protein stimulants was investigated for each sample. These tests were performed by Cisbio Bioassays. Human IFNy assay Kit (Cat No. 62HIFNGPEG) and Human IL10 Assay Kit (Cat No. 62HIL10PEG) ELISA based kits were used for the measurement of cytokines. Prior to the cytokine assays, the PBMCs were observed under the microscope to ensure that the cells were alive and healthy. Additionally, the cytokine response in the PBMCs was investigated with IMA/Ionomycin as a positive control to ensure that the PBMCs were functional.

The peptides were dissolved in 5-30µL of 10% DMSO based on solubility. 100µL of water was added, then the solution was made up to 1 ml using RPMI-1640 working buffer. Thus, the final concentration of the peptide was 2 mg/ml. Once the peptides were reconstituted, the vials were added together as described below. Since it was not possible to test each peptide individually due to the limitation with volunteer PBMCs samples, peptide mix were made as

follows, so that cytokine response from certain part of PA, LF or EF sequence could be tested: PA mix 1 - 253-267, 264-278, 275-289, PA mix 2 - 633-647, 644-658, 655-669, PA mix 3 - 397-411, 408-422, PA mix 4 - 501-515, 512-526, PA mix 5 - 709-723, 720-734, LF mix 1 - 570-584, 581-595, LF mix 2 - 650-664, 661-675, LF mix 3 - 672-686, 683-697, LF mix 4 - 710-724, 721-735. The final concentration of each mix was 2 mg/mL.

PBMCs (480K cells/well) were stimulated with 10 µg/ml of rPA, rLF or peptide mixes for 72 hours. Supernatant (50µL) was then transferred to new wells and cytokine levels were measured according to the instructions in the Cisbio kits. The cell count was underestimated for these experiments; the live cell count was decreased significantly post cryopreservation. Further, significantly higher cell count of PBMCs was required in the assay than anticipated, as was determined during preliminary experiments. Hence, the number of samples that could be tested for each stimulant varied, depending on the live cell count. Appendix 6 details the grid of samples and stimulants tested for cytokine response.

5.4 Results and Discussion

5.4.1 HLA tissue typing

The HLA types and immunisation history of volunteers are shown in Table 10.

Sample No.	Immunisation History (Primary Immunisation Year, Boosters Years)	HLA-DRB1		HLA-DQB1		HLA-DPB1	
1	2013, 2015, 2016	*01:01:01	*15:01:01	*06:02:01	*05:01	*04:02:01	*04:01:01
2	2012, 2014, 2016	*04:01/35/63/145/179	*11:01/11:08/11:37/11:175/13:14	*03:02:01	*03:01:01	*03:01:01	*03:01:01
3	2014, 2016	*15:01:01	*04:01:01	*06:02:01	*03:01:01	*04:01:01	*04:01:01
4	1999, 2016	*04:01:01	*11:02:01	*03:01:01	*03:19:01	*04:01:01	*04:01:01
5[A]	N/A	*15:01:01	*15:01:01	*06:02:01	*06:02:01	*02:01	*04:01:01
6	2015, 2016	*15:01:01	*15:01:01	*06:02:01	*06:02:01	*02:01	*04:01:01
7	2007, 2009, 2011, 2013, 2016	*15:01:01	*11:04:01	*06:02:01	*03:01:01	*04:01:01	*11:01:01
8	2014, 2016	*04:08:01	*07:01/79	*03:03:02	*03:01:01	*04:01:01	*04:01:01
9	2016, N/A	*03:01:01	*04:01:01	*02:01:01	*03:01:01	*01:01:01	*20:01:01
10[A]	N/A	*07:01/79	*07:01/79	*02:02:01	*02:02:01	*17:01:01	*17:01:01

[A]Samples from control volunteer

Table 10 – Volunteer HLA types and immunisation history

5.4.2 Anti-PA antibody, anti-LF antibody and TNA levels

The antibody titres measured in sera from volunteers is detailed in Table 11 and Figure 21. As expected, the antibody titre and TNA levels in the control samples were below the detection limit (Table 11). On the other hand, the antibody titres and TNA levels of the vaccinees are highly variable.

Sample No.	Anti-PA Antibody Titre	Anti-LF- Antibody Titre	TNA (NF_{50})*1000
1	263	561	66
2	261	139	38
3	784	734	493
4	724	128	166
5[A]	0	0	0
6	533	470	318
7	306	118	91
8	538	149	89
9	706	429	75
10[A]	0	0	0

[A]Samples from control volunteers

Table 11 – Average anti-PA and anti-LF antibody titres, and TNA levels in blood sera of AVP vaccinees. Measurement of antibody levels was performed with at least four replicates; TNA levels were measured in duplicates.

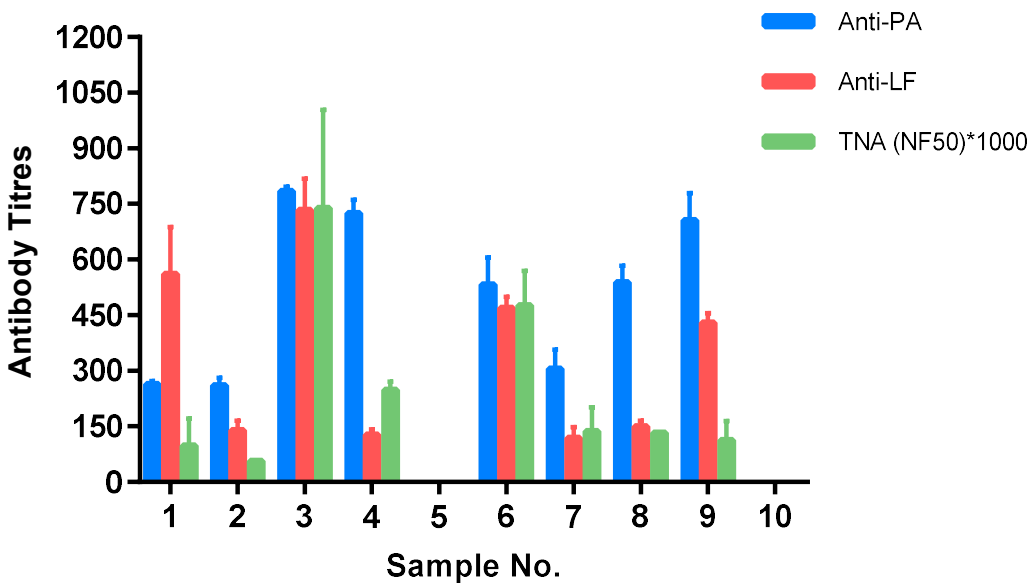

Figure 21 – Anti-PA antibody, Anti-LF antibody and TNA Levels in blood sera of AVP vaccinees. Measurement of antibody levels was performed with at least four replicates; TNA levels were measured in duplicates. Data has been plotted with 95% confidence interval about the mean. Sample 5 and 10 are from control volunteers.

An analysis of the vaccinee data in Tables 10 and 11 shows that there is no clear correlation between vaccinee immunisation history (whether the number and/or timing of vaccinations) and antibody titre (whether anti-PA and/or anti-LF antibody titre), nor between anti-PA and/or anti-LF antibody titre and TNA level (Figure 22). Although there is evidence that anti-PA antibodies and TNA levels have good correlation in human studies [135, 293, 294], strong correlation was not observed in this study, potentially due to the small sample size. Other studies have shown that antibody and TNA levels can be highly variable in AVA and AVP vaccinees [3, 160, 294]. It is likely that TNA levels are modulated by a range of other factors, such as age, gender, T cell and B cell memory, and genetic differences (including HLA allelic differences) in humans could be responsible for variable antibody levels [14, 169, 295]. Previous research had investigated the impact of HLA polymorphisms on anti-PA antibody response in AVA vaccinees and found that DRB1–DQA1–DQB1 haplotypes *1501–*0102–*0602, *0101–*0101–*0501 and *0102–*0101–*0501 were associated with significantly lower anti-PA antibody levels [163, 164]. However, it was not possible to identify such a correlation in this study.

Nevertheless, it is apparent that, whereas most vaccinees have higher anti-PA antibody titres than anti-LF titres, none of the vaccinees have low levels of anti-LF antibodies. Moreover, the TNA levels do not suggest that any vaccinees have negligible capacity to neutralise the anthrax toxin, although, in the absence of vaccinated humans becoming infected with *B. anthracis*, it is unclear what TNA levels are necessary to afford protection.

Given the current lack of knowledge about the TNA levels needed to provide protection against *B. anthracis* in humans, Anthrax vaccine studies have inevitable limitations, which are compounded here by the small-scale nature of the *in vitro* component of this study. Nevertheless, there are several important and novel conclusions.

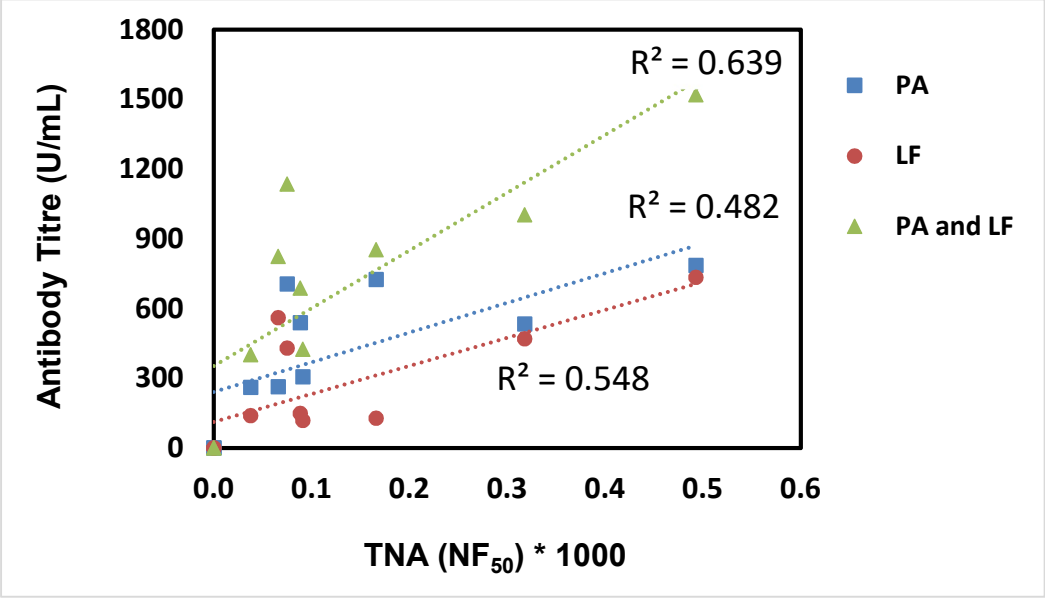

Figure 22 - Correlation between PA, LF and PA+LF antibody titres and TNA levels in blood sera of AVP vaccines was 0.482, 0.548 and 0.639 respectively. Measurement of antibody levels was performed with at least four replicates; TNA levels were measured in duplicates.

Although direct comparison of this study with other AVA studies is not possible, notably because of the different cell lines and different reference standard used for the TNA assay, it is interesting to contrast the results here with the large AVA study conducted by James and co-workers [25]. In that study, 69% of vaccinees had no detectable anti-LF antibodies, whereas all vaccinees in our study had moderate to high LF titres. Additionally, over 40% of the AVA vaccinees were deemed to have low toxin neutralisation activity; although it is hard to calibrate the TNA levels in our study, we do not see evidence of very low TNA activity, with only a single individual having a TNA (NF_{50})*1000 below 50. Taken together, these observations suggest that anti-LF antibody response from AVP potentially enhances protection, and are broadly consistent with previous observations about the efficacy of anti-LF antibodies in neutralising lethal toxin (formed by the association of PA and LF) [10, 11] and

about the speed and extent of the anti-LF antibody response in comparison to the anti-PA response in naturally-acquired cutaneous Anthrax patients [169].

5.4.3 Cytokine response

5.4.3.1 IFNγ response

PBMCs were found to be healthy when observed under the microscope. The cells were successfully stimulated with IMA/Ionomycin positive control, as expected. The average IFN**γ** response (pg/mL) was measured from PBMCs stimulated with rPA and rLF (Table 12, Figure 23). IFNγ response was measured in two biological replicates, read in duplicate.

Only AVP vaccinee sample 3 PBMCs showed a measurable IFNγ response when stimulated with rPA. Contrastingly, AVP vaccinee PBMCs samples 1, 3, 8 and 9 (50% of the sample set) showed a measurable IFNγ response when stimulated with rLF (Table 12, Figure 23).

Sample No.	rPA	rLF
1	0	477
2	0	0
3	130	623
4	0	0
5	0	0
6	0	0
7	0	0
8	0	91
9	0	398
10	0	661

Table 12 – IFNγ response in PBMCs from AVP vaccinees when stimulated with rPA or rLF

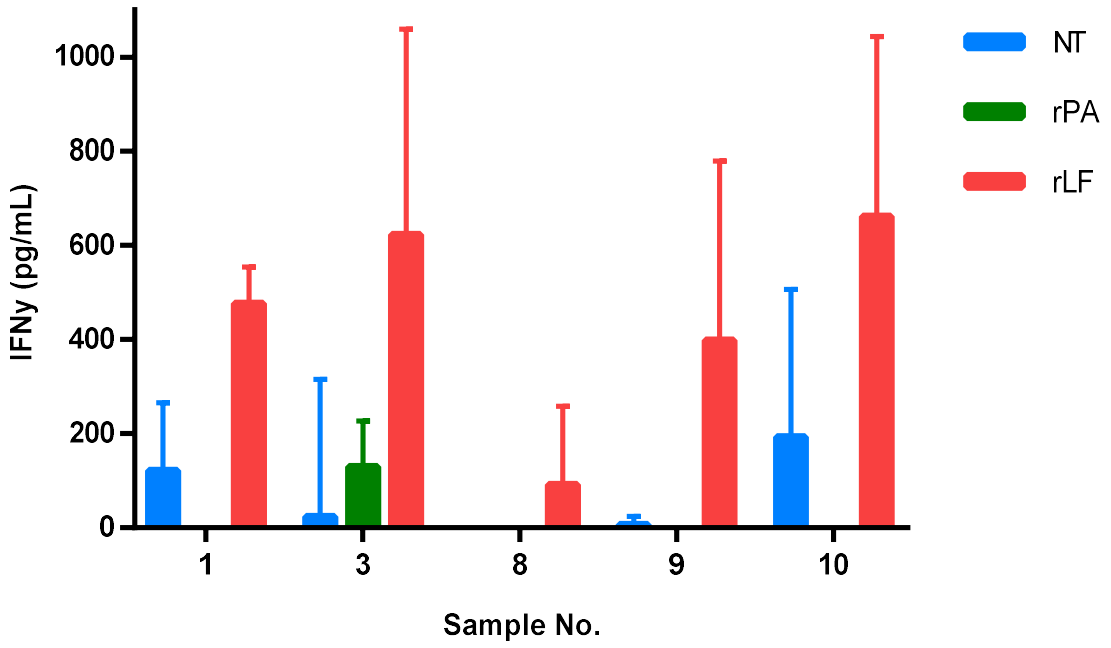

Figure 23 - IFNγ response in AVP vaccinees stimulated with rPA and rLF, only significant IFNγ response differences between non-treated and treated ($p<0.05$) have been reported with 95% confidence interval.

Again, the IFNγ levels were variable in AVP vaccinees. There are a number of factors that one might attribute such variation to, including: differences in the epitopes being presented by MHC molecules, and/or the impact of HLA haplotypes (i.e. different epitopes presented by different MHC molecules with a single individual); cytokine or cytokine receptor gene polymorphisms; differences in cell surface molecules, vaccination history, age, sex and/or environmental factors [160, 162, 163].

Control sample 5 PBMCs did not show IFNγ response when stimulated with rPA or rLF, as expected. Control sample 10 PBMCs showed a measurable IFNγ when stimulated with rLF (Figure 23). This was most certainly a non-specific response to rLF, as the anti-LF antibody titres was below the detection limit (Table 11). The sample did not show IFNγ response when stimulated with rPA. Ideally, the analysis should have been repeated, but due to lack of sample, this was not possible.

This data suggests that there is a longer-lasting T cell response to rLF than rPA in AVP vaccinees. Generally, AVP vaccinees who had their primary vaccination some years ago (Samples 2, 4 and 7 – immunisation in 2012, 1999 and 2007 respectively), did not show IFNγ response when stimulated with rPA or rLF. Only AVP vaccinee 6 had their primary vaccination in 2015, yet there was no IFNγ response from rPA or rLF.

Some attempts have been made to investigate the effect of HLA genotypes and haplotypes on cellular responses to PA. Ovsyannikova *et al.,* [295] have shown that AVA vaccinees with HLA-DQA1 and HLA-DQB1 homozygosity showed significantly decreased PA-specific lymphocyte proliferation in comparison to heterozygous individuals. Sample 6 PBMCs, from an individual who is homozygous at both HLA-DRB1 and HLA-DQB1 loci (Table 10), did not exhibit an IFNγ response to rPA or rLF, even though they had their primary immunisation recently (primary immunisation in 2015, booster in 2016). The individual's homozygosity at

both loci could explain the decreased cytokine response to rPA and rLF. Similarly, sample 2 PBMCs, from an individual who is homozygous at the HLA-DPB1 locus, did not exhibit an IFNy response to rPA and rLF. This individual was immunised in 2012 and had regular boosters every 2 years. However, due to the small sample size, it is not possible to make robust conclusion regarding the relationship between IFNy response and HLA homozygosity in AVP vaccinees.

The correlation between IFNy and anti-LF antibody titres (0.73) was considerably higher than that between IFNy and anti-PA antibody titres (0.21) (Figure 24). This data supports the hypothesis that LF has a T cell response that correlates with anti-LF antibody levels in AVP vaccinees. Previously, Ingram *et al.,* [169] had reported that a strong $CD4^+$ T cell response was observed in AVP vaccinees to LF only, whilst a T cell response to both PA and LF was observed in naturally-infected cutaneous Anthrax patients. Previous studies have concluded that PA-based humoral immunity may not be long lasting and that boosters may be essential [145, 293, 296-298]. This may be because of the shorter-lived memory T cell response from PA, as suggested by the results presented here.

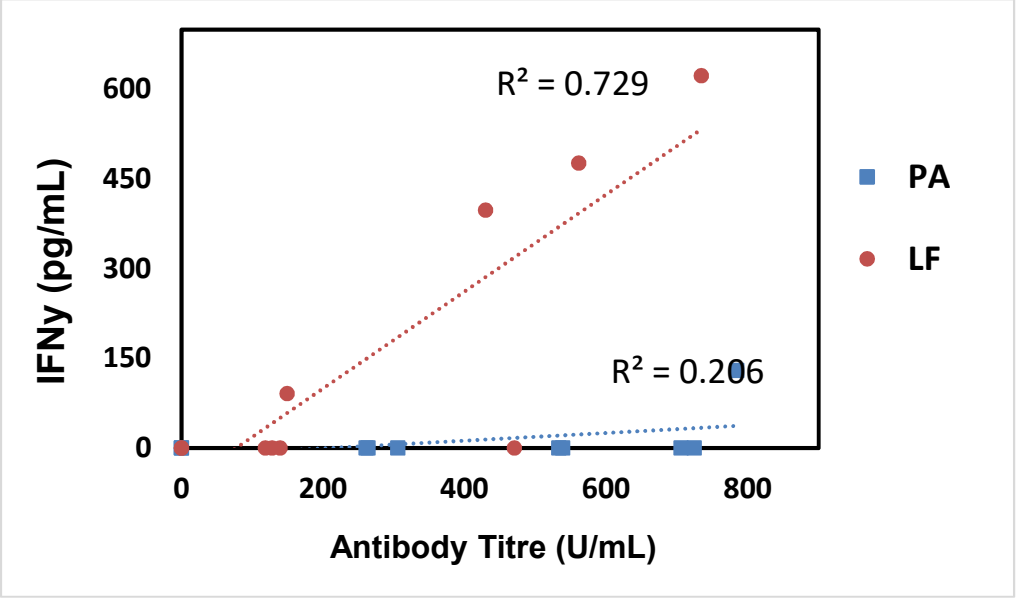

Figure 24 – Correlation between IFNy and Antibody levels. Only the significant IFNγ response differences between non-treated and treated ($p<0.05$) have been included in this comparison. IFNy cytokine response from control sample 10 was excluded from analysis.

There was no measurable IFNy response from PA peptides ($PA_{253-289}$, $PA_{633-669}$, $PA_{397-422}$, $PA_{501-526}$, $PA_{709-734}$) or LF peptides ($LF_{570-595}$, $LF_{650-675}$, $LF_{672-697}$, $LF_{710-735}$) in any of the samples. There are a number of possible explanations for this. It is possible that the assay was not optimised for IFNy response to rPA and rLF peptides. The availability of PBMCs from AVP vaccinees was the limiting factor, which meant that the optimisation work on the assay was also limited. Another possibility is that these epitopes are not immunodominant in these vaccinees. Further work would be required to investigate the underlying causes; however, this is beyond the scope of the current project.

5.4.3.2 IL10 cytokine response

There was no measurable IL10 response from rPA, rLF, PA peptides ($PA_{253-289}$, $PA_{633-669}$, $PA_{397-422}$, $PA_{501-526}$, $PA_{709-734}$) or LF peptides ($LF_{570-595}$, $LF_{650-675}$, $LF_{672-697}$, $LF_{710-735}$) in any of the

samples. This data confirmed that there is no IL10 response from rPA or rLF proteins in AVP vaccinees.

5.4.4 Limitations of this study

The major limitation of this study was that it was small, reflecting its proof-of-concept status. Consequently, it has been not been possible to draw firm conclusions regarding the effect of allelic differences in AVP vaccinees. In order to fully characterise the T cell response and contribution towards generation of protective antibodies, it would be necessary to conduct a large, ethnically diverse study (*e.g.* n=1000) with significant numbers of individuals of the same gender, and of similar age and vaccination history, *etc*.

In this study, another major problem was that the ELISA assay for measuring cytokines needed to be developed and optimised on study samples (PBMCs having memory response to AVP proteins is not available off the shelf). However, there were insufficient samples to conduct both these preliminary experiments and to repeat the sample analysis. In future, these issues should be given more consideration.

5.5 Conclusion

Anti-PA and anti-LF antibody data suggest that LF is an important component of AVP. Most vaccinees had high anti-PA antibody titres, but equally none of the vaccinees had low anti-LF antibodies levels. Although, it was not possible to differentiate the individual contribution of PA and LF towards TNA levels in AVP vaccinees, the presence of LF in AVP potentially enhances overall protection from AVP. Further, T cell study data supports the hypothesis that LF has a stronger T cell response than PA in AVP vaccinees. This is broadly consistent with data reported by Ingram *et al.*, [169] in AVP vaccinees and naturally infected cutaneous Anthrax patients.

6.0 CONCLUSION

6.1 Project Summary

LC-MS/MS studies found that AVP is a complex mixture of at least 138 *B. anthracis* proteins, including PA (65%), LF (8%) and EF (3%), using DIA based Hi3 label free quantitation. NetMHCIIpan predicted that peptides from all eight abundant proteins are likely to be presented to T cells, a pre-requisite for protection; however, the number of such peptides varied considerably for different HLA alleles. This work demonstrates that AVP contains many protein components that have not previously been identified and suggests that several proteins not normally considered relevant – notably LF, EF, PX01 and Chaperonin – are reasonably abundant within AVP and have the potential to afford protection for individuals with HLA allele combinations that are predicted to have relatively few PA epitopes.

These analyses highlighted two important properties of the AVP vaccine that have not been previously established. Firstly, the effectiveness of AVP within humans does not depend on PA alone; there is compelling evidence to suggest that LF has a protective role, with computational predictions suggesting that additional proteins may be important for individuals with specific HLA allele combinations. Secondly, in spite of differences in the sequences of key antigenic proteins from different *B. anthracis* strains, computational analysis suggested that these do not affect the protection that AVP affords to strains other than the vaccine's source strain. Nevertheless, there remains a small possibility that an individual's immunodominant vaccine response, induced by the Sterne strain, may be comparatively ineffective against a different strain if one or more critical epitopes are absent or different in that strain.

6.2 Future Directions

This work has demonstrated that AVP is composed of at least 138 proteins and computational studies have shown that many of these proteins are potentially important in inducing an immune response against Anthrax. Further work is needed to validate this data experimentally using *in vitro* MHC molecules and antigen-binding studies - by measuring binding affinity of antigen epitopes to MHC molecules using bio-layer interferometry technology or competitive ELISAs. Additionally, it would be beneficial to identify the frequency of cytokine-producing cells and visualise the T-cell response to a specific antigen using the intracellular cytokine staining method on a flow cytometer. It could also be combined with staining for phenotypic markers for identifying cell types (e.g. effector or memory T cell).

Intracellular cytokine staining (ICS) is a popular method for visualizing cellular responses, most often T-cell responses to antigenic or mitogenic stimulation. It can be coupled with staining for other functional markers, such as upregulation of CD107 or CD154, as well as phenotypic markers that define specific cellular subsets, e.g. effector and memory T-cell compartments.

Further, future studies should incorporate many more vaccinees and will need to explicitly evaluate the potential importance of HLA and protein specificity highlighted by the computational results. Further, AVP is known to have side effects (*e.g.* local reactions, fever and influenza-like symptoms). In future, it would be useful to identify proteins responsible for side effects and remove them from AVP to develop a next generation vaccine.

This work also shows the potential importance of considering inter-strain differences and identifies specific epitopes that are modified or absent in a subset of other *B. anthracis* strains. Further work is needed to identify whether these epitopes are important targets of the protective T cell response induced by the vaccine in some individuals.

7.0 REFERENCES

[1] Whiting G, Wheeler JX, Rijpkema S. Identification of peptide sequences as a measure of Anthrax vaccine stability during storage. Human vaccines & immunotherapeutics. 2014;10:1669-81. DOI: 10.4161/hv.28443.
[2] Whiting GC, Rijpkema S, Adams T, Corbel MJ. Characterisation of adsorbed anthrax vaccine by two-dimensional gel electrophoresis. Vaccine. 2004;22:4245-51. DOI: 10.1016/j.vaccine.2004.04.036.
[3] Dumas EK, Garman L, Cuthbertson H, Charlton S, Hallis B, Engler RJM, et al. Lethal factor antibodies contribute to lethal toxin neutralization in recipients of anthrax vaccine precipitated. Vaccine. 2017;35:3416-22. DOI: 10.1016/j.vaccine.2017.05.006.
[4] Turnbull PC. Anthrax vaccines: past, present and future. Vaccine. 1991;9:533-9. DOI: 10.1016/0264-410x(91)90237-z.
[5] Ivins BE, Pitt ML, Fellows PF, Farchaus JW, Benner GE, Waag DM, et al. Comparative efficacy of experimental anthrax vaccine candidates against inhalation anthrax in rhesus macaques. Vaccine. 1998;16:1141-8. DOI: 10.1016/s0264-410x(98)80112-6.
[6] Chen L, Schiffer JM, Dalton S, Sabourin CL, Niemuth NA, Plikaytis BD, et al. Comprehensive analysis and selection of anthrax vaccine adsorbed immune correlates of protection in rhesus macaques. Clinical and vaccine immunology : CVI. 2014;21:1512-20. DOI: 10.1128/CVI.00469-14.
[7] Brachman PS, Gold H, Plotkin SA, Fekety FR, Werrin M, Ingraham NR. Field Evaluation of a Human Anthrax Vaccine. Am J Public Health Nations Health. 1962;52:632-45. DOI: 10.2105/ajph.52.4.632.
[8] Price BM, Liner AL, Park S, Leppla SH, Mateczun A, Galloway DR. Protection against anthrax lethal toxin challenge by genetic immunization with a plasmid encoding the lethal factor protein. Infect Immun. 2001;69:4509-15. DOI: 10.1128/IAI.69.7.4509-4515.2001.
[9] Pezard C, Weber M, Sirard JC, Berche P, Mock M. Protective immunity induced by Bacillus anthracis toxin-deficient strains. Infect Immun. 1995;63:1369-72.
[10] Albrecht MT, Li H, Williamson ED, LeButt CS, Flick-Smith HC, Quinn CP, et al. Human monoclonal antibodies against anthrax lethal factor and protective antigen act independently to protect against Bacillus anthracis infection and enhance endogenous immunity to anthrax. Infect Immun. 2007;75:5425-33. DOI: 10.1128/IAI.00261-07.
[11] Staats HF, Alam SM, Scearce RM, Kirwan SM, Zhang JX, Gwinn WM, et al. In vitro and in vivo characterization of anthrax anti-protective antigen and anti-lethal factor monoclonal antibodies after passive transfer in a mouse lethal toxin challenge model to define correlates of immunity. Infect Immun. 2007;75:5443-52. DOI: 10.1128/IAI.00529-07.
[12] Winterroth L, Rivera J, Nakouzi AS, Dadachova E, Casadevall A. Neutralizing monoclonal antibody to edema toxin and its effect on murine anthrax. Infect Immun. 2010;78:2890-8. DOI: 10.1128/IAI.01101-09.
[13] Leysath CE, Chen KH, Moayeri M, Crown D, Fattah R, Chen Z, et al. Mouse monoclonal antibodies to anthrax edema factor protect against infection. Infect Immun. 2011;79:4609-16. DOI: 10.1128/IAI.05314-11.
[14] Dumas EK, Gross T, Larabee J, Pate L, Cuthbertson H, Charlton S, et al. Anthrax Vaccine Precipitated Induces Edema Toxin-Neutralizing, Edema Factor-Specific Antibodies in Human Recipients. Clinical and vaccine immunology : CVI. 2017;24. DOI: 10.1128/CVI.00165-17.
[15] Uchida M, Harada T, Enkhtuya J, Kusumoto A, Kobayashi Y, Chiba S, et al. Protective effect of Bacillus anthracis surface protein EA1 against anthrax in mice. Biochemical and biophysical research communications. 2012;421:323-8. DOI: 10.1016/j.bbrc.2012.04.007.
[16] Crowe SR, Ash LL, Engler RJ, Ballard JD, Harley JB, Farris AD, et al. Select human anthrax protective antigen epitope-specific antibodies provide protection from lethal toxin challenge. The Journal of infectious diseases. 2010;202:251-60. DOI: 10.1086/653495.
[17] CDC. Anthrax. 2015.
[18] PHE. Anthrax Vaccine Precipitated. 1 ed: Public Health England; 2014.

[19] Todar K. Online Textbook of Bacteriology. Bacillus anthracis and Anthrax2015.
[20] Driks A, Mallozzi M. Outer Structures of the *Bacillus anthracis* Spore. In: Bergman NH, editor. *Bacillus anthracis* and Anthrax. New Jersey: John Wiley and Sons; 2011. p. 17-38.
[21] Histroy of Vaccines. 2020.
[22] Fisher N, Carr KA, Giebel JD, Hanna PC. Anthrax Spore Germination. In: Bergman NH, editor. *Bacillus anthracis* and Anthrax. New Jersey: John Wiley and Sons; 2011. p. 39-52.
[23] Setlow P. Spore germination. Current opinion in microbiology. 2003;6:550-6.
[24] Moir A, Corfe BM, Behravan J. Spore germination. Cellular and molecular life sciences : CMLS. 2002;59:403-9.
[25] Driks A. The Bacillus anthracis spore. Molecular aspects of medicine. 2009;30:368-73. DOI: 10.1016/j.mam.2009.08.001.
[26] Leppla SH. Anthrax lethal factor. In: Rawlings ND, Salvesen GS, editors. Handbook of Proteolytic Enzymes. 3rd ed: Academic Press; 2013. p. 1257-61.
[27] Fouet A, Mock M. Regulatory networks for virulence and persistence of Bacillus anthracis. Curr Opin Microbiol. 2006;9:160-6.
[28] Liu S, Moayeri M, Leppla SH. Anthrax lethal and edema toxins in anthrax pathogenesis. Trends in microbiology. 2014;22:317-25. DOI: 10.1016/j.tim.2014.02.012.
[29] Baillie LW. Is new always better than old?: The development of human vaccines for anthrax. Human vaccines. 2009;5:806-16.
[30] BBC. http://www.bbc.co.uk/news/uk-scotland-glasgow-west-16424695. 2012.
[31] Altmann DM. Host immunity to Bacillus anthracis lethal factor and other immunogens: implications for vaccine design. Expert review of vaccines. 2015;14:429-34. DOI: 10.1586/14760584.2015.981533.
[32] Tasota FJ, Henker RA, Hoffman LA. Anthrax as a biological weapon: an old disease that poses a new threat. Critical care nurse. 2002;22:21-32, 4; quiz 5-6.
[33] Saile E, Quinn CP. Anthrax Vaccines. In: Bergman NH, editor. Anthrax Vaccines in Bacillus anthracis and anthrax: Wiley-Blackwell and sons; 2011. p. 269-93.
[34] Keim P, Smith KL, Keys C, Takahashi H, Kurata T, Kaufmann A. Molecular investigation of the Aum Shinrikyo anthrax release in Kameido, Japan. Journal of clinical microbiology. 2001;39:4566-7. DOI: 10.1128/JCM.39.12.4566-4567.2001.
[35] WHO. Anthrax in humans and animals. 2008. DOI: http://whqlibdoc.who.int/publications/2008/9789241547536_eng.pdf?ua=1.
[36] Athamna A, Athamna M, Abu-Rashed N, Medlej B, Bast DJ, Rubinstein E. Selection of Bacillus anthracis isolates resistant to antibiotics. J Antimicrob Chemother. 2004;54:424-8. DOI: 10.1093/jac/dkh258.
[37] Price LB, Vogler A, Pearson T, Busch JD, Schupp JM, Keim P. In vitro selection and characterization of Bacillus anthracis mutants with high-level resistance to ciprofloxacin. Antimicrob Agents Chemother. 2003;47:2362-5. DOI: 10.1128/aac.47.7.2362-2365.2003.
[38] Brook I, Elliott TB, Pryor HI, 2nd, Sautter TE, Gnade BT, Thakar JH, et al. In vitro resistance of Bacillus anthracis Sterne to doxycycline, macrolides and quinolones. Int J Antimicrob Agents. 2001;18:559-62. DOI: 10.1016/s0924-8579(01)00464-2.
[39] Pomerantsev AP, Shishkova NA, Marinin LI. [Comparison of therapeutic effects of antibiotics of the tetracycline group in the treatment of anthrax caused by a strain inheriting tet-gene of plasmid pBC16]. Antibiot Khimioter. 1992;37:31-4.
[40] Cavallo JD, Ramisse F, Girardet M, Vaissaire J, Mock M, Hernandez E. Antibiotic susceptibilities of 96 isolates of Bacillus anthracis isolated in France between 1994 and 2000. Antimicrob Agents Chemother. 2002;46:2307-9. DOI: 10.1128/aac.46.7.2307-2309.2002.
[41] Wright JG, Quinn CP, Shadomy S, Messonnier N. Use of anthrax vaccine in the United States: recommendations of the Advisory Committee on Immunization Practices (ACIP). MMWR Recomm Rep 2010. 2010;59:1-30. DOI: http://www.cdc.gov/mmwr/preview/mmwrhtml/rr5906a1.htm.

[42] Leuber M, Kronhardt A, Tonello F, Dal Molin F, Benz R. Binding of N-terminal fragments of anthrax edema factor (EF(N)) and lethal factor (LF(N)) to the protective antigen pore. Biochimica et biophysica acta. 2008;1778:1436-43. DOI: 10.1016/j.bbamem.2008.01.007.
[43] Petosa C, Collier RJ, Klimpel KR, Leppla SH, Liddington RC. Crystal structure of the anthrax toxin protective antigen. Nature. 1997;385:833-8. DOI: 10.1038/385833a0.
[44] Young JA, Collier RJ. Anthrax toxin: receptor binding, internalization, pore formation, and translocation. Annual review of biochemistry. 2007;76:243-65. DOI: 10.1146/annurev.biochem.75.103004.142728.
[45] Vuyisich M, Sanders CK, Graves SW. Binding and cell intoxication studies of anthrax lethal toxin. Molecular biology reports. 2012;39:5897-903. DOI: 10.1007/s11033-011-1401-2.
[46] Bradley KA, Mogridge J, Mourez M, Collier RJ, Young JA. Identification of the cellular receptor for anthrax toxin. Nature. 2001;414:225-9. DOI: 10.1038/n35101999.
[47] Thoren KL, Krantz BA. The unfolding story of anthrax toxin translocation. Molecular microbiology. 2011;80:588-95. DOI: 10.1111/j.1365-2958.2011.07614.x.
[48] Scobie HM, Rainey GJ, Bradley KA, Young JA. Human capillary morphogenesis protein 2 functions as an anthrax toxin receptor. Proc Natl Acad Sci U S A 2003;100:5170-4.
[49] Abrami L, Liu S, Cosson P, Leppla SH, van der Goot FG. Anthrax toxin triggers endocytosis of its receptor via a lipid raft-mediated clathrin-dependent process. The Journal of cell biology. 2003;160:321-8. DOI: 10.1083/jcb.200211018.
[50] Collier RJ. Membrane translocation by anthrax toxin. Molecular aspects of medicine. 2009;30:413-22. DOI: 10.1016/j.mam.2009.06.003.
[51] Miller CJ, Elliott JL, Collier RJ. Anthrax protective antigen: preporeto-pore conversion. Biochemistry. 1999;38:10432-41.
[52] Nassi S, Collier RJ, Finkelstein A. PA63 channel of anthrax toxin: an extended beta-barrel. Biochemistry. 2002;41:1445-50.
[53] Pannifer AD, Wong TY, Schwarzenbacher R, Renatus M, Petosa C, Bienkowska J, et al. Crystal structure of the anthrax lethal factor. Nature. 2001;414:229-33. DOI: 10.1038/n35101998.
[54] Klimpel KR, Arora N, Leppla SH. Anthrax toxin lethal factor contains a zinc metalloprotease consensus sequence which is required for lethal toxin activity. Molecular microbiology. 1994;13:1093-100.
[55] Zhang YL, Dong C. MAP kinases in immune responses. Cellular & molecular immunology. 2005;2:20-7.
[56] Duesbery NS, Webb CP, Leppla SH, Gordon VM, Klimpel KR, Copeland TD, et al. Proteolytic inactivation of MAP-kinase-kinase by anthrax lethal factor. Science. 1998;280:734-7.
[57] Moayeri M, Leppla SH. Cellular and systemic effects of anthrax lethal toxin and edema toxin. Molecular aspects of medicine. 2009;30:439-55. DOI: 10.1016/j.mam.2009.07.003.
[58] Pellizzari R, Guidi-Rontani C, Vitale G, Mock M, Montecucco C. Anthrax lethal factor cleaves MKK3 in macrophages and inhibits the LPS/IFNgamma-induced release of NO and TNFalpha. FEBS letters. 1999;462:199-204.
[59] Vitale G, Bernardi L, Napolitani G, Mock M, Montecucco C. Susceptibility of mitogen-activated protein kinase kinase family members to proteolysis by anthrax lethal factor. The Biochemical journal. 2000;352 Pt 3:739-45.
[60] Vitale G, Pellizzari R, Recchi C, Napolitani G, Mock M, Montecucco C. Anthrax lethal factor cleaves the N-terminus of MAPKKs and induces tyrosine/threonine phosphorylation of MAPKs in cultured macrophages. Biochemical and biophysical research communications. 1998;248:706-11. DOI: 10.1006/bbrc.1998.9040.
[61] Rincon M, Flavell RA, Davis RA. The JNK and P38 MAP kinase signaling pathways in T cell-mediated immune responses. Free radical biology & medicine. 2000;28:1328-37.
[62] Leppla SH. Anthrax toxin edema factor: a bacterial adenylate cyclase that increases cyclic AMP concentrations of eukaryotic cells. Proceedings of the National Academy of Sciences of the United States of America. 1982;79:3162-6.

[63] Gnade BT, Moen ST, Chopra AK, Peterson JW, Yeager LA. Emergence of Anthrax Edema Toxin as a Master Manipulator of Macrophage and B Cell Functions. Toxins. 2010;2:1881-97. DOI: 10.3390/toxins2071881.
[64] Tournier JN, Rossi Paccani S, Quesnel-Hellmann A, Baldari CT. Anthrax toxins: a weapon to systematically dismantle the host immune defenses. Molecular aspects of medicine. 2009;30:456-66. DOI: 10.1016/j.mam.2009.06.002.
[65] Choi YS, Kageyama R, Eto D, Escobar TC, Johnston RJ, Monticelli L, et al. ICOS receptor instructs T follicular helper cell versus effector cell differentiation via induction of the transcriptional repressor Bcl6. Immunity. 2011;34:932-46. DOI: 10.1016/j.immuni.2011.03.023.
[66] Aljurayyan A, Puksuriwong S, Ahmed M, Sharma R, Krishnan M, Sood S, et al. Activation and Induction of Antigen-Specific T Follicular Helper Cells Play a Critical Role in Live-Attenuated Influenza Vaccine-Induced Human Mucosal Anti-influenza Antibody Response. J Virol. 2018;92. DOI: 10.1128/JVI.00114-18.
[67] Kipps TJ. Williams Hematology - Chapter 5: The Organization and Structure of Lymphoid Tissues. 8th edition ed2010.
[68] Glomski IJ, Piris-Gimenez A, Huerre M, Mock M, Goossens PL. Primary involvement of pharynx and peyer's patch in inhalational and intestinal anthrax. PLoS pathogens. 2007;3:e76. DOI: 10.1371/journal.ppat.0030076.
[69] Moayeri M, Crown D, Newman ZL, Okugawa S, Eckhaus M, Cataisson C, et al. Inflammasome sensor Nlrp1b-dependent resistance to anthrax is mediated by caspase-1, IL-1 signaling and neutrophil recruitment. PLoS pathogens. 2010;6:e1001222. DOI: 10.1371/journal.ppat.1001222.
[70] During RL, Li W, Hao B, Koenig JM, Stephens DS, Quinn CP, et al. Anthrax lethal toxin paralyzes neutrophil actin-based motility. The Journal of infectious diseases. 2005;192:837-45. DOI: 10.1086/432516.
[71] Szarowicz SE, During RL, Li W, Quinn CP, Tang WJ, Southwick FS. Bacillus anthracis edema toxin impairs neutrophil actin-based motility. Infect Immun. 2009;77:2455-64. DOI: 10.1128/IAI.00839-08.
[72] Crawford MA, Aylott CV, Bourdeau RW, Bokoch GM. Bacillus anthracis toxins inhibit human neutrophil NADPH oxidase activity. Journal of immunology. 2006;176:7557-65.
[73] Serbina NV, Jia T, Hohl TM, Pamer EG. Monocyte-mediated defense against microbial pathogens. Annu Rev Immunol 2008;26:421-52. DOI: 10.1146/annurev.immunol.26.021607.090326.
[74] Chauncey KM, Lopez C, Sidhu G, Szarowicz SE, Baker HV, Quinn C, et al. Bacillus anthracis' lethal toxin induces broad transcriptional responses in human peripheral monocytes. BMC Immunology. 2012;13:33. DOI: 10.1186/1471-2172-13-33.
[75] Mosser DM. The many faces of macrophage activation. Journal of leukocyte biology. 2003;73:209-12.
[76] Koski GK, Lyakh LA, Rice NR. Rapid lipopolysaccharide-induced differentiation of CD14(+) monocytes into CD83(+) dendritic cells is modulated under serum-free conditions by exogenously added IFN-gamma and endogenously produced IL-10. Eur J Immunol. 2001;31:3773-81.
[77] van Furth R. Origin and turnover of monocytes and macrophages. Current topics in pathology Ergebnisse der Pathologie. 1989;79:125-50.
[78] Dozmorov M, Wu W, Chakrabarty K, Booth JL, Hurst RE, Coggeshall KM, et al. Gene expression profiling of human alveolar macrophages infected by B. anthracis spores demonstrates TNF-alpha and NF-kappab are key components of the innate immune response to the pathogen. BMC infectious diseases. 2009;9:152. DOI: 10.1186/1471-2334-9-152.
[79] Chaussabel D, Semnani RT, McDowell MA, Sacks D, Sher A, Nutman TB. Unique gene expression profiles of human macrophages and dendritic cells to phylogenetically distinct parasites. Blood. 2003;102:672-81. DOI: 10.1182/blood-2002-10-3232.
[80] Kassam A, Der SD, Mogridge J. Differentiation of human monocytic cell lines confers susceptibility to Bacillus anthracis lethal toxin. Cellular microbiology. 2005;7:281-92. DOI: 10.1111/j.1462-5822.2004.00458.x.

[81] Tournier JN, Paccani SR, Quesnel-Hellmann A, Baldari CT. Anthrax toxins: a weapon to systematically dismantle the host immune defenses. Mol Aspects Med. 2009;30:456-66. DOI: 10.1016/j.mam.2009.06.002.
[82] Bailly S, Ferrua B, Fay M, Gougerot-Pocidalo MA. Differential regulation of IL 6, IL 1 A, IL 1 beta and TNF alpha production in LPS-stimulated human monocytes: role of cyclic AMP. Cytokine. 1990;2:205-10.
[83] Hoover DL, Friedlander AM, Rogers LC, Yoon IK, Warren RL, Cross AS. Anthrax edema toxin differentially regulates lipopolysaccharide-induced monocyte production of tumor necrosis factor alpha and interleukin-6 by increasing intracellular cyclic AMP. Infect Immun. 1994;62:4432-9.
[84] Ingram RJ, Harris A, Ascough S, Metan G, Doganay M, Ballie L, et al. Exposure to anthrax toxin alters human leucocyte expression of anthrax toxin receptor 1. Clin Exp Immunol. 2013;173:84-91. DOI: 10.1111/cei.12090.
[85] Erwin JL, Dasilva LM, Bavari S, Little SF, Friedlander AM, Chanh TC, et al. Macrophage-Derived Cell Lines Do Not Express Proinflammatory Cytokines after Exposure to Bacillus anthracis Lethal Toxin. Infection and Immunity. 2001. DOI: 10.1128/IAI.69.2.1175-1177.2001.
[86] Paccani RS, Tonello F, Patrussi L, Capitani N, Simonato M, Montecucco C, et al. Anthrax toxins inhibit immune cell chemotaxis by perturbing chemokine receptor signalling. Cell Microbiol 2007;9:924-9.
[87] Fink SL, Bergsbaken T, Cookson BT. Anthrax lethal toxin and Salmonella elicit the common cell death pathway of caspase-1-dependent pyroptosis via distinct mechanisms. Proceedings of the National Academy of Sciences of the United States of America. 2008;105:4312-7. DOI: 10.1073/pnas.0707370105.
[88] Wickliffe KE, Leppla SH, Moayeri M. Killing of macrophages by anthrax lethal toxin: involvement of the N-end rule pathway. Cellular microbiology. 2008;10:1352-62. DOI: 10.1111/j.1462-5822.2008.01131.x.
[89] Yeager LA, Chopra AK, Peterson JW. Bacillus anthracis edema toxin suppresses human macrophage phagocytosis and cytoskeletal remodeling via the protein kinase A and exchange protein activated by cyclic AMP pathways. Infect Immun. 2009;77:2530-43. DOI: 10.1128/IAI.00905-08.
[90] Kau JH, Sun DS, Huang HS, Lien TS, Huang HH, Lin HC, et al. Sublethal doses of anthrax lethal toxin on the suppression of macrophage phagocytosis. PLoS One. 2010;5:e14289. DOI: 10.1371/journal.pone.0014289.
[91] Comer JE, Chopra AK, Peterson JW, Konig R. Direct inhibition of T-lymphocyte activation by anthrax toxins in vivo. Infect Immun. 2005;73:8275-81. DOI: 10.1128/IAI.73.12.8275-8281.2005.
[92] Kim C, Wilcox-Adelman S, Sano Y, Tang WJ, Collier RJ, Park JM. Antiinflammatory cAMP signaling and cell migration genes co-opted by the anthrax bacillus. Proceedings of the National Academy of Sciences of the United States of America. 2008;105:6150-5. DOI: 10.1073/pnas.0800105105.
[93] Cleret-Buhot A, Mathieu J, Tournier J, Quesnel-Hellmann A. Both Lethal and Edema Toxins of Bacillus anthracis Disrupt the Human Dendritic Cell Chemokine Network. PLoS One. 2012;7:e43266. DOI: 10.1371/journal.pone.0043266.
[94] Bettelli E, Korn T, Oukka M, Kuchroo VK. Induction and effector functions of T(H)17 cells. Nature. 2008;453:1051-7. DOI: 10.1038/nature07036.
[95] Dong C. TH17 cells in development: an updated view of their molecular identity and genetic programming. Nat Rev Immunol 2008;8:337-48. DOI: 10.1038/nri2295.
[96] Agrawal A, Lingappa J, Leppla SH, Agrawal S, Jabbar A, Quinn C, et al. Impairment of dendritic cells and adaptive immunity by anthrax lethal toxin. Nature. 2003;424:329-34. DOI: 10.1038/nature01794.
[97] Tournier JN, Quesnel-Hellmann A, Mathieu J, Montecucco C, Tang WJ, Mock M, et al. Anthrax edema toxin cooperates with lethal toxin to impair cytokine secretion during infection of dendritic cells. Journal of immunology. 2005;174:4934-41.
[98] Cleret A, Quesnel-Hellmann A, Mathieu J, Vidal D, Tournier JN. Resident CD11c+ lung cells are impaired by anthrax toxins after spore infection. The Journal of infectious diseases. 2006;194:86-94. DOI: 10.1086/504686.

[99] Brittingham KC, Ruthel G, Panchal RG, Fuller CL, Ribot WJ, Hoover TA, et al. Dendritic cells endocytose Bacillus anthracis spores: implications for anthrax pathogenesis. Journal of immunology. 2005;174:5545-52.
[100] Hahn AC, Lyons CR, Lipscomb MF. Effect of Bacillus anthracis virulence factors on human dendritic cell activation. Human immunology. 2008;69:552-61. DOI: 10.1016/j.humimm.2008.06.012.
[101] Raymond B, Batsche E, Boutillon F, Wu YZ, Leduc D, Balloy V, et al. Anthrax lethal toxin impairs IL-8 expression in epithelial cells through inhibition of histone H3 modification. PLoS Pathog 2009;5:e1000359. DOI: 10.1371/journal.ppat.1000359.
[102] Reig N, Jiang A, Couture R, Sutterwala FS, Ogura Y, Flavell RA, et al. Maturation modulates caspase-1-independent responses of dendritic cells to Anthrax lethal toxin. Cellular microbiology. 2008;10:1190-207. DOI: 10.1111/j.1462-5822.2008.01121.x.
[103] Maldonado-Arocho FJ, Bradley KA. Anthrax edema toxin induces maturation of dendritic cells and enhances chemotaxis towards macrophage inflammatory protein 3beta. Infect Immun. 2009;77:2036-42. DOI: 10.1128/IAI.01329-08.
[104] Hu H, Leppla SH. Anthrax toxin uptake by primary immune cells as determined with a lethal factor-beta-lactamase fusion protein. PLoS One. 2009;4:e7946. DOI: 10.1371/journal.pone.0007946.
[105] Premanandan C, Lairmore MD, Fernandez S, Phipps AJ. Quantitative measurement of anthrax toxin receptor messenger RNA in primary mononuclear phagocytes. Microbial pathogenesis. 2006;41:193-8. DOI: 10.1016/j.micpath.2006.05.003.
[106] Mosenden R, Tasken K. Cyclic AMP-mediated immune regulation--overview of mechanisms of action in T cells. Cellular signalling. 2011;23:1009-16. DOI: 10.1016/j.cellsig.2010.11.018.
[107] Paccani SR, Baldari CT. T cell targeting by anthrax toxins: two faces of the same coin. Toxins. 2011;3:660-71. DOI: 10.3390/toxins3060660.
[108] Paccani SR, Tonello F, Ghittoni R, Natale M, Muraro L, D'Elios MM, et al. Anthrax toxins suppress T lymphocyte activation by disrupting antigen receptor signaling. The Journal of experimental medicine. 2005;201:325-31. DOI: 10.1084/jem.20041557.
[109] Fang H, Cordoba-Rodriguez R, Lankford CS, Frucht DM. Anthrax lethal toxin blocks MAPK kinase-dependent IL-2 production in CD4+ T cells. Journal of immunology. 2005;174:4966-71.
[110] Fimia GM, Sassone-Corsi P. Cyclic AMP signalling. Journal of cell science. 2001;114:1971-2.
[111] Dal Molin F, Tonello F, Ladant D, Zornetta I, Zamparo I, Di Benedetto G, et al. Cell entry and cAMP imaging of anthrax edema toxin. The EMBO journal. 2006;25:5405-13. DOI: 10.1038/sj.emboj.7601408.
[112] Zornetta I, Brandi L, Janowiak B, Dal Molin F, Tonello F, Collier RJ, et al. Imaging the cell entry of the anthrax oedema and lethal toxins with fluorescent protein chimeras. Cellular microbiology. 2010;12:1435-45. DOI: 10.1111/j.1462-5822.2010.01480.x.
[113] Rossi Paccani S, Benagiano M, Capitani N, Zornetta I, Ladant D, Montecucco C, et al. The adenylate cyclase toxins of Bacillus anthracis and Bordetella pertussis promote Th2 cell development by shaping T cell antigen receptor signaling. PLoS pathogens. 2009;5:e1000325. DOI: 10.1371/journal.ppat.1000325.
[114] Viola A, Contento RL, Molon B. T cells and their partners: the chemokine dating agency. Trends in immunology. 2006;27:421-7.
[115] Sakata D, Yao C, Narumiya S. Prostaglandin E2, an immunoactivator. Journal of pharmacological sciences. 2010;112:1-5.
[116] Napolitani G, Acosta-Rodriguez EV, Lanzavecchia A, Sallusto F. Prostaglandin E2 enhances Th17 responses via modulation of IL-17 and IFN-gamma production by memory CD4+ T cells. European journal of immunology. 2009;39:1301-12. DOI: 10.1002/eji.200838969.
[117] Boniface K, Bak-Jensen KS, Li Y, Blumenschein WM, McGeachy MJ, McClanahan TK, et al. Prostaglandin E2 regulates Th17 cell differentiation and function through cyclic AMP and EP2/EP4 receptor signaling. J Exp Med. 2009;206:535-48. DOI: 10.1084/jem.20082293.
[118] Murphy KM, Stockinger B. Effector T cell plasticity: flexibility in the face of changing circumstances. Nature immunology. 2010;11:674-80. DOI: 10.1038/ni.1899.

[119] Zhou L, Littman DR. Transcriptional regulatory networks in Th17 cell differentiation. Current opinion in immunology. 2009;21:146-52. DOI: 10.1016/j.coi.2009.03.001.
[120] Zhu J, Yamane H, Paul WE. Differentiation of effector CD4 T cell populations. Annual review of immunology. 2010;28:445-89. DOI: 10.1146/annurev-immunol-030409-101212.
[121] Paccani SR, Benagiano M, Savino MT, Finetti F, Tonello F, D'Elios MM, et al. The adenylate cyclase toxin of Bacillus anthracis is a potent promoter of T(H)17 cell development. J Allergy Clin Immunol 2011;127:1635-7. DOI: 10.1016/j.jaci.2010.12.1104.
[122] Fang H, Xu L, Chen TY, Cyr JM, Frucht DM. Anthrax lethal toxin has direct and potent inhibitory effects on B cell proliferation and immunoglobulin production. J Immunol 2006;176:6155-61.
[123] Baillie LW, Huwar TB, Moore S, Mellado-Sanchez G, Rodriguez L, Neeson BN, et al. An anthrax subunit vaccine candidate based on protective regions of Bacillus anthracis protective antigen and lethal factor. Vaccine. 2010;28:6740-8.
[124] McHeyzer-Williams LJ, Pelletier N, Mark L, Fazilleau N, McHeyzer-Williams MG. Follicular helper T cells as cognate regulators of B cell immunity. Curr Opin Immunol. 2009;21:266-73. DOI: 10.1016/j.coi.2009.05.010.
[125] Berkowska MA, Driessen GJ, Bikos V, Grosserichter-Wagener C, Stamatopoulos K, Cerutti A, et al. Human memory B cells originate from three distinct germinal center-dependent and -independent maturation pathways. Blood. 2011;118:2150-8. DOI: 10.1182/blood-2011-04-345579.
[126] O'Garra A, Robinson D. Development and function of T helper 1 cells. Advances in immunology. 2004;83:133-62. DOI: 10.1016/S0065-2776(04)83004-9.
[127] Lee GR, Kim ST, Spilianakis CG, Fields PE, Flavell RA. T helper cell differentiation: regulation by cis elements and epigenetics. Immunity. 2006;24:369-79. DOI: 10.1016/j.immuni.2006.03.007.
[128] Kubo S, Takahashi HK, Takei M, Iwagaki H, Yoshino T, Tanaka N, et al. E-prostanoid (EP)2/EP4 receptor-dependent maturation of human monocyte-derived dendritic cells and induction of helper T2 polarization. The Journal of pharmacology and experimental therapeutics. 2004;309:1213-20. DOI: 10.1124/jpet.103.062646.
[129] Tokoyoda K, Tsujikawa K, Matsushita H, Ono Y, Hayashi T, Harada Y, et al. Up-regulation of IL-4 production by the activated cAMP/cAMP-dependent protein kinase (protein kinase A) pathway in CD3/CD28-stimulated naive T cells. International immunology. 2004;16:643-53. DOI: 10.1093/intimm/dxh072.
[130] Nirula A, Ho M, Phee H, Roose J, Weiss A. Phosphoinositide-dependent kinase 1 targets protein kinase A in a pathway that regulates interleukin 4. The Journal of experimental medicine. 2006;203:1733-44. DOI: 10.1084/jem.20051715.
[131] Klein-Hessling S, Jha MK, Santner-Nanan B, Berberich-Siebelt F, Baumruker T, Schimpl A, et al. Protein kinase A regulates GATA-3-dependent activation of IL-5 gene expression in Th2 cells. Journal of immunology. 2003;170:2956-61.
[132] Clement KH, Rudge TL, Jr., Mayfield HJ, Carlton LA, Hester A, Niemuth NA, et al. Vaccination of rhesus macaques with the anthrax vaccine adsorbed vaccine produces a serum antibody response that effectively neutralizes receptor-bound protective antigen in vitro. Clinical and vaccine immunology : CVI. 2010;17:1753-62. DOI: 10.1128/CVI.00174-10.
[133] Little SF, Ivins BE, Fellows PF, Friedlander AM. Passive protection by polyclonal antibodies against Bacillus anthracis infection in guinea pigs. Infect Immun. 1997;65:5171-5.
[134] Pitt ML, Little S, Ivins BE, Fellows P, Boles J, Barth J, et al. In vitro correlate of immunity in an animal model of inhalational anthrax. Journal of applied microbiology. 1999;87:304.
[135] Reuveny S, White MD, Adar YY, Kafri Y, Altboum Z, Gozes Y, et al. Search for correlates of protective immunity conferred by anthrax vaccine. Infect Immun. 2001;69:2888-93. DOI: 10.1128/IAI.69.5.2888-2893.2001.
[136] Welkos S, Little S, Friedlander A, Fritz D, Fellows P. The role of antibodies to Bacillus anthracis and anthrax toxin components in inhibiting the early stages of infection by anthrax spores. Microbiology. 2001;147:1677-85.

[137] Pitt ML, Little SF, Ivins BE, Fellows P, Barth J, Hewetson J, et al. In vitro correlate of immunity in a rabbit model of inhalational anthrax. Vaccine. 2001;19:4768-73.
[138] Little SF, Ivins BE, Fellows PF, Pitt ML, Norris SL, Andrews GP. Defining a serological correlate of protection in rabbits for a recombinant anthrax vaccine. Vaccine. 2004;22:422-30.
[139] Jawa V, Cousens LP, Awwad M, Wakshull E, Kropshofere H, De Groot AS. T-cell dependent immunogenicity of protein therapeutics: Preclinical assessment and mitigation. Clinical Immunology. 2013;149:534-55.
[140] Alberts B JA, Lewis J, et al. B Cells and Antibodies - Molecular Biology of the Cell.2002.
[141] Vidarsson G, Dekkers G, Rispens T. IgG subclasses and allotypes: from structure to effector functions. Frontiers in immunology. 2014;5:520. DOI: 10.3389/fimmu.2014.00520.
[142] Baillie LW, Fowler K, Turnbull PC. Human immune responses to the UK human anthrax vaccine. Journal of applied microbiology. 1999;87:306-8.
[143] Baillie L, Townend T, Walker N, Eriksson U, Williamson D. Characterization of the human immune response to the UK anthrax vaccine. FEMS immunology and medical microbiology. 2004;42:267-70. DOI: 10.1016/j.femsim.2004.05.011.
[144] Peterson JD, Herzenberg LA, Vasquez K, Waltenbaugh C. Glutathione levels in antigen-presenting cells modulate Th1 versus Th2 response patterns. Proceedings of the National Academy of Sciences of the United States of America. 1998;95:3071-6.
[145] Allen JS, Skowera A, Rubin GJ, Wessely S, Peakman M. Long-lasting T cell responses to biological warfare vaccines in human vaccinees. Clinical infectious diseases : an official publication of the Infectious Diseases Society of America. 2006;43:1-7. DOI: 10.1086/504806.
[146] Laughlin EM, Miller JD, James E, Fillos D, Ibegbu CC, Mittler RS, et al. Antigen-specific CD4+ T cells recognize epitopes of protective antigen following vaccination with an anthrax vaccine. Infect Immun. 2007;75:1852-60. DOI: 10.1128/IAI.01814-06.
[147] Kwok WW, Yang J, James E, Bui J, Huston L, Wiesen AR, et al. The anthrax vaccine adsorbed vaccine generates protective antigen (PA)-Specific CD4+ T cells with a phenotype distinct from that of naive PA T cells. Infect Immun 2008;76:4538-45. DOI: 10.1128/IAI.00324-08.
[148] Henderson DW, Peacock S, Belton FC. Observations on the prophylaxis of experimental pulmonary anthrax in the monkey. J Hygiene 1956;1:28-36.
[149] Hambleton P, Carman JA, Melling K. Anthrax: the disease in relation to vaccines. Vaccine. 1984;2:125-32.
[150] Darlow HM, Belton FC, Henderson DW. The use of anthrax antigen to immunise man and monkey. The Lancet. 1956;Sep 8 476-9.
[151] Belton FC, Strange RE. Studies on a protective antigen produced in vitro from Bacillus anthracis: medium and methods of production. Br J Exp Pathol. 1954;35:144-52.
[152] Schiffer JM, Chen L, Dalton S, Niemuth NA, Sabourin CL, Quinn CP. Bridging non-human primate correlates of protection to reassess the Anthrax Vaccine Adsorbed booster schedule in humans. Vaccine. 2015;33:3709-16. DOI: 10.1016/j.vaccine.2015.05.091.
[153] Turnbull PC, Broster MG, Carman JA, Manchee RJ, Melling J. Development of antibodies to protective antigen and lethal factor components of anthrax toxin in humans and guinea pigs and their relevance to protective immunity. Infect Immun. 1986;52:356-63.
[154] Turnbull PC, Leppla SH, Broster MG, Quinn CP, Melling J. Antibodies to anthrax toxin in humans and guinea pigs and their relevance to protective immunity. Med Microbiol Immunol 1988;177:293-303.
[155] Broster MG, Hibbs SE. Protective efficacy of anthrax vaccines against aerosol challenge. . Salisbury Medical Bulletin. 1990:91-2.
[156] Little SF, Knudson GB. Comparative efficacy of Bacillus anthracis live spore vaccine and protective antigen vaccine against anthrax in the guinea pig. Infect Immun. 1986;52:509-12.
[157] Fellows PF, Linscott MK, Ivins BE, Pitt ML, Rossi CA, Gibbs PH, et al. Efficacy of a human anthrax vaccine in guinea pigs, rabbits, and rhesus macaques against challenge by Bacillus anthracis isolates of diverse geographical origin. Vaccine. 2001;19:3241-7. DOI: 10.1016/s0264-410x(01)00021-4.

[158] Quinn CP, Dull PM, Semenova V, Li H, Crotty S, Taylor TH, et al. Immune responses to Bacillus anthracis protective antigen in patients with bioterrorism-related cutaneous or inhalation anthrax. The Journal of infectious diseases. 2004;190:1228-36. DOI: 10.1086/423937.
[159] Dumas EK, Nguyen ML, Cox PM, Rodgers H, Peterson JL, James JA, et al. Stochastic humoral immunity to Bacillus anthracis protective antigen: identification of anti-peptide IgG correlating with seroconversion to Lethal Toxin neutralization. Vaccine. 2013;31:1856-63. DOI: 10.1016/j.vaccine.2013.01.040.
[160] Crowe SR, Garman L, Engler RJ, Farris AD, Ballard JD, Harley JB, et al. Anthrax vaccination induced anti-lethal factor IgG: fine specificity and neutralizing capacity. Vaccine. 2011;29:3670-8.
[161] Marano N, Plikaytis BD, Martin SW, Rose C, Semenova VA, Martin SK, et al. Effects of a reduced dose schedule and intramuscular administration of anthrax vaccine adsorbed on immunogenicity and safety at 7 months: a randomized trial. JAMA. 2008;300:1532-43.
[162] Ingram R, Baillie L. It's in the genes! Human genetic diversity and the response to anthrax vaccines. Expert review of vaccines. 2012;11:633-5. DOI: 10.1586/erv.12.41.
[163] Pajewski NM, Shrestha S, Quinn CP, Parker SD, Wiener H, Aissani B, et al. A genome-wide association study of host genetic determinants of the antibody response to Anthrax Vaccine Adsorbed. Vaccine. 2012;30:4778-84. DOI: 10.1016/j.vaccine.2012.05.032.
[164] Pajewski NM, Parker SD, Poland GA, Ovsyannikova IG, Song W, Zhang K, et al. The role of HLA-DR-DQ haplotypes in variable antibody responses to anthrax vaccine adsorbed. Genes Immun. 2011;12:457-65. DOI: 10.1038/gene.2011.15.
[165] Baillie L, Hebdon R, Flick-Smith H, Williamson D. Characterisation of the immune response to the UK human anthrax vaccine. FEMS Immunology & Medical Microbiology. 2003;36:83-6. DOI: 10.1016/s0928-8244(03)00085-3.
[166] Garman L, Smith K, Farris AD, Nelson MR, Engler RJ, James JA. Protective antigen-specific memory B cells persist years after anthrax vaccination and correlate with humoral immunity. Toxins. 2014;6:2424-31. DOI: 10.3390/toxins6082424.
[167] Moayeri M, Leppla SH. The roles of anthrax toxin in pathogenesis. Current opinion in microbiology. 2004;7:19-24. DOI: 10.1016/j.mib.2003.12.001.
[168] Puziss M, Manning LC, Lynch JW, Barclaye, Abelow I, Wright GG. Large-scale production of protective antigen of Bacillus anthracis in anaerobic cultures. Applied microbiology. 1963;11:330-4.
[169] Ingram RJ, Metan G, Maillere B, Doganay M, Ozkul Y, Kim LU, et al. Natural exposure to cutaneous anthrax gives long-lasting T cell immunity encompassing infection-specific epitopes. Journal of immunology. 2010;184:3814-21. DOI: 10.4049/jimmunol.0901581.
[170] Brenneman KE, Doganay M, Akmal A, Goldman S, Galloway DR, Mateczun AJ, et al. The early humoral immune response to Bacillus anthracis toxins in patients infected with cutaneous anthrax. FEMS immunology and medical microbiology. 2011;62:164-72. DOI: 10.1111/j.1574-695X.2011.00800.x.
[171] Zhang Y, Fonslow BR, Shan B, Baek MC, Yates JR, 3rd. Protein analysis by shotgun/bottom-up proteomics. Chemical reviews. 2013;113:2343-94. DOI: 10.1021/cr3003533.
[172] Hervey WJt, Strader MB, Hurst GB. Comparison of digestion protocols for microgram quantities of enriched protein samples. Journal of proteome research. 2007;6:3054-61. DOI: 10.1021/pr070159b.
[173] Strader MB, Tabb DL, Hervey WJ, Pan C, Hurst GB. Efficient and specific trypsin digestion of microgram to nanogram quantities of proteins in organic-aqueous solvent systems. Analytical chemistry. 2006;78:125-34. DOI: 10.1021/ac051348l.
[174] Chen EI, Cociorva D, Norris JL, Yates JR, 3rd. Optimization of mass spectrometry-compatible surfactants for shotgun proteomics. Journal of proteome research. 2007;6:2529-38. DOI: 10.1021/pr060682a.
[175] Sun L, Tao D, Han B, Ma J, Zhu G, Liang Z, et al. Ionic liquid 1-butyl-3-methyl imidazolium tetrafluoroborate for shotgun membrane proteomics. Analytical and bioanalytical chemistry. 2011;399:3387-97. DOI: 10.1007/s00216-010-4381-5.

[176] Shimadzu. http://www.shimadzu.com/an/lcms/support/faq/ms/lcms-intro.html. 2016.
[177] Deracinois BF, C.; Duban-Deweer, S.; Karamanos, Y. Comparative and Quantitaive Global Proteomics Approaches: An overview. Proteomes. 2013;1:180-218.
[178] Aebersold R, Mann M. Mass spectrometry-based proteomics. Nature. 2003;422:198-207. DOI: 10.1038/nature01511.
[179] Glish GL, Vachet RW. The basics of mass spectrometry in the twenty-first century. Nature reviews Drug discovery. 2003;2:140-50. DOI: 10.1038/nrd1011.
[180] Wilm M, Mann M. Analytical properties of the nanoelectrospray ion source. Analytical chemistry. 1996;68:1-8.
[181] Banerjee S, Mazumdar S. Electrospray ionization mass spectrometry: a technique to access the information beyond the molecular weight of the analyte. International journal of analytical chemistry. 2012;2012:282574. DOI: 10.1155/2012/282574.
[182] Karas M, Bahr U, Dulcks T. Nano-electrospray ionization mass spectrometry: addressing analytical problems beyond routine. Fresenius' journal of analytical chemistry. 2000;366:669-76.
[183] Asara JM, Christofk HR, Freimark LM, Cantley LC. A label-free quantification method by MS/MS TIC compared to SILAC and spectral counting in a proteomics screen. Proteomics. 2008;8:994-9. DOI: 10.1002/pmic.200700426.
[184] Mamyrin BA. Time-of-flight mass spectrometry (concepts, achievements, and prospects). International Journal of Mass Spectrometry and Ion Physics. 2001;206:251–66.
[185] Angel TE, Aryal UK, Hengel SM, Baker ES, Kelly RT, Robinson EW, et al. Mass spectrometry-based proteomics: existing capabilities and future directions. Chemical Society reviews. 2012;41:3912-28. DOI: 10.1039/c2cs15331a.
[186] Zubarev RA. Electron-capture dissociation tandem mass spectrometry. Current opinion in biotechnology. 2004;15:12-6. DOI: 10.1016/j.copbio.2003.12.002.
[187] Coon JJ, Shabanowitz J, Hunt DF, Syka JE. Electron transfer dissociation of peptide anions. Journal of the American Society for Mass Spectrometry. 2005;16:880-2. DOI: 10.1016/j.jasms.2005.01.015.
[188] DDA. http://www.inf.fu-berlin.de/lehre/WS14/ProteomicsWS14/LUS/lu4b/397/objects/il_1600_mob_1102140/nmeth1004-16-F1.gif. 2017.
[189] Doerr A. Data-independent acquisition (DIA) mass spectrometry may change how proteomic data are generated. Nature methods. 2015;12:35.
[190] Tabb DL, Vega-Montoto L, Rudnick PA, Variyath AM, Ham AJ, Bunk DM, et al. Repeatability and reproducibility in proteomic identifications by liquid chromatography-tandem mass spectrometry. Journal of proteome research. 2010;9:761-76. DOI: 10.1021/pr9006365.
[191] Rost HL, Rosenberger G, Navarro P, Gillet L, Miladinovic SM, Schubert OT, et al. OpenSWATH enables automated, targeted analysis of data-independent acquisition MS data. Nature biotechnology. 2014;32:219-23. DOI: 10.1038/nbt.2841.
[192] Silva JC, Denny R, Dorschel CA, Gorenstein M, Kass IJ, Li GZ, et al. Quantitative proteomic analysis by accurate mass retention time pairs. Analytical chemistry. 2005;77:2187-200. DOI: 10.1021/ac048455k.
[193] Silva JC, Gorenstein MV, Li GZ, Vissers JP, Geromanos SJ. Absolute quantification of proteins by LCMSE: a virtue of parallel MS acquisition. Molecular & cellular proteomics : MCP. 2006;5:144-56. DOI: 10.1074/mcp.M500230-MCP200.
[194] MSE. http://www.slideshare.net/ramborao/discovery-and-analysis-of-peanut-allergens-using-proteomic-approaches-with-ion-mobility-and-high-resolution-mass-spectrometry-waters-corporation-food-research. 2017.
[195] Kramer G, Woolerton Y, van Straalen JP, Vissers JP, Dekker N, Langridge JI, et al. Accuracy and Reproducibility in Quantification of Plasma Protein Concentrations by Mass Spectrometry without the Use of Isotopic Standards. PLoS One. 2015;10:e0140097. DOI: 10.1371/journal.pone.0140097.

[196] Panchaud AS, A.; Shaffer. S. A.; von Haller, P. D.; Kulasekara, H. D.; Miller, S. I. and Goodlett. D. R. Precursor Acquisition Independent From Ion Count: How to Dive Deeper into the Proteomics Ocean. Anal Chem, . 2009;81:6481–8.
[197] Gillet LC, Navarro P, Tate S, Rost H, Selevsek N, Reiter L, et al. Targeted data extraction of the MS/MS spectra generated by data-independent acquisition: a new concept for consistent and accurate proteome analysis. Molecular & cellular proteomics : MCP. 2012;11:O111 016717. DOI: 10.1074/mcp.O111.016717.
[198] Eng JK, McCormack AL, Yates JR. An approach to correlate tandem mass spectral data of peptides with amino acid sequences in a protein database. Journal of the American Society for Mass Spectrometry. 1994;5:976-89. DOI: 10.1016/1044-0305(94)80016-2.
[199] Perkins DNP, D. J.; Creasy, D. M. and Cottrell, J. S. Probability-based protein identification by searching sequence databases using mass spectrometry data. Electrophoresis. 1999;20:3551-67.
[200] Cox JN, N.; Michalski, A.; Scheltema, R. A.; Olsen, J. V. and Mann, M. Andromeda: A peptide search engine integrated into the MaxQuant environment. J Proteome Res 2011;10:1794-805.
[201] PLGS. http://www.waters.com/waters/en_GB/ProteinLynx-Global-SERVER-%28PLGS%29/nav.htm?cid=513821&locale=en_GB. 2017.
[202] Geer LY, Markey SP, Kowalak JA, Wagner L, Xu M, Maynard DM, et al. Open mass spectrometry search algorithm. Journal of proteome research. 2004;3:958-64. DOI: 10.1021/pr0499491.
[203] Craig R, Beavis RC. TANDEM: matching proteins with tandem mass spectra. Bioinformatics. 2004;20:1466-7. DOI: 10.1093/bioinformatics/bth092.
[204] McIlwain S, Tamura K, Kertesz-Farkas A, Grant CE, Diament B, Frewen B, et al. Crux: rapid open source protein tandem mass spectrometry analysis. Journal of proteome research. 2014;13:4488-91. DOI: 10.1021/pr500741y.
[205] Distler U, Kuharev J, Navarro P, Levin Y, Schild H, Tenzer S. Drift time-specific collision energies enable deep-coverage data-independent acquisition proteomics. Nature methods. 2014;11:167-70. DOI: 10.1038/nmeth.2767.
[206] Xu H, Freitas MA. A mass accuracy sensitive probability based scoring algorithm for database searching of tandem mass spectrometry data. BMC bioinformatics. 2007;8:133. DOI: 10.1186/1471-2105-8-133.
[207] Keller A, Nesvizhskii AI, Kolker E, Aebersold R. Empirical statistical model to estimate the accuracy of peptide identifications made by MS/MS and database search. Analytical chemistry. 2002;74:5383-92.
[208] Nesvizhskii AI. A survey of computational methods and error rate estimation procedures for peptide and protein identification in shotgun proteomics. Journal of proteomics. 2010;73:2092-123. DOI: 10.1016/j.jprot.2010.08.009.
[209] Zhang NA, R. and Schwikowski, B. ProbID: A Probabilistic Algorithm to Identify Peptides Through Sequence Database Searching Using Tandem Mass Spectral Data. Proteomics. 2002;2:1406-12.
[210] Higgs RE, Knierman MD, Gelfanova V, Butler JP, Hale JE. Comprehensive label-free method for the relative quantification of proteins from biological samples. Journal of proteome research. 2005;4:1442-50. DOI: 10.1021/pr050109b.
[211] Wang WZ, H., Lin, H.; Roy, S., Shaler, T. A.; Hill, L. R.; Norton, S.; Kumar, P.; Anderle, M; and Becker, C. H. Quantification of Proteins and Metabolites by Mass Spectrometry without Isotopic Labeling or Spiked Standards. Analytical chemistry. 2003;75:4818–26.
[212] Radulovic DJ, S.; Ryu, S; Hamilton, T. G.; Foss, E.; Mao, Y. and Emili, A. Informatics Platform for Global Proteomic Profiling and Biomarker Discovery Using Liquid Chromatography-Tandem Mass Spectrometry. Molecular & Cellular Proteomics. 2004;3:984-97.
[213] Wiener MC, Sachs JR, Deyanova EG, Yates NA. Differential mass spectrometry: a label-free LC-MS method for finding significant differences in complex peptide and protein mixtures. Analytical chemistry. 2004;76:6085-96. DOI: 10.1021/ac0493875.
[214] Mayr BM, Kohlbacher O, Reinert K, Sturm M, Gropl C, Lange E, et al. Absolute myoglobin quantitation in serum by combining two-dimensional liquid chromatography-electrospray ionization

mass spectrometry and novel data analysis algorithms. Journal of proteome research. 2006;5:414-21. DOI: 10.1021/pr050344u.
[215] Nahnsen S, Bielow C, Reinert K, Kohlbacher O. Tools for label-free peptide quantification. Molecular & cellular proteomics : MCP. 2013;12:549-56. DOI: 10.1074/mcp.R112.025163.
[216] Timm W, Scherbart A, Bocker S, Kohlbacher O, Nattkemper TW. Peak intensity prediction in MALDI-TOF mass spectrometry: a machine learning study to support quantitative proteomics. BMC bioinformatics. 2008;9:443. DOI: 10.1186/1471-2105-9-443.
[217] Schwanhausser B, Busse D, Li N, Dittmar G, Schuchhardt J, Wolf J, et al. Corrigendum: Global quantification of mammalian gene expression control. Nature. 2013;495:126-7. DOI: 10.1038/nature11848.
[218] Kwok WW, Tan V, Gillette L, Littell CT, Soltis MA, LaFond RB, et al. Frequency of epitope-specific naive CD4(+) T cells correlates with immunodominance in the human memory repertoire. Journal of immunology. 2012;188:2537-44. DOI: 10.4049/jimmunol.1102190.
[219] Ascough S, Ingram RJ, Chu KK, Reynolds CJ, Musson JA, Doganay M, et al. Anthrax Lethal Factor as an Immune Target in Humans and Transgenic Mice and the Impact of HLA Polymorphism on CD4+ T Cell Immunity. PLOS Pathogens. 2014;10:e1004085.
[220] Andreatta M, Karosiene E, Rasmussen M, Stryhn A, Buus S, Nielsen M. Accurate pan-specific prediction of peptide-MHC class II binding affinity with improved binding core identification. Immunogenetics. 2015;67:641-50. DOI: 10.1007/s00251-015-0873-y.
[221] Wilson DB, Wilson DH, Schroder K, Pinilla C, Blondelle S, Houghten RA, et al. Specificity and degeneracy of T cells. Molecular immunology. 2004;40:1047-55. DOI: 10.1016/j.molimm.2003.11.022.
[222] Sewell AK. Why must T cells be cross-reactive? Nature reviews Immunology. 2012;12:669-77. DOI: 10.1038/nri3279.
[223] Birnbaum ME, Mendoza JL, Sethi DK, Dong S, Glanville J, Dobbins J, et al. Deconstructing the peptide-MHC specificity of T cell recognition. Cell. 2014;157:1073-87. DOI: 10.1016/j.cell.2014.03.047.
[224] Dimitrov I, Garnev P, Flower DR, Doytchinova I. MHC Class II Binding Prediction-A Little Help from a Friend. Journal of biomedicine & biotechnology. 2010;2010:705821. DOI: 10.1155/2010/705821.
[225] Monzavi-Karbassi B, Shamloo S, Kieber-Emmons M, Jousheghany F, Luo P, Lin KY, et al. Priming characteristics of peptide mimotopes of carbohydrate antigens. Vaccine. 2003;21:753-60.
[226] Mueller R, Karle A, Vogt A, Kropshofer H, Ross A, Maeder K, et al. Evaluation of the immuno-stimulatory potential of stopper extractables and leachables by using dendritic cells as readout. Journal of pharmaceutical sciences. 2009;98:3548-61. DOI: 10.1002/jps.21672.
[227] Verthelyi D, Wang V. Trace levels of innate immune response modulating impurities (IIRMIs) synergize to break tolerance to therapeutic proteins. PLoS One. 2010;5:e15252. DOI: 10.1371/journal.pone.0015252.
[228] van Beers MM, Jiskoot W, Schellekens H. On the role of aggregates in the immunogenicity of recombinant human interferon beta in patients with multiple sclerosis. Journal of interferon & cytokine research : the official journal of the International Society for Interferon and Cytokine Research. 2010;30:767-75. DOI: 10.1089/jir.2010.0086.
[229] Weaver JM, Lazarski CA, Richards KA, Chaves FA, Jenks SA, Menges PR, et al. Immunodominance of CD4 T Cells to Foreign Antigens Is Peptide Intrinsic and Independent of Molecular Context: Implications for Vaccine Design. The Journal of Immunology. 2008;181:3039-48.
[230] webpage E. https://www.ebi.ac.uk/ipd/imgt/hla/stats.html. Accessed Mar 2020.
[231] Wang P, Sidney J, Kim Y, Sette A, Lund O, Nielsen M, et al. Peptide binding predictions for HLA DR, DP and DQ molecules. BMC bioinformatics. 2010;11:568. DOI: 10.1186/1471-2105-11-568.
[232] Godkin AJ, Smith KJ, Willis A, Tejada-Simon MV, Zhang J, Elliott T, et al. Naturally processed HLA class II peptides reveal highly conserved immunogenic flanking region sequence preferences that reflect antigen processing rather than peptide-MHC interactions. Journal of immunology. 2001;166:6720-7.

[233] Chicz RM, Urban RG, Gorga JC, Vignali DA, Lane WS, Strominger JL. Specificity and promiscuity among naturally processed peptides bound to HLA-DR alleles. The Journal of experimental medicine. 1993;178:27-47.
[234] Sette A, Adorini L, Colon SM, Buus S, Grey HM. Capacity of intact proteins to bind to MHC class II molecules. Journal of immunology. 1989;143:1265-7.
[235] Carson RT, Vignali KM, Woodland DL, Vignali DA. T cell receptor recognition of MHC class II-bound peptide flanking residues enhances immunogenicity and results in altered TCR V region usage. Immunity. 1997;7:387-99.
[236] Southwood S, Sidney J, Kondo A, del Guercio MF, Appella E, Hoffman S, et al. Several common HLA-DR types share largely overlapping peptide binding repertoires. J Immunol 1998;160:3363-73.
[237] De Groot AS, Martin W. Reducing risk, improving outcomes: bioengineering less immunogenic protein therapeutics. Clinical immunology. 2009;131:189-201. DOI: 10.1016/j.clim.2009.01.009.
[238] Zhang L, Chen Y, Wong HS, Zhou S, Mamitsuka H, Zhu S. TEPITOPEpan: extending TEPITOPE for peptide binding prediction covering over 700 HLA-DR molecules. PLoS One. 2012;7:e30483. DOI: 10.1371/journal.pone.0030483.
[239] Jensen KK, Andreatta M, Marcatili P, Buus S, Greenbaum JA, Yan Z, et al. Improved methods for predicting peptide binding affinity to MHC class II molecules. Immunology. 2018;154:394-406. DOI: 10.1111/imm.12889.
[240] Andreatta M, Nielsen M. Gapped sequence alignment using artificial neural networks: application to the MHC class I system. Bioinformatics. 2016;32:511-7. DOI: 10.1093/bioinformatics/btv639.
[241] Liepe J, Marino F, Sidney J, Jeko A, Bunting DE, Sette A, et al. A large fraction of HLA class I ligands are proteasome-generated spliced peptides. Science. 2016;354:354-8. DOI: 10.1126/science.aaf4384.
[242] Eichmann M, de Ru A, van Veelen PA, Peakman M, Kronenberg-Versteeg D. Identification and characterisation of peptide binding motifs of six autoimmune disease-associated human leukocyte antigen-class I molecules including HLA-B*39:06. Tissue antigens. 2014;84:378-88. DOI: 10.1111/tan.12413.
[243] Rist MJ, Theodossis A, Croft NP, Neller MA, Welland A, Chen Z, et al. HLA peptide length preferences control CD8+ T cell responses. Journal of immunology. 2013;191:561-71. DOI: 10.4049/jimmunol.1300292.
[244] Rammensee HG, Falk K, Rotzschke O. Peptides naturally presented by MHC class I molecules. Annual review of immunology. 1993;11:213-44. DOI: 10.1146/annurev.iy.11.040193.001241.
[245] Falk K, Rotzschke O, Stevanovic S, Jung G, Rammensee HG. Allele-specific motifs revealed by sequencing of self-peptides eluted from MHC molecules. Nature. 1991;351:290-6. DOI: 10.1038/351290a0.
[246] Rapin N, Hoof I, Lund O, Nielsen M. The MHC motif viewer: a visualization tool for MHC binding motifs. Current protocols in immunology. 2010;Chapter 18:Unit 18 7. DOI: 10.1002/0471142735.im1817s88.
[247] Theodossis A, Guillonneau C, Welland A, Ely LK, Clements CS, Williamson NA, et al. Constraints within major histocompatibility complex class I restricted peptides: presentation and consequences for T-cell recognition. Proceedings of the National Academy of Sciences of the United States of America. 2010;107:5534-9. DOI: 10.1073/pnas.1000032107.
[248] Kim Y, Sidney J, Pinilla C, Sette A, Peters B. Derivation of an amino acid similarity matrix for peptide: MHC binding and its application as a Bayesian prior. BMC bioinformatics. 2009;10:394. DOI: 10.1186/1471-2105-10-394.
[249] Wang Y, Zhou P, Lin Y, Shu M, Hu Y, Xia Q, et al. Quantitative prediction of class I MHC/epitope binding affinity using QSAR modeling derived from amino acid structural information. Combinatorial chemistry & high throughput screening. 2015;18:75-82.
[250] Hoof I, Peters B, Sidney J, Pedersen LE, Sette A, Lund O, et al. NetMHCpan, a method for MHC class I binding prediction beyond humans. Immunogenetics. 2009;61:1-13. DOI: 10.1007/s00251-008-0341-z.

[251] Koch CP, Perna AM, Pillong M, Todoroff NK, Wrede P, Folkers G, et al. Scrutinizing MHC-I binding peptides and their limits of variation. PLoS computational biology. 2013;9:e1003088. DOI: 10.1371/journal.pcbi.1003088.
[252] Kuksa PP, Min MR, Dugar R, Gerstein M. High-order neural networks and kernel methods for peptide-MHC binding prediction. Bioinformatics. 2015;31:3600-7. DOI: 10.1093/bioinformatics/btv371.
[253] Nielsen M, Andreatta M. NetMHCpan-3.0; improved prediction of binding to MHC class I molecules integrating information from multiple receptor and peptide length datasets. Genome medicine. 2016;8:33. DOI: 10.1186/s13073-016-0288-x.
[254] Lundegaard C, Lund O, Nielsen M. Accurate approximation method for prediction of class I MHC affinities for peptides of length 8, 10 and 11 using prediction tools trained on 9mers. Bioinformatics. 2008;24:1397-8. DOI: 10.1093/bioinformatics/btn128.
[255] Peters B, Bui HH, Frankild S, Nielson M, Lundegaard C, Kostem E, et al. A community resource benchmarking predictions of peptide binding to MHC-I molecules. PLoS computational biology. 2006;2:e65. DOI: 10.1371/journal.pcbi.0020065.
[256] Marrack P, McKee AS, Munks MW. Towards an understanding of the adjuvant action of aluminium. Nature reviews Immunology. 2009;9:287-93. DOI: 10.1038/nri2510.
[257] Wen Y, Shi Y. Alum: an old dog with new tricks. Emerg Microbes Infect. 2016;5:e25. DOI: 10.1038/emi.2016.40.
[258] Glenny AT PC, Waddington H, Wallace U. The antigenic value of toxoid precipitated by potassium alum. J Pathol Bacteriol. 1926;3:8-45.
[259] Vessely C, Estey T, Randolph TW, Henderson I, Cooper J, Nayar R, et al. Stability of a trivalent recombinant protein vaccine formulation against botulinum neurotoxin during storage in aqueous solution. Journal of pharmaceutical sciences. 2009;98:2970-93. DOI: 10.1002/jps.21498.
[260] Zhu D, Huang S, McClellan H, Dai W, Syed NR, Gebregeorgis E, et al. Efficient extraction of vaccines formulated in aluminum hydroxide gel by including surfactants in the extraction buffer. Vaccine. 2012;30:189-94. DOI: 10.1016/j.vaccine.2011.11.025.
[261] Lindblad EB. Aluminium compounds for use in vaccines. Immunology and Cell Biology. 2004;82:497-505.
[262] Gupta N, Bandeira N, Keich U, Pevzner PA. Target-decoy approach and false discovery rate: when things may go wrong. Journal of the American Society for Mass Spectrometry. 2011;22:1111-20. DOI: 10.1007/s13361-011-0139-3.
[263] Rinella JV WJ, Hem SL. Effect of pH on the elution of model antigens
from aluminium-containing adjuvants. . J Colloid Interface Sci 1998;205:161-5.
[264] al-Shakhshir RH, Regnier FE, White JL, Hem SL. Contribution of electrostatic and hydrophobic interactions to the adsorption of proteins by aluminium-containing adjuvants. Vaccine. 1995;13:41-4.
[265] Iyer S, Robinett RS, HogenEsch H, Hem SL. Mechanism of adsorption of hepatitis B surface antigen by aluminum hydroxide adjuvant. Vaccine. 2004;22:1475-9. DOI: 10.1016/j.vaccine.2003.10.023.
[266] Jully V, Mathot F, Moniotte N, Preat V, Lemoine D. Mechanisms of Antigen Adsorption Onto an Aluminum-Hydroxide Adjuvant Evaluated by High-Throughput Screening2016.
[267] Chittineni SPaM, S. C. Improved method for Hepatitis B vaccine in-vitro potency. International Journal of Pharmaceutical Science Invention. 2014;3:39-42.
[268] Synapt. https://pubs.acs.org/cen/coverstory/88/8813cover3.html. 2017.
[269] Li GZ, Vissers JP, Silva JC, Golick D, Gorenstein MV, Geromanos SJ. Database searching and accounting of multiplexed precursor and product ion spectra from the data independent analysis of simple and complex peptide mixtures. Proteomics. 2009;9:1696-719. DOI: 10.1002/pmic.200800564.
[270] Venn I. http://www.interactivenn.net/. 2019.
[271] Chevreux G, Tilly N, Bihoreau N. Quantification of proteins by data independent acquisition: Performance assessment of the Hi3 methodology. Anal Biochem. 2018;549:184-7. DOI: 10.1016/j.ab.2018.03.019.

[272] Hart DP, Uzun N, Skelton S, Kakoschke A, Househam J, Moss DS, et al. Factor VIII cross-matches to the human proteome reduce the predicted inhibitor risk in missense mutation hemophilia A. Haematologica. 2019;104:599-608. DOI: 10.3324/haematol.2018.195669.
[273] IEDB. http://wwwiedborg/Accessed June 2017.
[274] Gfeller D, Bassani-Sternberg M. Predicting Antigen Presentation-What Could We Learn From a Million Peptides? Frontiers in immunology. 2018;9:1716. DOI: 10.3389/fimmu.2018.01716.
[275] Jurtz V, Paul S, Andreatta M, Marcatili P, Peters B, Nielsen M. NetMHCpan-4.0: Improved Peptide-MHC Class I Interaction Predictions Integrating Eluted Ligand and Peptide Binding Affinity Data. Journal of immunology. 2017;199:3360-8. DOI: 10.4049/jimmunol.1700893.
[276] MegAlign. https://www.dnastar.com/t-megalign.aspx. Sep 2016.
[277] NCBI. https://www.ncbi.nlm.nih.gov/. Jul 2016.
[278] Solberg OD, Mack SJ, Lancaster AK, Single RM, Tsai Y, Sanchez-Mazas A, et al. Balancing selection and heterogeneity across the classical human leukocyte antigen loci: a meta-analytic review of 497 population studies. Human immunology. 2008;69:443-64. DOI: 10.1016/j.humimm.2008.05.001.
[279] Solberg OD, Mack SJ, Lancaster AK, Single RM, Tsai Y, Sanchez-Mazas A, et al. http://www.pypop.org/popdata/. 2017.
[280] Jenkins MK, Moon JJ. The role of naive T cell precursor frequency and recruitment in dictating immune response magnitude. Journal of immunology. 2012;188:4135-40. DOI: 10.4049/jimmunol.1102661.
[281] Ford ML, Koehn BH, Wagener ME, Jiang W, Gangappa S, Pearson TC, et al. Antigen-specific precursor frequency impacts T cell proliferation, differentiation, and requirement for costimulation. The Journal of experimental medicine. 2007;204:299-309. DOI: 10.1084/jem.20062319.
[282] Martinez RJ, Andargachew R, Martinez HA, Evavold BD. Low-affinity CD4+ T cells are major responders in the primary immune response. Nat Commun. 2016;7:13848. DOI: 10.1038/ncomms13848.
[283] Edwards LJ, Evavold BD. T cell recognition of weak ligands: roles of signaling, receptor number, and affinity. Immunol Res. 2011;50:39-48. DOI: 10.1007/s12026-011-8204-3.
[284] Musson JA, Walker N, Flick-Smith H, Williamson ED, Robinson JH. Differential processing of CD4 T-cell epitopes from the protective antigen of Bacillus anthracis. The Journal of biological chemistry. 2003;278:52425-31. DOI: 10.1074/jbc.M309034200.
[285] Sadegh-Nasseri S, Kim A. Selection of immunodominant epitopes during antigen processing is hierarchical. Molecular immunology. 2018. DOI: 10.1016/j.molimm.2018.08.011.
[286] Fontaine M, Vogel I, Van Eycke YR, Galuppo A, Ajouaou Y, Decaestecker C, et al. Regulatory T cells constrain the TCR repertoire of antigen-stimulated conventional CD4 T cells. The EMBO journal. 2018;37:398-412. DOI: 10.15252/embj.201796881.
[287] Schroder K, Hertzog PJ, Ravasi T, Hume DA. Interferon-gamma: an overview of signals, mechanisms and functions. Journal of leukocyte biology. 2004;75:163-89. DOI: 10.1189/jlb.0603252.
[288] Glomski IJ, Corre JP, Mock M, Goossens PL. Cutting Edge: IFN-gamma-producing CD4 T lymphocytes mediate spore-induced immunity to capsulated Bacillus anthracis. Journal of immunology. 2007;178:2646-50.
[289] Kang TJ, Fenton MJ, Weiner MA, Hibbs S, Basu S, Baillie L, et al. Murine macrophages kill the vegetative form of Bacillus anthracis. Infect Immun. 2005;73:7495-501. DOI: 10.1128/IAI.73.11.7495-7501.2005.
[290] Gold JA, Hoshino Y, Hoshino S, Jones MB, Nolan A, Weiden MD. Exogenous gamma and alpha/beta interferon rescues human macrophages from cell death induced by Bacillus anthracis. Infect Immun. 2004;72:1291-7.
[291] Couper KN, Blount DG, Riley EM. IL-10: the master regulator of immunity to infection. Journal of immunology. 2008;180:5771-7.
[292] I SJ. Interleukin 10 (IL-10) British Society of Immunology; 2019.
[293] Pittman PR, Leitman SF, Oro JG, Norris SL, Marano NM, Ranadive MV, et al. Protective antigen and toxin neutralization antibody patterns in anthrax vaccinees undergoing serial plasmapheresis.

Clinical and diagnostic laboratory immunology. 2005;12:713-21. DOI: 10.1128/CDLI.12.6.713-721.2005.
[294] Quinn CP, Sabourin CL, Schiffer JM, Niemuth NA, Semenova VA, Li H, et al. Humoral and Cell-Mediated Immune Responses to Alternate Booster Schedules of Anthrax Vaccine Adsorbed in Humans. Clinical and vaccine immunology : CVI. 2016;23:326-38. DOI: 10.1128/CVI.00696-15.
[295] Ovsyannikova IG, Pankratz VS, Vierkant RA, Pajewski NM, Quinn CP, Kaslow RA, et al. Human leukocyte antigens and cellular immune responses to anthrax vaccine adsorbed. Infect Immun. 2013;81:2584-91. DOI: 10.1128/IAI.00269-13.
[296] Little SF, Ivins BE, Webster WM, Fellows PF, Pitt ML, Norris SL, et al. Duration of protection of rabbits after vaccination with Bacillus anthracis recombinant protective antigen vaccine. Vaccine. 2006;24:2530-6. DOI: 10.1016/j.vaccine.2005.12.028.
[297] Pittman PR, Norris SL, Barrera Oro JG, Bedwell D, Cannon TL, McKee KT, Jr. Patterns of antibody response in humans to the anthrax vaccine adsorbed (AVA) primary (six-dose) series. Vaccine. 2006;24:3654-60. DOI: 10.1016/j.vaccine.2006.01.054.
[298] Phipps AJ, Premanandan C, Barnewall RE, Lairmore MD. Rabbit and nonhuman primate models of toxin-targeting human anthrax vaccines. Microbiol Mol Biol Rev. 2004;68:617-29. DOI: 10.1128/MMBR.68.4.617-629.2004.

8.0 APPENDICES

Appendix 1 – Python Script to enable automated prediction of MHC class II peptides

```
#!/usr/bin/env python
# -*- coding: utf-8 -*-

#Import modules
import os
import time
import requests
import re
from datetime import datetime

#Splits allele list into evenly sized chunks of 20
def split_alleles(list):
    for i in range(0, len(list), 20):
        yield list[i:i + 20]

#Sets data for POST submission
post_data = {
        "configfile" : (None, "/usr/opt/www/pub/CBS/services/NetMHCIIpan-3.2/NetMHCIIpan-
3.2.cf"),
        "inp" : (None, "0"),
        "SEQSUB" : (None, ""),
        "length" : (None, "15"),
        "PEPPASTE" : (None, ""),
        "PEPSUB" : (None, ""),
```

```
        "master" : (None, "1"),
        "slave0" : (None, "DRB1_0104"),
        "MHCSEQPASTEa" : (None, ""),
        "MHCSEQSUBa" : (None, ""),
        "MHCSEQPASTEb" : (None, ""),
        "MHCSEQSUBb" : (None, ""),
        "thrs" : (None, "2"),
        "thrw" : (None, "10"),
        "thrf" : (None, "10"),
        "sort" : (None, "on"),
        "histhr" : (None, "10")
}

#Lists all HLA alleles for MHCII
#REPLACE THIS WITH LIST OF YOUR ALLELES
alleles = ["HLA-DPA10201-DPB10101", "HLA-DPA10103-DPB10201", "HLA-DPA10103-
DPB10401", "HLA-DPA10301-DPB10402", "HLA-DPA10201-DPB10501", "HLA-DQA10501-
DQB10201", "HLA-DQA10501-DQB10301", "HLA-DQA10301-DQB10302", "HLA-
DQA10401-DQB10402", "HLA-DQA10101-DQB10501", "HLA-DQA10102-DQB10602",
"DRB1_0101", "DRB1_0301", "DRB1_0401", "DRB1_0404", "DRB1_0405", "DRB1_0701",
"DRB1_0802", "DRB1_0901", "DRB1_1101", "DRB1_1302", "DRB1_1501", "DRB3_0101",
"DRB4_0101", "DRB5_0101", "H-2-IAb"]

#Opens all FASTA files in given directory
#REPLACE THIS WITH THE LOCATION OF YOUR FILES
FASTA_directory = "C:\Tapasvi\PhD\BioInformatics Stuff\Protective antigen\Fasta
files\python"
FASTA_files = os.listdir(FASTA_directory)
```

```
i = 1
i_max = len(FASTA_files)

#For each FASTA in directory
for _FASTA_file in FASTA_files:

	#Prints progress
	print("File %s of %s: %s" % (i, i_max, _FASTA_file))

	#Sets empty lists for results
	allele_50_results = []
	allele_500_results = []

	#Extract sequence from FASTA file
	with open(FASTA_directory + "\\" + _FASTA_file, "r") as _file:
		_file_contents = _file.read()
	_file.close()
	_protein_seq = "".join(_file_contents.strip().split("\n")[1:])

	#Set session
	session = requests.session()

	#Adds sequence and allele
	post_data["SEQPASTE"] =  (None, _protein_seq)

	#Uploads results in chunks of 20 alleles
	for allele_list in split_alleles(alleles):
```

```
        #Uploads alleles in packets of 20 (maximum allowed by server)
        post_data["allele"] = (None, ",".join(allele_list))

        #Makes POST request to server
        response = session.post("http://www.cbs.dtu.dk/cgi-bin/webface2.fcgi",
files=post_data)

        #Processes initial response to fetch job ID
        job_ID = re.findall(r"\!\-\- jobid\: (.+?) status", response.text, re.DOTALL)[0]
        print("\tJob ID: %s" % job_ID)

        #Waits and checks job progress every 5 seconds
        _processing = True
        response = ""
        u_i = 1
        while _processing:
                response = session.get("http://www.cbs.dtu.dk/cgi-
bin/webface2.fcgi?jobid=%s" % job_ID)
                if "Number of strong binders" in response.text:
                        break
                print("\t\tWaiting for results ... %s" % u_i)
                u_i += 1
                time.sleep[85]

        #Gets results from response table and adds to appropriate list
        result_tables = re.findall(r"Allele\:.+?\-[85].+?\-[85](.+?)\-[85]", response.text,
re.DOTALL)
```

```
            for result_table in result_tables:
                new_50_table = []
                new_500_table = []

                for row in result_table.strip().split("\n"):
                    row_cells = re.split(r"\s{2,}If", row.strip())

                    if float(row_cells[8]) <= 50:
                        new_50_table.append(",".join(row_cells))

                    if float(row_cells[8]) <= 500:
                        new_500_table.append(",".join(row_cells))

                allele_50_results += new_50_table
                allele_500_results += new_500_table

        #Saves all alleles with <50nM affinity to own file
        with open("%s-50nM Results.csv" % _FASTA_file.split(".")[0], "w") as _file:
            _file.write("Seq,Allele,Peptide,Identity,Pos,Core,Core_Rel,1-
log50k(aff),Affinity(nM),%Rank,Exp_Bind,BindingLevel\n" + "\n".join(allele_50_results))
        _file.close()

        #Saves all alleles with <500nM affinity to own file
        with open("%s-500nM Results.csv" % _FASTA_file.split(".")[0], "w") as _file:
            _file.write("Seq,Allele,Peptide,Identity,Pos,Core,Core_Rel,1-
log50k(aff),Affinity(nM),%Rank,Exp_Bind,BindingLevel\n" + "\n".join(allele_500_results))
        _file.close()
```

```
print("COMPLETE!")
```

Appendix 2 – Python Script to enable automated prediction of MHC class I peptides

```
#!/usr/bin/env python
# -*- coding: utf-8 -*-

#Import modules
import os
import time
import requests
import re
from datetime import datetime

#Splits allele list into evenly sized chunks of 20
def split_alleles(list):
    for i in range(0, len(list), 20):
        yield list[i:i + 20]

#Sets data for POST submission
post_data = {
        "configfile" : (None, "/usr/opt/www/pub/CBS/services/NetMHCpan-
3.0/NetMHCpan.cf"),
        "inp" : (None, "0"),
        "SEQSUB" : (None, ""),
        "length" : (None, "9"),
        "PEPPASTE" : (None, ""),
        "PEPSUB" : (None, ""),
        "master" : (None, "1"),
        "slave0" : (None, "HLA-A01:01"),
```

```
        "MHCSEQPASTEa" : (None, ""),
        "MHCSEQSUBa" : (None, ""),
        "MHCSEQPASTEb" : (None, ""),
        "MHCSEQSUBb" : (None, ""),
        "thrs" : (None, "2"),
        "thrw" : (None, "10"),
        "thrf" : (None, "10"),
        "sort" : (None, "on"),
        "histhr" : (None, "10")
}

#Lists all HLA alleles for MHCI
#REPLACE THIS WITH LIST OF YOUR ALLELES
alleles = ["HLA-A02:01", "HLA-A11:01", "HLA-A01:01", "HLA-A03:01", "HLA-A31:01", "HLA-
A33:03", "HLA-A02:06", "HLA-A26:01", "HLA-A30:01", "HLA-B35:01", "HLA-B51:01", "HLA-
B40:01", "HLA-B44:03", "HLA-B07:02", "HLA-B15:01", "HLA-B08:01", "HLA-B58:01", "HLA-
B27:05", "HLA-B39:05", "HLA-C07:02", "HLA-C04:01", "HLA-C03:04", "HLA-C01:02", "HLA-
C07:01", "HLA-C06:02", "HLA-C03:03", "HLA-C08:01", "HLA-C15:02", "HLA-C12:02"]

#Opens all FASTA files in given directory
#REPLACE THIS WITH THE LOCATION OF YOUR FILES
FASTA_directory = "C:\Tapasvi_11Sep19\PhD\BioInformatics Stuff\Protective antigen\Fasta
files\python"
FASTA_files = os.listdir(FASTA_directory)

i = 1
i_max = len(FASTA_files)
```

```
#For each FASTA in directory
for _FASTA_file in FASTA_files:

        #Prints progress
        print("File %s of %s: %s" % (i, i_max, _FASTA_file))

        #Sets empty lists for results
        allele_SB_results = []
        allele_WB_results = []

        #Extract sequence from FASTA file
        with open(FASTA_directory + "\\" + _FASTA_file, "r") as _file:
                _file_contents = _file.read()
        _file.close()
        _protein_seq = "".join(_file_contents.strip().split("\n")[1:])

        #Set session
        session = requests.session()

        #Adds sequence and allele
        post_data["SEQPASTE"] =  (None, _protein_seq)

        #Uploads results in chunks of 20 alleles
        for allele_list in split_alleles(alleles):

                #Uploads alleles in packets of 20 (maximum allowed by server)
                post_data["allele"] = (None, ",".join(allele_list))
```

```
#Makes POST request to server
response = session.post("http://www.cbs.dtu.dk/cgi-bin/webface2.fcgi",
files=post_data)

#Processes initial response to fetch job ID
job_ID = re.findall(r"\!\-\- jobid\: (.+?) status", response.text, re.DOTALL)[0]
print("\tJob ID: %s" % job_ID)

#Waits and checks job progress every 5 seconds
_processing = True
response = ""
u_i = 1
while _processing:
        response = session.get("http://www.cbs.dtu.dk/cgi-
bin/webface2.fcgi?jobid=%s" % job_ID)
        if "Number of strong binders" in response.text:
                break
        print("\t\tWaiting for results ... %s" % u_i)
        u_i += 1
        time.sleep[85]

#Gets results from response table and adds to appropriate list
result_tables = re.findall(r"Allele\:.+?\-[85].+?\-[85](.+?)\-[85]", response.text,
re.DOTALL)
for result_table in result_tables:
        new_SB_table = []
        new_WB_table = []
```

```
                    for row in result_table.strip().split("\n"):
                        row_cells = re.split(r"\s{2,}", row.strip())

                        if "sb" in row_cells[-1].lower():
                            new_SB_table.append(",".join(row_cells))

                        if "wb" in row_cells[-1].lower():
                            new_WB_table.append(",".join(row_cells))

                    allele_SB_results += new_SB_table
                    allele_WB_results += new_WB_table

        #Saves all alleles with <50nM affinity to own file
        with open("%s-SB Results.csv" % _FASTA_file.split(".")[0], "w") as _file:
            _file.write("Allele,pos,HLA,peptide,Core
Offset,I_pos,I_len,D_pos,D_len,iCore,Identity 1-log50k(aff),Affinity(nM),%Rank,BindLevel\n"
+ "\n".join(allele_SB_results))
        _file.close()

        #Saves all alleles with <500nM affinity to own file
        with open("%s-WB Results.csv" % _FASTA_file.split(".")[0], "w") as _file:
            _file.write("Allele,pos,HLA,peptide,Core
Offset,I_pos,I_len,D_pos,D_len,iCore,Identity 1-log50k(aff),Affinity(nM),%Rank,BindLevel\n"
+ "\n".join(allele_WB_results))
        _file.close()

print("COMPLETE!")
```

Appendix 3 – *B. anthracis* Strain Collection

Strain Name	Genbank No.	Source
Ames A0462	CP010793.1	American Type Culture Collection
Ames BA1004	CP009980.1	USAMRIID
A0248	CP001599.1	No information
A1144	CP010853.1	Argentinian isolate with mucoid colony morphology
A16R	CP001975.1	analysed in China, souce unknown
A16	CP001971.1	analysed in China, souce unknown
A2012	AE011190.1	Florida isolate
BA0052	CP007703	USARMIID
BA1015	CP009543.1	USAMRIID
BA1035	CP009699.1	USAMRIID
BFV	CP007703.1	USAMRIID
Canadian Bison	CP010321.1	USAMRIID
CDC 684	CP001216.1	Los Alamos National Laboratory
Delta Sterne	CP008752	USARMIID
HYU01	CP008847.1	Soil Samples in the Korean Peninsula
H9401	CP002092.1	isolate from korean patient
Isolate IT Carb 1-6241	AJ413937.1	B. *anthracis* 'Carbosap' vaccine strain, used as vaccine in Italy
Isolate IT Carb3-6254	AJ413936.1	B. *anthracis* 'Carbosap' vaccine strain, used as vaccine in Italy
K3	CP009331.1	USAMRIID

Larissa	CP012520.1	human cutaneous Anthrax stain in Greece
Ohio	CP009340.1	USAMRIID
PAK-1	CP009324.1	USAMRIID
Pasteur	CP009476.1	USAMRIID
Pasteur-like	JNOD01000001	USARMIID
Pollino	NZ_CP010813.1	Cattle Italy
P.NO2	KT186230.1	analysed in China, px01 from attenuated pasteur vaccine strains
RA3	CP009696.1	USAMRIID
Scotland A.Br.003	JMPV01000001-JMPV01000008	USARMIID
Shikan-NIID	AP014834.1	horses Tokyo Japan
SK-102	CP009463.1	USAMRIID
Stendel	CP014177.1	cattle in germany
Sterne	CP009540.1	USAMRIID
Sterne NG	CP035988.1	N/A
SVA11	NZ_CP006742.1	National Veterinary Institute in Sweden
Turkey32	CP009316.1	USAMRIID
VCM1168	KP213102.1	northern Vietnam
V770-NP-1R	CP009597.1	USAMRIID
Vollum 1B	CP009327.1	USAMRIID
Vollum	CP007665.1	USARMIID
Zimbabwe 89	JMPU01000001-JMPU01000017	USARMIID
1C3	KP213104	northern Vietnam
4NS	KP213103.1	northern Vietnam

52-40-NIAH	BBWY01000001 to B BWY01000036	horses Tokyo Japan
44-NIAH	BBWX01000001 to B BWX01000124	horses Tokyo Japan
34F2	JQ798178.1	recombinant PA
2002013094	CP009902.1	USAMRIID
2000031021	CP007617	USARMIID

Appendix 4 – Proteins identified in CF using LC-MS/MS analysis

Uniprot Accession No.	*B. Anthracis* Protein Name
P13423	Protective antigen
P15917	Lethal factor
P40136	Calmodulin-sensitive adenylate cyclase
Q81X78	Enolase
Q9X360	PXO1-90
Q81VE1	60 kDa chaperonin
Q81QZ5	Alcohol dehydrogenase
Q81X75	Phosphoglycerate kinase
Q81K80	L-lactate dehydrogenase 2
Q81KZ1	Pyruvate kinase
P02769	Unknown Entry
Q81K75	Glucose-6-phosphate isomerase
Q81M66	Leucine dehydrogenase
Q81YX1	Formate acetyltransferase
Q81VT3	Elongation factor G
Q81X76	Triosephosphate isomerase
Q81VE0	GMP synthase [glutamine-hydrolyzing]
Q81P59	Chorismate mutase
P94217	S-layer protein EA1
Q81M07	Probable glycine dehydrogenase (decarboxylating) subunit 1
Q81Y15	Transketolase
Q81ZG8	Bifunctional purine biosynthesis protein PurH
Q81XT6	Glutamine synthetase

Q81M06	Aminomethyltransferase
Q81LL7	Aldehyde-alcohol dehydrogenase
Q81X77	2_3-bisphosphoglycerate-independent phosphoglycerate mutase
Q81KZ0	ATP-dependent 6-phosphofructokinase
TRYP_PIG	Entry Unknown Entry
Q81W29	Inosine-5'-monophosphate dehydrogenase
Q81ZF8	1-pyrroline-5-carboxylate dehydrogenase
Q81W27	Pyridoxal 5'-phosphate synthase subunit PdxS
Q81Y22	N-acetylmuramoyl-L-alanine amidase
Q81ZC4	Alkyl hydroperoxide reductase
Q81WM8	Polyribonucleotide nucleotidyltransferase
Q81RT5	Peptidase P60
Q81VV3	Glutamate--tRNA ligase
Q81JY4	Serine hydroxymethyltransferase
Q81ZH6	Adenylosuccinate lyase
Q81UH4	Amidase
Q81SA0	Fumarate hydratase class II
Q81VN5	Glutamine--fructose-6-phosphate aminotransferase [isomerizing]
Q81Z72	Chemical-damaging agent resistance protein C
Q81UL6	Glyceraldehyde-3-phosphate dehydrogenase
Q81RQ4	3-dehydroshikimate dehydratase
Q81KW3	Alanine dehydrogenase
Q81VU0	50S ribosomal protein L7/L12
Q81Y95	Serine protease
Q81JI9	Adenylosuccinate synthetase
Q81MR3	Dihydrolipoamide acetyltransferase component of pyruvate dehydrogenase complex

Q81ZH1	Amidophosphoribosyltransferase
Q81LS1	Protein GrpE
Q81VN7	Phosphoglucosamine mutase
Q81WN5	Aspartate-semialdehyde dehydrogenase
Q81UA1	Putative S-layer protein
Q81L19	Peptidase M28
Q81SV8	Nucleoside diphosphate kinase
Q81L45	Cell surface protein
Q81QP8	Isochorismatase
Q81KQ7	Aminopeptidase
Q6HSF4	Malate dehydrogenase
Q81KP6	Peptidase_ M42 family
Q81YG1	Putative lipoprotein
D1MPY3	Putative malate dehydrogenase
Q81LL9	High-affinity heme uptake system protein isdE
Q81XS0	Ferredoxin--NADP reductase 2
Q81KU8	Probable thiol peroxidase
Q81RE1	Formate--tetrahydrofolate ligase
Q81VX2	Cysteine synthase
Q81X74	Glyceraldehyde-3-phosphate dehydrogenase
Q81JT1	Agmatinase
Q81V80	Putative pyridoxal phosphate-dependent acyltransferase
Q81ZH8	N5-carboxyaminoimidazole ribonucleotide mutase
Q81WK9	Elongation factor Ts
Q81TL8	Tryptophan synthase beta chain
Q81M65	Phosphate butyryltransferase
Q81RW4	L-lactate dehydrogenase 1

Q81UU2	Nitroreductase
Q81M84	Peptidase_ M20/M25/M40 family
Q81XP7	NifU domain protein
Q81TL7	Tryptophan synthase alpha chain
Q81LG0	Nicotinate-nucleotide diphosphorylase (Carboxylating)
Q81JR4	Phosphate acetyltransferase
Q81V19	Cell wall-binding protein
Q81VE2	10 kDa chaperonin
Q81TX2	Putative S-layer protein
Q81VA6	Alanine dehydrogenase
Q81XS5	Probable cytosol aminopeptidase
Q81L73	Thioredoxin
Q81NS6	Signal peptidase I
Q81RP6	Peptidase
Q81JF9	3-oxoacyl-[acyl-carrier-protein] synthase 2
Q81VZ2	Putative septation protein SpoVG
Q81L44	Cell surface protein
Q81X16	UDP-N-acetylglucosamine 2-epimerase
Q81SX5	30S ribosomal protein S1
Q81K96	1_4-dihydroxy-2-naphthoyl-CoA synthase
Q81JW4	Fructose-bisphosphate aldolase
Q81ZG7	Phosphoribosylamine--glycine ligase
Q81JI2	30S ribosomal protein S6
Q81JY0	PTS system glucose-specific EIIA component
Q81V33	Probable transaldolase 1
Q81WW9	Conserved domain protein
Q81JT0	Polyamine aminopropyltransferase 1

Q81Z71	Chemical-damaging agent resistance protein C
Q81U41	HIT family protein
Q81MG5	Peptidyl-prolyl cis-trans isomerase
Q81MB5	6_7-dimethyl-8-ribityllumazine synthase
Q81KX5	Metallopeptidase
Q81MH4	N-acetylglucosamine-6-phosphate deacetylase
Q81KU3	3-demethylubiquinone-9 3-methyltransferase
Q81UU2	Nitroreductase
Q81L43	Heme uptake protein IsdC
Q81SW2	GTP cyclohydrolase 1
Q81T83	Thioredoxin
Q81VP8	30S ribosomal protein S9
Q81UR6	Uncharacterized protein
Q81LD0	Glutamate-1-semialdehyde 2_1-aminomutase 2
Q81VW3	Lysine--tRNA ligase
Q81PX6	Uncharacterized protein
Q81MR2	2-oxoisovalerate dehydrogenase
Q81U22	Ferrochelatase 1
Q81WK7	GTP-sensing transcriptional pleiotropic repressor CodY
Q81TB9	Abortive phage infection protein
Q81T55	D-isomer specific 2-hydroxyacid dehydrogenase family protein
Q81WQ9	2-oxoacid ferredoxin oxidoreductase
Q81QQ0	Isochorismate synthase
Q81K32	UDP-N-acetylglucosamine 2-epimerase
Q81WN7	4-hydroxy-tetrahydrodipicolinate synthase
Q81R67	ESAT-6-like protein
Q81MR4	Dihydrolipoyl dehydrogenase

Q81VU3	50S ribosomal protein L11
Q81JR3	Putative heme-dependent peroxidase BA_5637
Q81XJ7	L-lactate dehydrogenase 3
Q81W25	Serine--tRNA ligase
Q81LK9	Transcription elongation factor GreA
Q81L16	50S ribosomal protein L35
Q81WY2	Lipoteichoic acid synthase-like yqgS
Q6I4E9	tRNA N6-adenosine threonylcarbamoyltransferase
Q81UR3	Efflux transporter periplasmic adaptor subunit
Q81P32	Antibiotic biosynthesis monooxygenase
Q81KI0	S-adenosylmethionine synthase
Q81JI3	Single-stranded DNA-binding protein
Q81X56	Thioredoxin reductase
Q81SU0	4-hydroxy-tetrahydrodipicolinate reductase
Q81V38	Ribokinase
Q81SP8	Uncharacterized protein
Q81UR3	Efflux transporter periplasmic adaptor subunit
Q81R29	Cell division protein FtsK
Q81JI3	Single-stranded DNA-binding protein
Q81VP0	Arginase
B9ZW32	Hypoxanthine phosphoribosyltransferase
Q81VV4	2-C-methyl-D-erythritol 2_4-cyclodiphosphate synthase
Q81SB6	Uncharacterized protein
Q81ZF6	Isochorismatase
Q81JX8	Uncharacterized protein ywrF
Q81LJ1	HTH-type transcriptional regulator CymR
Q81PA3	Sporulation protein

Q81XF6	DNA methyltransferase
Q81L16	50S ribosomal protein L35
Q81K32	UDP-N-acetylglucosamine 2-epimerase
Q81YR9	Ankyrin repeat domain protein
Q81QQ0	Isochorismate synthase
Q81JI3	Single-stranded DNA-binding protein
Q81SP6	Uncharacterized protein
Q81T89	Transcriptional regulator_ Bla/Mec family
Q81JR3	Putative heme-dependent peroxidase BA_5637
Q81U47	Uncharacterized protein
Q81WT0	Probable N-acetyl-alpha-D-glucosaminyl L-malate deacetylase 2
Q81VW7	7_8-dihydroneopterin aldolase
Q81VR5	50S ribosomal protein L6
Q81SX3	Uncharacterized protein
Q6I4E9	tRNA N6-adenosine threonylcarbamoyltransferase
Q81YT0	Internalin
Q81LL6	Cys/Met metabolism PLP-dependent enzyme
Q81LW0	Superoxide dismutase [Mn] 1
Q81L16	50S ribosomal protein L35
Q81UH0	Ornithine cyclodeaminase
Q81WQ6	Stage V sporulation protein S
Q81R02	Putative lipoprotein
Q81JW2	Uncharacterized protein
Q81VT2	Elongation factor Tu
Q81MR1	Pyruvate dehydrogenase
Q81XN4	Putative lipoprotein
Q81KN9	RNA 2'_3'-cyclic phosphodiesterase

Appendix 5 – Proteins identified in AVP using LC-MS/MS analysis

Uniprot Accession No.	Protein Description
P13423	Protective antigen
P15917	Lethal factor
P40136	Calmodulin-sensitive adenylate cyclase
Q81X78	Enolase
Q9X360	PXO1-90
Q81QZ5	Alcohol dehydrogenase
Q81VE1	60 kDa chaperonin
Q81KZ1	Pyruvate kinase
Q81K80	L-lactate dehydrogenase 2
Q81VT3	Elongation factor G
Q81YX1	Formate acetyltransferase
P02769	Unknown Entry
Q81M66	Leucine dehydrogenase
Q81X75	Phosphoglycerate kinase
Q81K75	Glucose-6-phosphate isomerase
Q81VE0	GMP synthase [glutamine-hydrolyzing]
P94217	S-layer protein EA1
Q81ZF8	1-pyrroline-5-carboxylate dehydrogenase
TRYP_PIG	Entry Unknown Entry
Q81XT6	Glutamine synthetase
Q81W29	Inosine-5'-monophosphate dehydrogenase
Q81M08	Probable glycine dehydrogenase (decarboxylating) subunit 2
Q81Y15	Transketolase

Q81Y95	Serine protease
Q81X77	2_3-bisphosphoglycerate-independent phosphoglycerate mutase
Q81UH4	Amidase
Q81JY4	Serine hydroxymethyltransferase
Q81ZC4	Alkyl hydroperoxide reductase
Q81M07	Probable glycine dehydrogenase (decarboxylating) subunit 1
Q81V19	Cell wall-binding protein
Q81L45	Cell surface protein
Q81WM8	Polyribonucleotide nucleotidyltransferase
Q81ZG8	Bifunctional purine biosynthesis protein PurH
Q81M06	Aminomethyltransferase
Q81X74	Glyceraldehyde-3-phosphate dehydrogenase
Q81ZH6	Adenylosuccinate lyase
Q81VN5	Glutamine--fructose-6-phosphate aminotransferase [isomerizing]
Q81P59	Chorismate mutase
Q81QQ0	Isochorismate synthase
Q81SV8	Nucleoside diphosphate kinase
D1MPY3	Putative malate dehydrogenase
Q81UA1	Putative S-layer protein
Q81VV3	Glutamate--tRNA ligase
Q81Y22	N-acetylmuramoyl-L-alanine amidase
Q81TX2	Putative S-layer protein
Q81KZ0	ATP-dependent 6-phosphofructokinase
Q81TL7	Tryptophan synthase alpha chain
Q81JW4	Fructose-bisphosphate aldolase
Q81W27	Pyridoxal 5'-phosphate synthase subunit PdxS
Q81KW3	Alanine dehydrogenase

Q81VN7	Phosphoglucosamine mutase
Q81VU0	50S ribosomal protein L7/L12
Q81LL7	Aldehyde-alcohol dehydrogenase
Q81X76	Triosephosphate isomerase
Q81JI9	Adenylosuccinate synthetase
Q6HSF4	Malate dehydrogenase
Q81LB8	Trigger factor
Q81L43	Heme uptake protein IsdC
Q81UR6	Uncharacterized protein
Q81LL9	High-affinity heme uptake system protein isdE
Q81TS4	Dipeptide-binding protein dppE
Q81TL8	Tryptophan synthase beta chain
Q81Z71	Chemical-damaging agent resistance protein C
Q81LS1	Protein GrpE OS=Bacillus anthracis GN=grpE PE=3 SV=1
Q81ZC5	Alkyl hydroperoxide reductase subunit F
Q81LG0	Nicotinate-nucleotide diphosphorylase (Carboxylating)
Q81Z72	Chemical-damaging agent resistance protein C
Q81R29	Cell division protein FtsK
Q81SA0	Fumarate hydratase class II
Q81XS0	Ferredoxin--NADP reductase 2
Q81RP6	Peptidase
Q81UL6	Glyceraldehyde-3-phosphate dehydrogenase
Q81SX5	30S ribosomal protein S1
Q81LW0	Superoxide dismutase [Mn] 1
Q81WN5	Aspartate-semialdehyde dehydrogenase
Q81WK9	Elongation factor Ts
Q81KP6	Peptidase_ M42 family

Q81RQ4	3-dehydroshikimate dehydratase
Q81K96	1_4-dihydroxy-2-naphthoyl-CoA synthase
Q81MR4	Dihydrolipoyl dehydrogenase
Q81QP8	Isochorismatase
Q81VE2	10 kDa chaperonin
Q81ZG7	Phosphoribosylamine--glycine ligase
Q81RW4	L-lactate dehydrogenase 1
Q81JT0	Polyamine aminopropyltransferase 1
Q81XP7	NifU domain protein
Q81L19	Peptidase M28
Q81JT1	Agmatinase
Q81VT2	Elongation factor Tu
Q81ZH8	N5-carboxyaminoimidazole ribonucleotide mutase
Q81RT5	Peptidase P60
Q81NS6	Signal peptidase I
Q81M65	Phosphate butyryltransferase
Q81JI3	Single-stranded DNA-binding protein
Q81LL6	Cys/Met metabolism PLP-dependent enzyme
Q81KW2	Universal stress protein
Q81VW3	Lysine--tRNA ligase
Q81XJ7	L-lactate dehydrogenase 3
Q81V33	Probable transaldolase 1
Q81WY2	Lipoteichoic acid synthase-like yqgS
Q81WW9	Conserved domain protein
Q81JF9	3-oxoacyl-[acyl-carrier-protein] synthase 2
Q81VX2	Cysteine synthase
Q81T09	Purine nucleoside phosphorylase DeoD-type

Q81MR2	2-oxoisovalerate dehydrogenase
Q81MB5	6_7-dimethyl-8-ribityllumazine synthase
Q81TX0	Isocitrate lyase
Q81W04	Transition state regulator Abh
Q81VA6	Alanine dehydrogenase
Q81KQ7	Aminopeptidase
Q81RR7	LytR family transcriptional regulator
Q81V80	Putative pyridoxal phosphate-dependent acyltransferase
Q81L44	Cell surface protein
Q81ZG0	Putative lipoprotein
Q81JI2	30S ribosomal protein S6
Q81WL1	Ribosome-recycling factor
Q81VZ2	Putative septation protein SpoVG
Q81UU2	Nitroreductase
Q81ZH1	Amidophosphoribosyltransferase
Q81U83	UPF0145 protein BA_1001/GBAA_1001/BAS0936
Q81SW3	DNA-binding protein
Q81LS2	Chaperone protein DnaK
Q81V16	LPXTG-site transpeptidase family protein
Q81VU1	50S ribosomal protein L10
Q81T55	D-isomer specific 2-hydroxyacid dehydrogenase family protein
Q81L70	Enoyl-CoA hydratase
Q81TN0	Putative phosphoesterase BA_1241/GBAA_1241/BAS1148
Q81VQ4	DNA-directed RNA polymerase subunit alpha
Q81LK9	Transcription elongation factor GreA
Q81ZE6	Diacylglycerol kinase
Q81TC3	Conserved domain protein

Q81P32	Antibiotic biosynthesis monooxygenase
Q81VS2	50S ribosomal protein L29
Q81MG5	Peptidyl-prolyl cis-trans isomerase
Q81X22	Endopeptidase lytF
Q81X22	Endopeptidase lytF
Q81MY9	Probable transaldolase 2
Q81KI0	S-adenosylmethionine synthase
Q81L32	Asparagine--tRNA ligase
Q9X366	PXO1-97
Q81VR5	50S ribosomal protein L6
Q81L73	Thioredoxin
Q81LB4	Uncharacterized protein
Q81MP6	Uncharacterized protein
Q81L70	Enoyl-CoA hydratase
Q81VZ2	Putative septation protein SpoVG
B9ZW32	Hypoxanthine phosphoribosyltransferase
Q81L73	Thioredoxin
Q81U83	UPF0145 protein BA_1001/GBAA_1001/BAS0936
Q81WL1	Ribosome-recycling factor
Q81W77	Transcriptional regulator
Q81L70	Enoyl-CoA hydratase
B9ZW32	Hypoxanthine phosphoribosyltransferase
Q81VZ2	Putative septation protein SpoVG
Q81R20	FMN-dependent NADH-azoreductase 3
Q81L44	Cell surface protein
P49051	S-layer protein sap
Q81KI0	S-adenosylmethionine synthase

Q81U83	UPF0145 protein BA_1001/GBAA_1001/BAS0936
Q81WK7	GTP-sensing transcriptional pleiotropic repressor CodY
Q81VZ2	Putative septation protein SpoVG
Q81L70	Enoyl-CoA hydratase
B9ZW32	Hypoxanthine phosphoribosyltransferase
Q81ME6	Transcriptional regulator_ MarR family
Q81L44	Cell surface protein
Q81TB9	Abortive phage infection protein
Q81VL4	Lipoprotein
Q81TC1	Phosphoglycerate mutase
Q81UN3	Acetyltransferase
Q9X388	PXO1-131
Q81JU4	Methionine aminopeptidase
Q81M74	UPF0403 protein BA_4378/GBAA_4378/BAS4061
Q81QA3	TetR family transcriptional regulator
Q81XS7	Phosphoglucomutase
Q81XK8	Glycine cleavage system H protein
Q81Q77	Uncharacterized protein
Q81T89	Transcriptional regulator_ Bla/Mec family
Q81PW3	Spore cortex-lytic enzyme
Q81LW2	Penicillin-binding protein
Q81U72	3'-5' exoribonuclease YhaM
Q81KU8	Probable thiol peroxidase
Q81VT8	DNA-directed RNA polymerase subunit beta
D1MPU6	Ribonucleoside-diphosphate reductase
Q81VV9	ATP-dependent Clp protease ATP-binding subunit ClpC
Q81JR3	Putative heme-dependent peroxidase BA_5637

Q81JW7	Fructose-1_6-bisphosphatase
Q81ZH0	Phosphoribosylformylglycinamidine cyclo-ligase
Q81V01	Quinol oxidase subunit 2
Q81LC9	Delta-aminolevulinic acid dehydratase
Q81VP0	Arginase
Q81MR1	Pyruvate dehydrogenase
Q81TC4	NADPH-dependent 7-cyano-7-deazaguanine reductase
Q81RP3	NH(3)-dependent NAD(+) synthetase
Q81KU3	3-demethylubiquinone-9 3-methyltransferase
Q81L18	DUTPase
Q81R24	Penicillin-binding protein
Q81RE1	Formate--tetrahydrofolate ligase
Q81TD1	Oligoendopeptidase F
Q81T62	Histidinol dehydrogenase
Q81LH1	S-adenosylmethionine:tRNA ribosyltransferase-isomerase
Q81KI3	Molybdenum cofactor biosynthesis protein B
Q81KP8	Thiol reductase thioredoxin
Q81MS8	GTP-binding protein TypA
Q81T83	Thioredoxin
Q81U22	Ferrochelatase 1
Q81P72	Peptidoglycan-N-acetylglucosamine deacetylase
Q81M67	Probable butyrate kinase
Q81PY0	Uncharacterized protein
Q81Y62	Putative S-layer protein
Q81RT6	Nitroreductase
Q81KX5	Metallopeptidase
Q81Z93	Chemotaxis protein

Q81UR3	Efflux transporter periplasmic adaptor subunit
Q81L80	D-alanyl-D-alanine carboxypeptidase
Q81SQ5	Xanthine phosphoribosyltransferase
Q81TM0	Indole-3-glycerol phosphate synthase
Q81T97	D-alanine--poly(phosphoribitol) ligase subunit 1
Q8RPQ2	DNA protection during starvation protein 2
Q81LF7	Transcriptional regulator
Q81Y06	LexA repressor
Q81JP0	Bifunctional hydroxymethylpyrimidine kinase/phosphomethylpyrimidine kinase
Q81WI1	Uncharacterized protein
Q81VV4	2-C-methyl-D-erythritol 2_4-cyclodiphosphate synthase
Q81SF5	IMP dehydrogenase
Q81LJ1	HTH-type transcriptional regulator CymR
Q81XP1	HAD family hydrolase
Q81UB2	FMN-dependent NADH-azoreductase 1
Q81XK7	Uncharacterized protein
Q81TC7	7-cyano-7-deazaguanine synthase
Q81ZG9	Phosphoribosylglycinamide formyltransferase
Q81TE0	2-aminoethylphosphonate--pyruvate transaminase
Q81M87	DUF3932 domain-containing protein
Q81KA6	2-dehydro-3-deoxyphosphooctonate aldolase
Q81L14	Threonine--tRNA ligase
Q81L31	Phenylalanine--tRNA ligase beta subunit
Q81XS5	Probable cytosol aminopeptidase
Q81W25	Serine--tRNA ligase
Q81ML7	Alpha-amylase

Q81US7	LytR family transcriptional regulator
Q81X56	Thioredoxin reductase
Q81L80	D-alanyl-D-alanine carboxypeptidase
Q81VQ9	Adenylate kinase
Q81JG0	3-oxoacyl-[acyl-carrier-protein] synthase 3 protein 1
Q81JI7	50S ribosomal protein L9
Q81WK8	30S ribosomal protein S2
Q81SQ5	Xanthine phosphoribosyltransferase
Q81LJ1	HTH-type transcriptional regulator CymR
Q81KY8	Acetyl-coenzyme A carboxylase carboxyl transferase subunit beta
Q81Z66	UPF0435 protein BA_0406/GBAA_0406/BAS0392
Q81SP8	Uncharacterized protein
Q81W25	Serine--tRNA ligase
Q81SB6	Uncharacterized protein
Q81MQ2	2_3_4_5-tetrahydropyridine-2_6-dicarboxylate N-acetyltransferase
Q81L80	D-alanyl-D-alanine carboxypeptidase
Q81VQ9	Adenylate kinase
Q81SQ5	Xanthine phosphoribosyltransferase
Q81U05	Lipoate--protein ligase
Q81KU5	NAD kinase 2
Q81WQ6	Stage V sporulation protein S
Q81ZG9	Phosphoribosylglycinamide formyltransferase
Q81WI7	Acyl carrier protein
Q81RT9	Putative lipoprotein
Q81Y62	Putative S-layer protein
Q81L31	Phenylalanine--tRNA ligase beta subunit
Q81US7	LytR family transcriptional regulator

Q81W25	Serine--tRNA ligase
Q81L46	Iron compound ABC transporter_ iron compound-binding protein
Q81JG0	3-oxoacyl-[acyl-carrier-protein] synthase 3 protein 1
Q81KX5	Metallopeptidase
Q81L80	D-alanyl-D-alanine carboxypeptidase
Q81MQ2	2_3_4_5-tetrahydropyridine-2_6-dicarboxylate N-acetyltransferase
Q81VQ9	Adenylate kinase
Q81JI7	50S ribosomal protein L9
Q81PH9	Probable manganese-dependent inorganic pyrophosphatase
Q81KU5	NAD kinase 2
Q81QP3	Cold-shock protein
Q81RQ5	Petrobactin biosynthesis protein AsbE
Q81WK8	30S ribosomal protein S2
Q81LJ1	HTH-type transcriptional regulator CymR
Q81W26	Pyridoxal 5'-phosphate synthase subunit PdxT
Q81UK5	UPF0342 protein BA_0863/GBAA_0863/BAS0820

Appendix 6 – List of Synthetic Peptides

rPA peptides

1. NTGTAPIYNVLPTTS (PA 397-411)
2. PTTSLVLGKNQTLAT (PA 408-422)
3. DTGSNWSEVLPQIQE (PA 501-515)
4. QIQETTARIIFNGKD (PA 512-526)
5. KYNDKLPLYISNPNY (PA 709-723)
6. NPNYKVNVYAVTKEN (PA 720-734)
7. SDNLQLPELKQKSSN (PA 177-191)
8. KSSNSRKKRSTSAGP (PA 188-202)
9. EKWSTASDPYSDFEK (PA 253-267)
10. DFEKVTGRIDKNVSP (PA 264-278)
11. NVSPEARHPLVAAYP (PA 275-289)
12. AVGADESVVKEAHRE (PA 633-647)
13. AHREVINSSTEGLLL (PA 644-658)
14. GLLLNIDKDIRKILS (PA 655-669)

rLF peptides

1. QSEKEYIRIDAKVVP (LF 570-584)
2. KVVPKSKIDTKIQEA (LF 581-595)
3. KVTNYLVDGNGRFVF (LF 650-664)
4. RFVFTDITLPNIAEQ (LF 661-675)
5. IAEQYTHQDEIYEQV (LF 672-686)
6. YEQVHSKGLYVPESR (LF 683-697)
7. LRNDSEGFIHEFGHA (LF 710-724)
8. FGHAVDDYAGYLLDK (LF 721-735)
9. DALLHQSIGSTLYNK (LF 453-467)

10. LYNKIYLYENMNINN (LF 464-478)
11. NINNLTATLGADLVD (LF 475-489)
12. RAGYLENGKLILQRN (LF 543-557)
13. LQRNIGLEIKDVQII (LF 554-568)

Appendix 7 – Samples that were tested for cytokine response to rPA, rLF, IMA/PNA and PA and LF peptide mixes

Stimulant	Sample No.									
	1	**2**	**3**	**4**	**5**	**6**	**7**	**8**	**9**	**10**
Blank	X	X	X	X	X	X	X	X	X	X
rPA	X	X	X	X	X	X	X	X	X	X
rLF	X	X	X	X	X	X	X	X	X	X
IMA/PNA	X	X	X	X	X	X	X	X	X	X
PA1 mix	X	X	X	X	X	X	X	X	X	X
PA2 mix	X	X	X	X	X	X	X	X	X	X
PA3 mix	X	X		X	X		X	X	X	X
PA4 mix		X		X	X		X	X	X	X
PA5 mix		X		X	X		X	X	X	X
LF1 mix		X		X	X		X	X	X	
LF2 mix		X		X	X		X	X	X	
LF3 mix		X		X	X		X	X	X	
LF4 mix		X			X		X	X	X	